APPLIED COMPUTER SCIENCE

The Journal is a peer-reviewed, international, multidisciplinary journal covering a broad spectrum of topics of computer application in production engineering, technology, management and economy.

The main purpose of Applied Computer Science is to publish the results of cutting-edge research advancing the concepts, theories and implementation of novel solutions in computer technology. Papers presenting original research results related to applications of computer technology in production engineering, management, economy and technology are welcomed.

We welcome original papers written in English. The Journal also publishes technical briefs, discussions of previously published papers, book reviews, and editorials. Especially we welcome papers which deals with the problem of computer applications in such areas as:

- manufacturing,
- engineering,
- technology,
- designing,
- organization,
- management,
- economics,
- innovations,
- competitiveness,
- quality and costs.

The Journal is published quarterly and is indexed in: BazTech, Cabell's Directory, CNKI Scholar (China National Knowledge Infrastucture), ERIH PLUS, Index Copernicus, J-Gate, Google Scholar, TEMA Technik und Management.

Letters to the Editor-in-Chief or Editorial Secretary are highly encouraged.

CONTENTS

Applied Computer Science, vol. 15, no. 3, pp. 5–20
doi:10.23743/acs-2019-17

Submitted: 2019-08-23
Revised: 2019-09-03
Accepted: 2019-09-11

optimization, UAVs , routing and scheduling

Grzegorz RADZKI [0000-0002-0688-1764]*,
Amila THIBBOTUWAWA [0000-0002-5443-8839]**,
Grzegorz BOCEWICZ [0000-0002-5181-2872]*

UAVS FLIGHT ROUTES OPTIMIZATION IN CHANGING WEATHER CONDITIONS – CONSTRAINT PROGRAMMING APPROACH

Abstract

The problem of delivering goods in a distribution network is considered in which a fleet of Unmanned Aerial Vehicles (UAV) carries out transport operations. The changing weather conditions in which the transport operations take place and the UAVs energy capacity levels influenced by the weather conditions are taken into account as factors that affect the determination of a collision-free route. The goods must be delivered to the customers in a given time window. Establishing the routes are the focus of this study. Solutions maximizing the level of customer satisfaction are focused and the computational experiments presented in the study show the impact of weather conditions on route determination.

1. INTRODUCTION

Every day, transport companies face the challenge of keeping their outlays as small as possible while making sure that the customers are fully satisfied. Decision support in this domain often comes down to solving an appropriate Vehicle Routing Problem (VRP) (Adbelhafiz, Mostafa & Girard, 2010).

* Koszalin University of Technology, Department of Computer Science and Management, Sniadeckich 2, Koszalin, Poland, radzki.grzegorz@gmail.com, bocewicz@ie.tu.koszalin.pl
** Aalborg University, Department of Materials and Production, Aalborg, Denmark, amila@mp.aau.dk

The dynamic development of unmanned aerial vehicle (UAV) technology in the recent decade has allowed the use of those machines, commonly referred to as drones, for the logistic services mainly in transportation of goods. Transportation companies quickly came to realize that the delivery of goods to customers by UAVs was associated with numerous benefits such as a short delivery time, easy movement (e.g. less traffic congestion), lower energy costs and reduced operational costs. It was also noticed that such solutions had no adverse effect on the environment and enables sustainable logistics operations (Chiang, Li, Shang & Urban, 2019).

The use of UAVs for transportation tasks, however, gives rise to new challenges related to the organization of transport. Typical limitations of air transport systems that use UAVs include the need for periodical (frequent) battery replacement, a pre-determined distance range limited by battery capacity, a limited payload capacity, the possibility of collision between UAVs performing their missions, etc. (Bocewicz, Nielsen, Banaszak & Thibbotuwawa, 2019).

Viewed in this way, the problem under consideration is an extension of the classical VRP that takes into account the weather-related changeable energy consumption (Adbelhafiz, Mostafa & Girard, 2010). In general, this type of problem belongs to the class of NP-hard problems (Bocewicz, Nielsen, Banaszak & Thibbotuwawa, 2019). The model of the VRP developed in this study, which is implemented in a constraint programming environment (IBM ILOG) assumes that energy consumption is a non-linear function that depends on weather conditions, carrying payload, UAVs' "geometry" (Thibbotuwawa, Nielsen, Zbigniew & Bocewicz, 2018a) and the flight trajectory (route) (Guerriero, Surace, Loscrí & Natalizio, 2014). The goal is to find flight mission plans (routings and schedules) which are collision-free and allow to maximize the quantity of goods delivered to customers by a fleet of UAVs with energy capacity limit flying in a given weather condition.

The paper is organized as follows: Section 2 discusses the state-of-the-art on the subject. Section 3 provides an example illustrating the UAV routing problem. Sections 4 and 5 present the proposed model and formulation of the problem. Section 6 reports experiments, which were conducted to verify the correctness of the model. The experiments were carried out in the IBM ILOG declarative programming environment. This illustrate the possibilities of practical application of the proposed solution. The key conclusions are formulated and the main directions of future research are suggested in Section 7.

2. LITERATURE REVIEW

The problem of transporting goods by UAVs is an extension of VRP. In the simplest version, the VRP assumes that one type of product is delivered using one mode of transport. Solutions are sought to minimize the total cost of travel (Golden, Raghavan & Wasil, 2011). The VRP extended to include the assumption that goods should be delivered to customers within specific time intervals is called the Vehicle Routing Problem with Time Windows (VRPTW). It is this type of problem that is most commonly encountered in practice. VRPTW for UAVs are used in both military and civilian settings (Adbelhafiz, Mostafa & Girard, 2010; Yakıcı, 2016; Ullah, et al., 2019).

According to the literature (Bocewicz, Nielsen, Banaszak & Thibbotuwawa, 2019; Chauhan, Unnikrishnan & Figliozzi, 2019; Dai, Fotedar, Radmanesh & Kumar, 2018), the UAV routing problem is usually modeled as a standard VRP with additional constraints reflecting the specific applications of this type of vehicle. The first studies on the UAV routing problem were focused on developing methods that would allow to obtain acceptable solutions within a given time interval. Apart from minimizing the cost of travel, other criteria that must also be considered include: reducing the individual UAVs operation costs (battery consumption), shortening the operation time, and increasing the safety of operations (Enright, Frazzoli, Pavone & Savla, 2014). Another aspect that distinguishes a VRP with UAVs from the standard version of the VRP is the environment in which routes are planned. For surface transport, routes are designed in 2D space (Karpenko, Konovalenko, Miller, Miller & Nikolaev, 2015). By contrast, routes for UAV must be planned in 3D space (Goerzen, Kong & Mettler, 2009). Article (Guerriero, Surace, Loscrí & Natalizio, 2014) presents a mathematical model of routing of UAV in three-dimensional space. It should be noted that the UAV routing approaches found in the literature fail to take into account the variability of weather conditions and the associated non-linearity of energy consumption (Wang, Poikonen & Golden, 2016). Routes established using those methods must be continuously adjusted as the flight progresses. The process of adjustment is very complex and does not protect the mission plan against potential failure due to battery depletion or other causes (Bocewicz, Nielsen, Banaszak & Thibbotuwawa, 2019). Certain studies has formulated the mission planning problem for a fleet of unmanned aerial vehicles (UAVs) as a mixed-integer nonlinear programming problem (MINLP) but approximating the problem of MINLP by a mixed-integer linear program (MILP), and used a solver (GUROBI) (Fügenschuh & Müllenstedt, 2015). They have considered energy limitations of UAVs but has not considered the effects of weather conditions in deriving the energy consumptions and used linier approximations of the energy consumption of UAVs which not realistic in practical context.

An alternative solution is to take into account the uncertainty/variability of weather conditions and the related level of energy consumption already at the stage of planning flight missions. This type of problem is an extension of the VRPTW that incorporates elements related to weather and route-dependent energy consumption (Guerriero, Surace, Loscrí & Natalizio, 2014). Studies (Thibbotuwawa, Nielsen, Zbigniew & Bocewicz, 2018a, 2018b) propose preliminary heuristics that allow to find such solutions. The present paper expands on these studies by using a declarative programming environment (IBM ILOG).

3. A MOTIVATION EXAMPLE

The problem studied can be described as follows: Given is a company that provides air transport services using a fleet of UAVs. In the case under consideration, the fleet consists of three UAVs with identical technical parameters (Tab. 1). The UAVs deliver goods to six customers located in an area covering 10 km^2 – the network of connections is shown in Fig. 1. Vertex N_1 marks the location of the company (the base which the UAVs take off from/land at) and vertices N_2–N_7 mark the locations of the individual customers. It is assumed that UAVs travel at a constant speed v = 20 m/s. The flight times along edge $\{N_i,N_j\}$ of the graph are shown in Fig. 1. For example, the flight time between node N_6 and node N_2 is 185 seconds.

Known is the demand of the individual customers for the goods transported by the UAVs (Tab. 2). It is assumed that the UAVs must deliver the exact quantity of goods demanded by a given customer.

Tab. 1. Technical parameters of UAVs

Technical parameters of UAVs	Value	Unit
Payload capacity Q	100	kg
Battery capacity CAP	6000	kJ
Flight speed v	20	m/s
Drag coefficient C_D	0.54	–
Front surface of UAV A	1.2	m
UAV width b	8.7	m

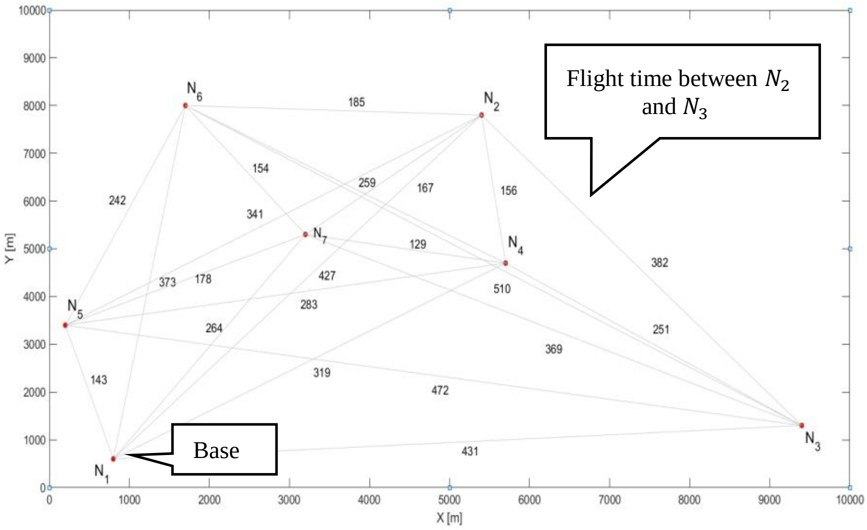

Fig.1. Map of drop-off locations

Tab. 2. Customer demand for transported goods

Node	Demand for goods [kg]
N1	0
N2	60
N3	70
N4	30
N5	40
N6	20
N7	30

Tab. 3. Weather conditions

Weather conditions	**Value**	**Unit**
Wind speed v_w	10	m/s
Wind direction Θ	30	°
Air density D	1.225	kg/m^3

It is additionally assumed that goods are transported in various weather conditions which affect the rate of battery discharge (the speed and direction of wind are both taken into account – Tab. 3). It is assumed that each of the UAVs must travel at the given constant flight speed (v = 20 m/s) regardless of atmospheric conditions. This means that the adoption of fixed, time-invariable delivery plans (that include UAV routes and flight schedules) may result in varying degrees of battery utilization and, in special cases, complete battery depletion. Fig. 2 presents an example of UAV flight routings and schedule that guarantee that the requested goods are delivered to customers (100% customer satisfaction) in the given weather conditions (Tab. 3). As it is easy to see, in this set-up, the freight will be delivered in under 2000 s.

In this set-up, UAVs move along routes Π: $\Pi_1 = (N_1, N_3, N_1)$, $\Pi_2 = (N_1, N_6, N_2, N_5, N_1)$, $\Pi_3 = (N_1, N_5, N_7, N_4, N_3, N_1)$. For example, UAV D_1 (route marked by the blue line) moves from the base N_1 to node N_3, to which it delivers 52 kg of goods and then returns to the base. UAV one D_2 (route marked by the red line) travels from the base N_1 through vertices N_6, N_2 and N_5, at which it drops off 20, 60 and 18 kg of goods, respectively, and then flies back to the base N_1. UAV D_3 (route marked by the green line) delivers goods to customers at the following nodes: N_5 – 22 kg, N_7 – 30 kg, N_4 – 30 kg, N_3 – 18 kg, and then returns to the base.

a)

b)

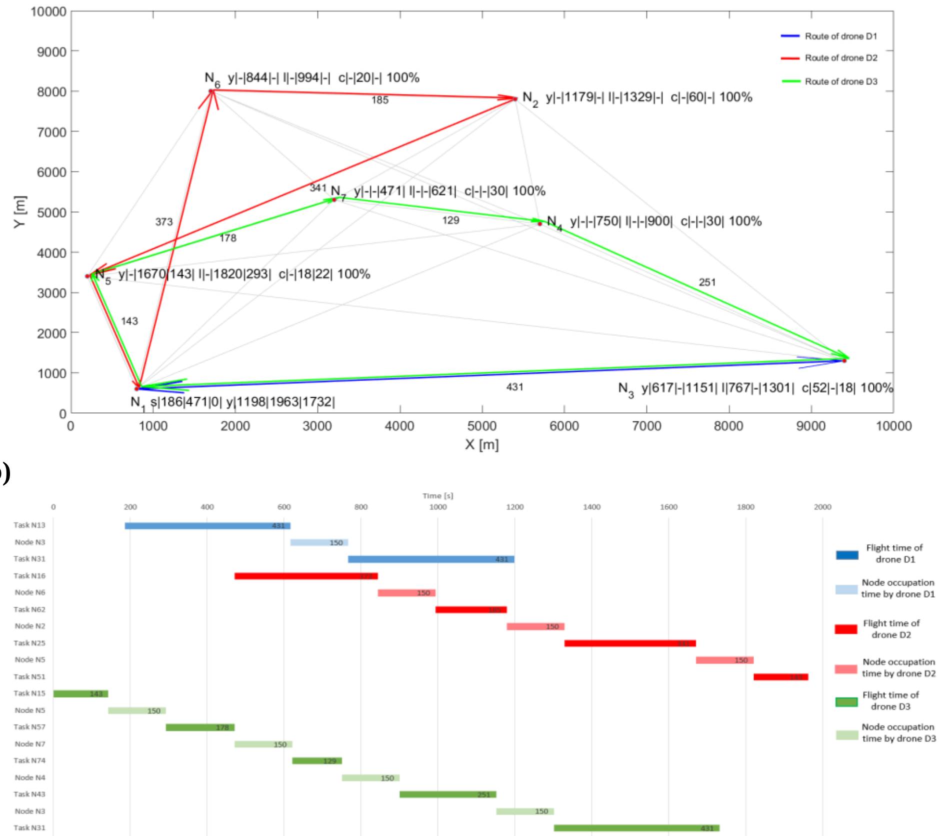

Fig. 2. Routes (a) and flight schedule (b) for a UAV fleet that guarantee delivery of requested goods to customers (weather conditions: wind speed = 10 m/s, wind direction = 30°)

A flight plan like this does not lead to collisions (the UAVs do not use shared edges at the same time – for example, the edge that connects vertices N_3 and N_1) and guarantees that the battery is still charged at the end of the mission. The battery utilization level for the UAVs is 77.58%, 88.93% and 97.53% respectively.

Unfortunately, this set-up cannot be used in all weather conditions. For example, when the wind direction changes from 30° to 60° and the wind speed changes from 10 m/s to 12 m/s, the use of the flight plan from Fig. 2 will lead to the complete depletion of the batteries of UAVs D_2 and D_3 before they return to the base. This situation is illustrated in Fig. 3. As it is easy to notice, UAV D_2 will end its flight while flying from vertex N_5 to N_1 and UAV D_3 will have to land while moving from node N_3 to N_1. This means that flight plans must be tailored to given weather conditions.

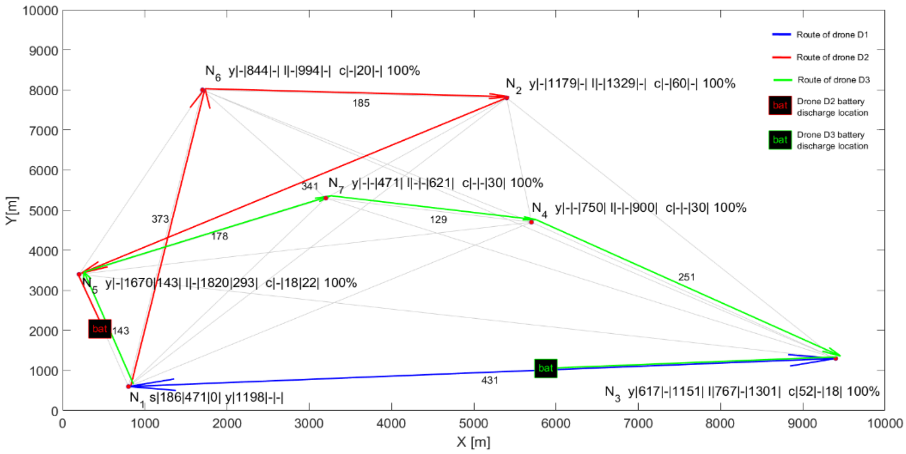

Fig. 3. Simulation results for wind speed = 12 m/s and wind direction = 60°

Taking into account the fact that the adopted weather conditions may affect the possibility of implementing the given flight plan, the problem under consideration boils down to seeking the answer to the following question: *Is the given fleet of UAVs sufficient to meet customer needs (deliver the required quantity of goods) in the given transport network under the specific weather conditions?*

To put it differently, the problem discussed can be considered as a problem of routing and scheduling a fleet of UAVs subject to variable weather conditions (wind speed and direction). Solutions are sought that will maximize customer satisfaction (a function that describes the degree to which customers' needs are satisfied) under the specific weather conditions and given the limited battery life.

4. DECLARATIVE MODEL

The problem discussed in the present paper assumes that the structure of the goods distribution network (number and location of customers and customer demand) is known. The goods are transported by UAVs. Also known is the time horizon in which all flights should be completed. In this context, the following assumptions are taken into account:

- The weather conditions are known (wind speed v_w and wind direction θ),
- The weather conditions are constant over the entire time horizon,
- All UAVs are in the base before the start of the delivery mission,
- The same type of freight is delivered to all customers,
- During the flight, the total weight of the UAV remains constant (i.e. no reduction in weight due to leaving part of the load at a drop-off location is planned for),

- The UAVs travel at a constant speed v = 20 m/s,
- The goal is to find collision-free flight plans and routes that guarantee the highest level of customer satisfaction.

The model is defined as follows:

Parameters

Network:

I – number of nodes,

$t_{i,j}$ – flight time between nodes N_i and N_j,

m_i – demand for goods at the i-th node $i = 1..I$, $m_1 = 0$,

w_i – priority of the i-th node $i = 1..I$, $w_1 = 0$,

TN – node occupation time (unloading time),

TS – time interval at which UAVs can start from the base,

$block_{\{i,j\};\{a,b\}}$ – binary variable corresponding to intersecting edges:

$$block_{\{i,j\};\{a,b\}} = \begin{cases} 1 \; when\; edges\; \{i,j\}\; and\; \{a,b\}\; intersect \\ 0 \quad\quad\quad\quad otherwise \end{cases}.$$

Technical parameters of the UAV fleet:

K – size of the UAV fleet,

Q – payload capacity of a UAV,

CAP – UAV battery capacity,

$e_{i,j}$ – energy consumed by a UAV during a flight from node N_i to node N_j,

C_D − drag coefficient

A − front surface of UAV,

b − UAV width,

W − total weight of UAV,

$va_{i,j}$ − motor thrust speed.

Environmental parameters:

H – planning horizon $H = [0, t_{max}]$,

D − air density,

v_w − wind speed,

Θ − wind direction.

Decision variables

$x_{i,j}^k$ – a binary variable describing whether the k-th UAV travels from node N_i to node N_j,

$$x_{i,j}^k = \begin{cases} 1 \;\; when\; k-th\; drone\; travels\; from\; node\; N_i to\; node\; N_j \\ 0 \quad\quad\quad\quad otherwise \end{cases}.$$

s^k – take-off time of the k-th UAV,

y_i^k – time at which the k-th UAV arrives at node N_i,
c_i^k – weight of freight delivered to node N_i by the k-th UAV,
cp_i – total weight of freight delivered to node N_i,
bat^k – battery level of the k-th UAV.

Sets

$Y^k -$ set of times y_i^k – schedule of the k-th UAV,
$Y -$ family $Y^k -$ schedule of the UAV fleet,
$C^k -$ set $c_i^k -$ weight of freight delivered by the k-th UAV,
$C -$ family C^k,
$\Pi -$ set of UAV fleet routes.

Constraints

Routing. Relationships between variables describing start times and task order.

$$s^k \geq 0\,, k = 1 \ldots K \tag{1}$$

$$(k \neq q) \Rightarrow \left(\left|s^k - s^q\right| \geq TS\right), k, q = 1 \ldots K \tag{2}$$

$$\sum_{j=1}^{I} x_{1,j}^k = 1\,, k = 1 \ldots K \tag{3}$$

$$\left(x_{1,j}^k = 1\right) \Rightarrow y_j^k = s^k + t_{1,j}\,, j = 1 \ldots I, k = 1 \ldots K \tag{4}$$

$$\left(k \neq q\ \wedge y_i^k \neq 0\ \wedge y_i^q \neq 0\right) \Rightarrow \left(\left|y_i^k - y_i^k\right| \geq TN\right), i = 1 \ldots I, k, q = 1 \ldots K \tag{5}$$

$$\left(x_{i,j}^k = 1\right) \Rightarrow y_j^k = y_i^k + t_{i,j} + TN, \quad j = 1 \ldots I, i = 2..I, k = 1 \ldots K \tag{6}$$

$$y_i^k \geq 0, i = 1 \ldots I, k = 1 \ldots K \tag{7}$$

$$\sum_{j=1}^{I} x_{i,j}^k = \sum_{j=1}^{I} x_{j,i}^k\,, i = 1 \ldots I, k = 1 \ldots K \tag{8}$$

$$y_i^k \leq H * \sum_{j=1}^{I} x_{i,j}^k \ \ \forall i \in I, \forall k \in K \tag{9}$$

Collision avoidance. Intersecting edges ($b_{\{i,j\};\{a,b\}} = 1$) cannot be occupied at the same time by UAVs ($x_{i,j}^k = 1, x_{i,j}^q = 1$)

$$\begin{gathered}\left(block_{\{i,j\}\{a,b\}} \wedge\ x_{i,j}^k = 1\ \wedge x_{a,b}^q = 1\right) \\ \Rightarrow \left(y_b^q \leq y_j^k - t_{i,j}\right) \vee \left(y_j^k \leq y_b^q - t_{a,b}\right) \\ i, j = 1 \ldots I,, k, q = 1 \ldots K, k \neq q\end{gathered} \tag{10}$$

Delivery of freight. Relationships between variables describing the amount of freight delivered to nodes by UAVs and the demand for goods at a given node.

$$c_i^k \geq 0, i = 1 \dots I, k = 1 \dots K \tag{11}$$

$$c_i^k \leq Q * \sum_{j=1}^{I} x_{i,j}^k, i = 1 \dots I, k = 1 \dots K \tag{12}$$

$$\sum_{i=1}^{I} c_i^k \leq Q, k = 1 \dots K \tag{13}$$

$$\left(x_{i,j}^k = 1\right) \Rightarrow c_j^k \geq 1, k = 1 \dots K, i = 1 \dots I, j = 2 \dots I \tag{14}$$

$$x_{i,i}^k = 0, i = 1 \dots I, k = 1 \dots K \tag{15}$$

$$cp_i \leq m_i, i = 1 \dots I \tag{16}$$

$$\sum_{k=1}^{K} c_i^k = cp_i, i = 1 \dots I \tag{17}$$

$$\sum_{j=1}^{I} x_{1,j}^k = 1, k = 1 \dots K \tag{18}$$

Battery consumption. The amount of energy needed to complete a task may not exceed the maximum battery capacity of the UAV.

$$bat^k \leq CAP, k = 1 \dots K \tag{19}$$

$$\sum_{i=0}^{I} \sum_{j=0}^{I} x_{i,j}^k * t_{i,j} * e_{i,j}, k = 1 \dots K \tag{20}$$

$$e_{i,j} = \frac{1}{2} C_D A D \left(va_{i,j}\right)^3 + \frac{W^2}{Db^2 va_{i,j}}, i, j = 1 \dots I \tag{21}$$

$$va_{i,j} = \sqrt{(vcos\vartheta - v_{\mathrm{w}} cos\theta)^2 + (vsin\vartheta - v_w sin\theta)^2}, i, j = 1 \dots I \tag{22}$$

Objective function. Maximization of customer satisfaction. Customer satisfaction is expressed as the sum of the product of the variables w_i and cp_i. Customer satisfaction should be understood as the ratio of the amount of goods delivered to the demand for goods at a given node expressed as a percentage.

$$CS = \max \sum_{i=0}^{I} w_i * cp_i \tag{23}$$

5. PROBLEM FORMULATION

In the context of the proposed model, the problem under consideration can be formulated as follows: *Given is a fleet of K UAVs moving in a transport network consisting of I vertices. Do there exist routes Π in that network that guarantee maximum customer satisfaction CS while satisfying the constraints associated with collision avoidance (10), delivery of the required quantity of goods (11)–(18) and energy consumption (19)–(22)?*

This problem can be considered as a *Constraint Optimization Problem* (COP) [12]:

$$COP = (\mathcal{V}, \mathcal{D}, \mathcal{C}, \mathrm{CS}) \tag{24}$$

where: $\mathcal{V} = \{\Pi, Y, C\}$ – a set of decision variables: Π – variables describing UAV routes, Y – variables describing the schedule of UAV fleet tasks, C – variables describing the quantity of goods delivered by UAVs,
$\mathcal{D}$ – a finite set of descriptions of decision variables,
$\mathcal{C}$ – a set of constraints describing the relationship between routes, the flight schedule and the transported loads (1)–(22),
CS – an objective function representing the level of customer satisfaction.

To solve the *COP*, one has to determine the values of the decision variables for which all constraints are satisfied and for which the objective function reaches a maximum. By implementing the *COP* in a constraint programming environment, such as IBM ILOG, one can build a computational engine for use in decision support systems (DSS).

6. COMPUTATIONAL EXPERIMENTS

In Section 3, it was noted that in the considered delivery network, the route from Fig. 2, cannot be used under weather conditions $v_w = 12$ m/s ; $\Theta = 60°$, as it leads to battery depletion in UAVs D_2 and D_3 before the completion of their missions. The model developed in this study can be used to determine a flight mission that would guarantee the return of all UAVs to the base under the given weather conditions, while maximizing the level of customer satisfaction. To put it differently, what is sought is the answer to the following question: *Given a fleet of 3-UAVs moving in the transport network from Fig. 1, do there exist routes Π that can ensure the maximum level of customer satisfaction in the given weather conditions ($v_w = 12\frac{m}{s}$; $\Theta = 60°$)?*

To answer this question one must solve problem (23). This problem was implemented and solved in the declarative programming environment IBM ILOG (Intel Core i7-M4800MQ 2.7 GHz, 32 GB RAM). The solution was obtained in 5.14 s.

Fig. 4 shows the computed routes and flight schedule. A set-up like this guarantees that the demanded quantity of goods are delivered to customers in the given weather conditions. Customer satisfaction at all nodes is 100%. Battery consumption for the UAVs traveling along these routes under the given weather conditions is 94.86%, 98.12%, 30%, and 99.5%, respectively.

a)

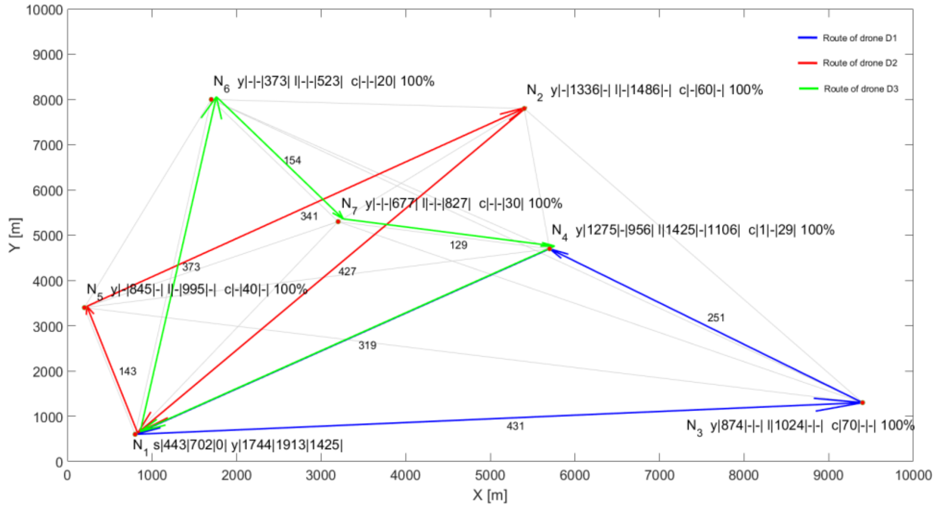

b)

Fig. 4. UAV routes (a) and a flight schedule (b) that guarantee delivery of the requested quantity of goods to customers (weather conditions: wind speed = 12 m/s, wind direction = 60°)

The model we developed was used in a series of experiments performed to assess the effect of weather on the solutions obtained and the scale of problems that could be effectively solved online at a calculation time < 300s.

In the first case, missions were determined for the given network (Fig. 1) and a fixed fleet of 3 UAVs (Tab. 1) for variable weather conditions, i.e. v_w = 5–15 m/s; Θ = 30°–360°. The results are shown in Tab. 4 and 5.

Tab.4. Simulation results for a constant wind speed = 10 m/s and variable wind direction

Wind direction [°]	Customer satisfaction [%]	Simulation time [s]
30	100	6.03
60	100	5.33
90	100	6.39
120	100	6.27
150	100	6.52
180	100	6.82
210	100	5.47
240	100	5.31
270	100	6.32
300	100	5.29
330	100	5.3
360	100	6.33

Tab.5. Simulation results for a variable wind speed and a constant wind direction = 30°

Wind speed [m/s]	Customer satisfaction [%]	Simulation time [s]
5	100	5.91
6	100	6.25
7	100	26.83
8	100	6.42
9	100	6.11
11	100	7.62
12	100	5.02
13	83.3	21.73
14	66.6	23.59
15	66.6	12.03

Tab. 4 clearly shows that at wind speed v_w = 10 m/s and a wind direction in the range 30°–360°, it is possible to designate routes that guarantee 100% customer satisfaction. When the wind direction is constant and the value of wind speed changes as indicated in Tab. 5. then, at wind speeds greater than 13 m/s it is no longer possible to find a solution that guarantees 100% customer satisfaction. In other words, the given UAV fleet allows to meet all customer needs only when the wind speed does not exceed 12 m/s .

In the next stage of our research, we assessed the effectiveness of the proposed approach. During the experiments, it was assumed that a UAV's payload capacity Q was balanced against the total weight of goods to be delivered to all nodes. The results are shown in Tab. 6. As it is easy to see, getting an answer to the question posed, in under 300 s is only possible for networks in which the number of UAVs is lower than or equal to 4 and the number of customers is lower than or equal to 8.

Tab.6. Results of the search for maximum network complexity, for wind speed = 10 m/s and wind direction = 30°

No.	No. customers	No. UAVs	Customer satisfaction = 100%	Calculation time [s]
1	6	2	Yes	7.46
2	6	3	Yes	6.03
3	6	4	Yes	10.18
4	6	5	Yes	113.93
5	6	6	No solution	300
6	7	2	Yes	5.6
7	7	3	Yes	11.05
8	7	4	Yes	187.57
9	7	5	No	300
10	7	6	No	300
11	8	2	Yes	15.82
12	8	3	No	28.81
13	8	4	Yes	253.22
14	8	5	No solution	300
15	8	6	No	300
16	9	2	No	300
17	9	3	No solution	300
18	9	4	No	300
19	9	5	No solution	300
20	9	6	No solution	300

7. CONCLUSION

The proposed declarative model (implemented in the IBM ILOG environment) allows to design UAV flight routes that guarantee the maximum level of customer satisfaction for various weather conditions. As the results of the experiments show, the admissible size of the network for which this type of solution is possible is 8 nodes for a fleet of 4 UAVs. This means that the proposed approach can be used with methods in which a network is partitioned into many small clusters. From this perspective, the approach developed in this study can be used as an element of the heuristics presented in (Thibbotuwawa, Nielsen, Zbigniew, & Bocewicz, 2018a) and (Thibbotuwawa, Nielsen, Zbigniew, & Bocewicz, 2018b).

In our future research, we plan to extend the model so that it can take into account the variable weight of a UAV and allow to search for routes that are robust to given weather conditions.

REFERENCES

Adbelhafiz, M., Mostafa, A., & Girard, A. (2010). Vehicle Routing Problem Instances: Application to Multi-UAV Mission Planning. In *AIAA Guidance, Navigation, and Control Conference*. Toronto, Canada. doi:10.2514/6.2010-8435

Bocewicz, G., Nielsen, P., Banaszak, Z., & Thibbotuwawa, A. (2019). Routing and Scheduling of Unmanned Aerial Vehicles Subject to Cyclic Production Flow Constraints. In *Advances in Intelligent Systems and Computing Distributed Computing and Artificial Intelligence, Special Sessions, 15th International Conference* (pp. 75–86, vol. 801). doi:10.1007/978-3-319-99608-0_9

Chauhan, D., Unnikrishnan, A., & Figliozzi, M. (2019). Maximum coverage capacitated facility location problem with range constrained drones. *Transportation Research Part C: Emerging Technologies*, *99*, 1-18. doi:10.1016/j.trc.2018.12.001

Chiang, W., Li, Y., Shang, J., & Urban, T. L. (2019). Impact of drone delivery on sustainability and cost: Realizing the UAV potential through vehicle routing optimization. *Applied Energy, 242*, 1164–1175. doi:10.1016/j.apenergy.2019.03.117

Dai, R., Fotedar, S., Radmanesh, M., & Kumar, M. (2018). Quality-aware UAV coverage and path planning in geometrically complex environments. *Ad Hoc Networks, 73*, 95–105. doi:10.1016/j.adhoc.2018.02.008

Enright, J. J., Frazzoli, E., Pavone, M., & Savla, K. (2014). UAV Routing and Coordination in Stochastic, Dynamic Environments. *Handbook of Unmanned Aerial Vehicles*, 2079–2109. doi:10.1007/978-90-481-9707-1_28

Fügenschuh, A., & Müllenstedt, D. (2015). *Flight planning for unmanned aerial vehicles*. Hamburg: Professur für Angewandte Mathematik, Helmut-Schmidt-Universität/Universität der Bundeswehr Hamburg, Fachbereich Maschinenbau.

Goerzen, C., Kong, Z., & Mettler, B. (2009). A Survey of Motion Planning Algorithms from the Perspective of Autonomous UAV Guidance. *Journal of Intelligent and Robotic Systems, 57*(1–4), 65–100. doi:10.1007/s10846-009-9383-1

Golden, B. L., Raghavan, S., & Wasil, E. A. (2011). *The vehicle routing problem: Latest advances and new challenges* (Ser. 43). New York, USA: Springer. doi:10.1007/978-0-387-77778-8

Guerriero, F., Surace, R., Loscrí, V., & Natalizio, E. (2014). A multi-objective approach for unmanned aerial vehicle routing problem with soft time windows constraints. *Applied Mathematical Modelling, 38*(3), 839–852. doi:10.1016/j.apm.2013.07.002

Karpenko, S., Konovalenko, I., Miller, A., Miller, B., & Nikolaev, D. (2015). UAV Control on the Basis of 3D Landmark Bearing-Only Observations. *Sensors, 15*(12), 29802–29820. doi:10.3390/s151229768

Thibbotuwawa, A., Nielsen, P., Zbigniew, B., & Bocewicz, G. (2018a). Energy Consumption in Unmanned Aerial Vehicles: A Review of Energy Consumption Models and Their Relation to the UAV Routing. *Advances in Intelligent Systems and Computing Information Systems Architecture and Technology: Proceedings of 39th International Conference on Information Systems Architecture and Technology – ISAT 2018* (pp. 173–184). doi:10.1007/978-3-319-99996-8_16

Thibbotuwawa, A., Nielsen, P., Zbigniew, B., & Bocewicz, G. (2018b). Factors Affecting Energy Consumption of Unmanned Aerial Vehicles: An Analysis of How Energy Consumption Changes in Relation to UAV Routing. *Advances in Intelligent Systems and Computing Information Systems Architecture and Technology: Proceedings of 39th International Conference on Information Systems Architecture and Technology – ISAT 2018* (pp. 228–238). doi:10.1007/978-3-319-99996-8_21

Ullah, S., Kim, K., Kim, K. H., Imran, M., Khan, P., Tovar, E., & Ali, F. (2019). UAV-enabled healthcare architecture: Issues and challenges. *Future Generation Computer Systems, 97*, 425–432. doi:10.1016/j.future.2019.01.028

Wang, X., Poikonen, S., & Golden, B. (2016). The vehicle routing problem with drones: Several worst-case results. *Optimization Letters, 11*(4), 679–697. doi:10.1007/s11590-016-1035-3

Yakıcı, E. (2016). Solving location and routing problem for UAVs. *Computers & Industrial Engineering, 102*, 294-301. doi:10.1016/j.cie.2016.10.029

Applied Computer Science, vol. 15, no. 3, pp. 21–33
doi:10.23743/acs-2019-18

Submitted: 2019-08-30
Revised: 2019-09-14
Accepted: 2019-09-18

genetic algorithm, neural network, crossover, mutation

Wafaa Mustafa HAMEED [0000-0002-2454-6185]*, *Asan Baker KANBAR* *

USING GA FOR EVOLVING WEIGHTS IN NEURAL NETWORKS

Abstract

This article aims at studying the behavior of different types of crossover operators in the performance of Genetic Algorithm. We have also studied the effects of the parameters and variables (crossover probability (Pc), mutation probability (Pm), population size (popsize) and number of generation (NG) for controlling the algorithm. This research accumulated most of the types of crossover operators these types are implemented on evolving weights of Neural Network problem. The article investigates the role of crossover in GAs with respect to this problem, by using a comparative study between the iteration results obtained from changing the parameters values (crossover probability, mutation rate, population size and number of generation). From the experimental results, the best parameters values for the Evolving Weights of XOR-NN problem are NG = 1000, popsize = 50, Pm = 0.001, Pc = 0.5 and the best operator is Line Recombination crossover.

1. INTRODUCTION

Genetic algorithms are a type of optimization algorithm, meaning they are used to find the optimal solution(s) to a given computational problem that maximizes or minimizes a particular function. Genetic algorithms represent one branch of the field of study called evolutionary computation (Koza, 1992), in that they imitate the biological processes of reproduction and natural selection to solve for the 'fittest' solutions (Mitchell, 1998). Like in evolution, many of a genetic algorithm's processes are random, however this optimization technique allows one to set the level of randomization and the level of control (Mitchell, 1998). These algorithms are far more powerful and efficient than random search and exhaustive search algorithms (Koza, 1992; Hameed, 2016; Hameed & Kanbar, 2017), yet require no extra information about the given problem. This feature allows them to find

* Cihan University, Department of Computer Science, Sulaimaniya, Iraq,
wafaa.mustafa.sulicihan@edu.krd, asan.baker.sulicihan@edu.krd

solutions to problems that other optimization methods cannot handle due to a lack of continuity, derivatives, linearity, or other features. Genetic algorithm and neural networks are both inspired by computation in biological genetically. Neural networks and genetic algorithms are two techniques for optimization and learning, each having its own strengths and weaknesses. The two have generally evolved along separate paths. (Montana & Davis, 1989; Arjona, 1991; Whitley, 1995), The article investigates the role of crossover in GAs with respect to this problem, by using a comparative study between the iteration results obtained from changing the parameters values (crossover probability, mutation rate, population size and number of generation) system. A good deal of biological neural architecture is determined.

2. PROBLEM DEFINITION

Neural Networks (NN) are biologically motivated approaches to machine learning, inspired by ideas from neuroscience. Recently, some efforts have been made to use genetic algorithms to evolve aspects of NN. (Wright, 1991). A NN consists of layers of processing units called nodes joined by directional links: one input layer, one output layer, zero or more hidden layers in between, and finally, the NN uses bias nodes (in some problems, NN needs no bias nodes) (see Fig. 1).

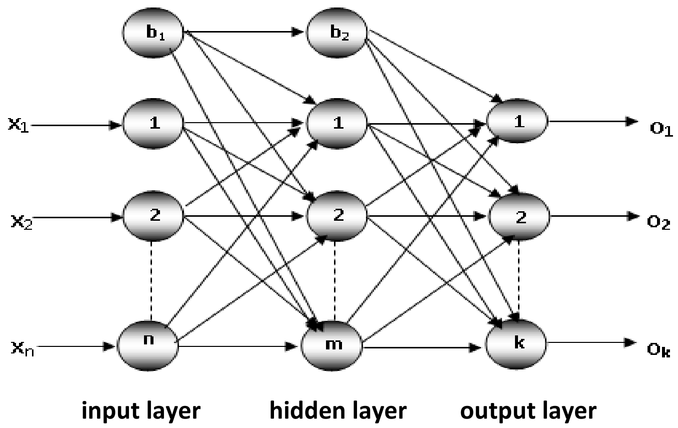

Fig. 1. A schematic diagram of a simple feed forward NN

(Montana & Davis, 1989) took the first approach of evolving the weights in a fixed network. They were using the GA instead of Back-Propagation algorithm and it is desirable to find alternative weight training scheme (Michalewicz, 1996). The simplest Boolean function that is not linearly separable, therefore, this problem cannot be solved by a neural net without the hidden neurons. Table 1 shows the desired relationships between input and output units for this function.

Tab. 1. Training pattern for Exclusive-OR (XOR)

Input		Desired Output
x_1	x_2	
0	0	**0**
0	1	**1**
1	0	**1**
1	1	**0**

3. PROBLEM REPRESENTATION

Each chromosome was a list or vector of 14 weights. Fig. 2 shows how the encoding was done: the weights were read off the network in a fixed order (from left to right and from top to bottom) and placed in a list. Notice that each "gene" in the chromosome is a real number rather than a bit.

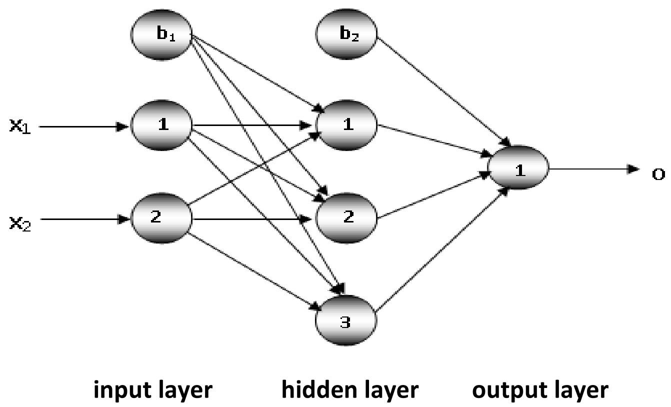

Fig. 2. 2-party XOR (2 – 3 – 1) NN

3.1. Initial Population

The genetic algorithm must create the initial population, which is comprised of multiple chromosome or solutions. An initial population of 13 weight vectors was chosen randomly, with each value based on the proper way to choose the weight W_{ij} in the range of $[-1,1]$ or $[-\frac{3}{\sqrt{k_i}}, \frac{3}{\sqrt{k_i}}]$, where k_i is the number of connection of j to that feed forward to i (the number of input links to i) (Whitley, Starkweather & Fuquay, 1989).

3.2. Evaluation Function

To calculate the fitness of a given chromosome, the weights in the chromosome were assigned to the links in the corresponding network, the network was run on the training set, and the sum of the squares of the errors (collected over all the training cycles) was returned. Here, an "error" was the activation value. The error here is the Mean Squared Error (*MSE*) which represents the square of the difference between the desired output (d_i) activation and actual output (a_i), where $1 \le i \le n$, n is the number of all possible output values.

$$MSE = \frac{1}{n}\sum_{i=1}^{n}(d_i - a_i)^2, \tag{1}$$

For the particular problem, $n = 4$.

Low *MSE* meant a high fitness. In another word, we can obtain the maximum fitness as follows:

$$Fit. = 1 - MSE \tag{2}$$

4. GENETIC OPERATORS

During the alteration phase of the algorithm, we will use the operators described below (Hameed, 2016; Hameed & Kanbar, 2017; Goldberg, 1989).

4.1. Selection Operator

The selection of individuals for crossover and mutation is based toward good individuals. In the classical fitness based roulette-wheel, the chance of an individual. The selected is based on its relative fitness in the population.

4.2. Crossover Operator

Crossover is the operator that creates new candidate solution, in this problem; we can say the One-Point crossover was used. A position is randomly chosen on the string and the two parents are crossed over at this point crossover is mapped, where this occurs at two points along the string.

4.3. Mutation Operator

The mutation operator used in this problem selects *n*-non input units and for each incoming link to those units, adds a random value between (–1.0) and (+1.0) to the weight on the link.

4. GENETIC PARAMETERS

For this particular problem, (Weisman & Pollack, 2002; Al-Inazy, 2005) used the following parameters: population size *popsize* = 20, probability of crossover *Pc* = 0.7, probability of mutation *Pm* = 0.001.

6. EXPERIMENTAL RESULTS

In table 2 we provide the generation number for which we noted improvement in the evaluation function, together with the value of the function. The best chromosome after 1000 generations was:
v_{max} = 2.1433; –2.6102; –0.2982; 4.4594; 4.5946; –0.1168; –4.0; –4.7712; –0.3300; 2.5095; –5.7542; 6.1160; 0.2693. Which is slightly less than 0.0111.

Tab. 2. Results of 1000 generations for evolving weights in NN

Generation number	Evolution function	Fitness
0	0.2610	0.7390
34	0.2457	0.7543
177	0.2195	0.7895
289	0.1883	0.8117
402	0.1325	0.8675
498	0.0861	0.9139
576	0.0364	0.9636
622	0.0262	0.9738
695	0.0159	0.9841
734	0.0121	0.9879
867	0.0111	0.9889

For this problem, a simulation has been constructed in order to apply the GA, using the crossover parameters mentioned above, the v_{min} value has many different sets of weights give *MSE* = 0.010, then the fit. value is 0.99.

7. THE EFFECT OF DIFFERENT TYPES OF CROSSOVER ON EVOLVING WEIGHTS OF XOR-NN PROBLEM

In this part, we will try to study the effect of applying different types of crossover on the reported algorithms, on their performance, speed, and ability to find the solution.

To see the effect of using different types of crossover operators on this problem, Weisman (Weisman & Pollack, 2002; Al-Inazy, 2005) used the Guaranteed Average crossover depending on the following parameters: Pc = 0.7, Pm = 0.001, $popsize$ = 20, NG = 1500. Table 3 describes the comparison study of the iterations results between the above crossover and the other kinds which are implemented on this problem. In addition, the table shows the average of iterations results for 10 runs.

Tab. 3. Comparison study of Guaranteed Average crossover and other kinds

Crossover	NG	Fitness
GUA	748	0.9900
ARITH	851	0.9881
DR	870	0.0868
HU	838	0.9900
EX	845	0.9882
IR	762	0.9900
LR	793	0.9900

From table 3, the average iterations results shows that the Guaranteed Average (followed by Intermediate Recombination and Line Recombination) is the best because when a = 0.5 this will makes approximate balance between the vectors x_1 and x_2. The Discrete Recombination is the worst because it generates corners of the hyper cube defined by the parents this may effect on the fitness value.

8. THE EFFECT OF DIFFERENT PARAMETERS ON CROSSOVER

The crossover is an extremely important component of a genetic algorithm. Many GA practitioners believe that if we delete the crossover operators from a GA the result is no longer a GA. In fact; many GA practitioners believe that the use of a crossover operator distinguishes GA from all other optimization algorithms. In this section we will try to study the effect of different genetic parameters on the performance of the proposed algorithms.

9. STUDYING THE EFFECT OF THE PROBABILITY OF CROSSOVER ON EVOLVING WEIGHTS OF XOR-NN PROBLEM

This operator owns a major role in GA, so specifying the probability of crossover, that should not be done randomly, but it must depend on many runs of the simulation to this problem, in order to tune this operator to obtain the fine probability of crossover. We will apply this operator with different values and so other operators. This problem, table 4 shows that the population size, the number of generation and the mutation rate are all fixed, while the crossover probability takes the values 0.0, 0.3, 0.5 and 0.8.

Tab. 4. Crossover probability effect when *NG* = 1000, *popsize* = 50, *Pm* = 0.001.

Crossover	Pc	Iteration	Max. Fit.	Min. Error
GUA	0.0	967	0.99	0.0
	0.5	800	0.99	0.0
	0.8	820	0.99	0.0
ARITH	0.0	980	0.99	0.0
	0.5	725	0.99	0.0
	0.8	646	0.99	0.0
DR	0.0	947	0.99	0.0
	0.5	836	0.99	0.0
	0.8	814	0.99	0.0
HU	0.0	988	0.99	0.0
	0.5	728	0.99	0.0
	0.8	706	0.99	0.0
EX	0.0	904	0.99	0.0
	0.5	911	0.99	0.0
	0.8	837	0.99	0.0
LR	0.0	955	0.99	0.0
	0.5	696	0.99	0.0
	0.8	835	0.99	0.0
IR	0.0	923	0.99	0.0
	0.5	887	0.99	0.0
	0.8	821	0.99	0.0

From table 4 we note the following analytic aspects:

1. The worst iteration results (high iteration levels) are be obtained when the effect of the crossover probability is eliminated (when *Pc* = 0.0).
2. In the most kinds of the used crossovers, including the Guaranteed Average crossover, the iteration results is be improved when using *Pc* = 0.5.
3. the results which appeared shows that the Guaranteed Average crossover, which is used previously, is better than the other operators, which are used to solve this problem.

10. STUDYING THE MUTATION RATE EFFECT ON CROSSOVER FOR EVOLVING WEIGHTS OF XOR-NN PROBLEM

This operator plays a dual role in genetic algorithm, it provides and maintains diversity in a population, so that other operators can continue to work and it can work as a search operator in its own right. We will apply this operator with different numbers of mutation rate and so other operators. In this problem, table 5 shows that the population size, the number of generation and the crossover probability are all fixed, while the mutation rate takes the values 0.0, 0.001 and 0.003.

Tab. 5. Mutation rate effect when *NG* = 1000, *popsize* = 50, *Pc* = 0.8.

Crossover	Pm	Iteration	Max. Fit.	Min. Error
GUA	0.0	888	0.99	0.0
	0.001	820	0.99	0.0
	0.003	1000	0.789	0.25
ARITH	0.0	798	0.99	0.0
	0.001	646	0.99	0.0
	0.003	1000	0.739	0.75
DR	0.0	815	0.99	0.0
	0.001	814	0.99	0.0
	0.003	1000	0.745	0.5
HU	0.0	824	0.99	0.0
	0.001	806	0.99	0.0
	0.003	1000	0.99	0.0
EX	0.0	807	0.99	0.0
	0.001	737	0.99	0.0
	0.003	1000	0.831	0.25
LR	0.0	745	0.99	0.0
	0.001	535	0.99	0.0
	0.003	1000	0.745	5.0
IR	0.0	878	0.99	0.0
	0.001	821	0.99	0.0
	0.003	1000	0.728	1.0
	0.003	**1000**	**0.728**	**1.0**

From table 5 we note the following analytic aspects:

1. When increasing the value of *Pm*, no positive results are gotten.
2. When using *Pm* = 0.001, the Line Recombination and Extended crossovers will give good results.

11. STUDYING THE EFFECT POPULATION SIZE ON CROSSOVER FOR EVOLVING WEIGHTS OF XOR-NN PROBLEM:

The operation which determines the population size is depending on the nature of the problem, that we require solving it. When increasing the complexity of search space, then it needs to a large population. In general, we cannot estimate the real size, but we can give the domain of it. In this operator we use different populations with other operators

In this problem, table 6 shows that the number of generation, the mutation rate and the crossover probability are all fixed, while the population size takes the values 20, 50 and 100.

Tab. 6. Population size effect when *NG* = 1000, *Pm* = 0.001, *Pc* = 0.8.

Crossover	popsize	Iteration	Max. Fit.	Min. Error
GUA	20	738	0.99	0.0
	50	520	0.99	0.0
	100	793	0.99	0.0
ARITH	20	877	0.99	0.0
	50	646	0.99	0.0
	100	1000	0.759	0.25
DR	20	810	0.99	0.0
	50	814	0.99	0.0
	100	1000	0.896	0.0
HU	20	881	0.99	0.0
	50	706	0.99	0.0
	100	851	0.738	0.75
EX	20	909	0.99	0.0
	50	737	0.99	0.0
	100	957	0.99	0.0
LR	20	772	0.99	0.0
	50	635	0.99	0.0
	100	850	0.944	0.0
IR	20	846	0.99	0.0
	50	821	0.99	0.0
	100	1000	0.897	0.0

From table 6 we note the following analytic aspects:

1. For most kinds of the used crossovers, the best results obtained when *popsize* parameter equals 50.
2. The best two crossover operators from all kinds of the used crossovers are the Guaranteed Average and Line Recombination crossovers.

12. STUDUING THE EFFECT OF NUMBER OF GENERATION ON CROSSOVER FOR EVOLVING WEIGHTS OF XOR-NN PROBLEM

In this problem, table 7 shows that the population size, the mutation rate and the crossover probability are all fixed, while the number of generation takes the values 500, 1000 and 1500.

Tab. 8. Number of generation effect when *popsize* = 50, *Pm* = 0.001, *Pc* = 0.8.

Crossover	NG	Iteration	Max. Fit.	Min. Error
GUA	500	500	0.90	0.0
	1000	820	0.99	0.0
	1500	752	0.99	0.0
ARITH	500	500	0. 738	0.75
	1000	646	0.99	0.0
	1500	776	0.99	0.0
DR	500	500	0.739	0.75
	1000	814	0.99	0.0
	1500	756	0.99	0.0
HU	500	500	0.824	0.25
	1000	806	0.99	0.0
	1500	824	0.99	0.0
EX	500	500	0.743	0.5
	1000	737	0.99	0.0
	1500	764	0.99	0.0
LR	500	500	0.879	0.0
	1000	535	0.99	0,0
	1500	699	0.99	0.0
IR	500	500	0.803	0.25
	1000	821	0.99	0.0
	1500	803	0.99	0.0

From tables 6, 7 and 8 we note the following analytic aspects:

1. It is important to mention that, there is a relation between the execution time and the control parameters (number of generation and population size).
2. In XOR Problem by NN, there is no solution to be obtained, when the low levels of generation (NG = 500) are to be chosen.

13. PARAMETRIC STUDY FOR ALL CROSSOVER OPERATORS

From our experiences and experimental results, the best parameters values for all crossover kinds are chosen to make a comparative study for each kind of crossover, for Evolving Weights of Xor-Nn problem and for several runs. The minimum iteration results are shown in tables with statistical diagram to illustrate these results.

For this problem, the best values are: when *NG* = 1000, *popsize* = 50, *Pm* = 0.001 and *Pc* = 0.5. Table 9 shows the comparison between iterations results for 10 runs and Fig. 3 Illustrates the statistical diagram of the comparison study results.

Tab. 9. Comparison study of crossover iterations results for evolving weights of XOR-NN problem

Crossover	NG	Fitness
GUA	816	0.9900
ARITH	871	0.9868
DR	882	0.0881
HU	850	0.9900
EX	872	0.9880
IR	879	0.9882
LR	775	0.9900

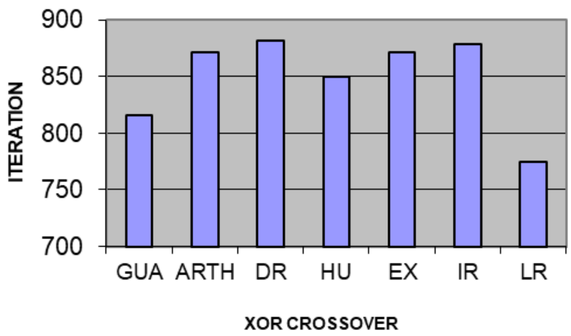

Fig. 3. Statistical diagram of the comparison study results for evolving weights of XOR-NN problem

In this particular problem, from table 9 and Fig. 3, we notes that the operator is the Line Recombination because its selects only one value of the alpha that is generates any point on the line define by the parents and keep the values of chromosome closed to each other.

14. CONCLUSIONS

This research concludes the following points. For evolving weights of XOR-NN problem, the Line Recombination was the best to be applied. For the parametric study, the research concludes: The worst iteration results (high iteration levels) are obtained when the effect of the crossover probability is eliminated (when $Pc = 0.0$), since the search in this state is closed to the random search. For the population size parameters, the result reveals that due to the founder effect, the GA's cannot always locate the peaks of the fitness landscape, even with higher crossover rate. Although, the mutation rate parameter preferred to be chosen as minimum as possible ($Pm \leq 0.01$), but it is still related to the problem which is discussed. It's natural that, there is a relation between the number of generation and population size. This parameter specification is related to the problem which is discussed.

REFERENCES

Al-Inazy, Q. A. (2005). *A Comparison between Lamarckian Evolution and Behavior Evolution of Neural Network* (Unpublished M.Sc. Thesis). Al- Mustansriyah University, Baghdad, Iraq.

Arjona, D. (1996). A hybrid artificial neural network/genetic algorithm approach to on-line operations for the optimization of electrical power systems. In *IECEC 96. Proceedings of the 31st Intersociety Energy Conversion Engineering Conference* (pp. 2286–2290 vol. 4). Washington, DC, USA. doi:10.1109/IECEC.1996.561174

Goldberg, D. E. (1989). *Genetic Algorithms in search, Optimization, and Machine Learning*. Boston, MA, USA: Addison–Wesley Longman Publishing Co., Inc.

Koza, J. R. (1992). *Genetic programming: on the programming of computers by means of natural selection.* Cambridge, MA, USA: MIT Press.

Michalewicz, Z. (1996). *Genetic Algorithm + Data Structure = Evolution Programs*, 3rd Revised Extended Edition. New York, USA: Springer – Verlag Berlin Heidelberg.

Mitchell, M. (1998). *An Introduction of Genetic Algorithms*. Cambridge, MA, USA: MIT Press.

Montana, D., & Davis, L. (1989). Training Feed Forward neural networks using Genetic Algorithms, In *IJCAI'89 Proceedings of the 11th international joint conference on Artificial intelligence* (pp. 762–767). San Francisco, CA, USA: Morgan Kaufmann Publishers Inc.

Hameed, W. M., & Kanbar, A. B. (2017). A Comparative Study of Crossover Operators for Genetic Algorithms to Solve Travelling Salesman Problem. *International Journal of Research – Granthaalayah, 5*(2), 284–291. doi:10.5281/zenodo.345734

Hameed, W. M. (2016). The Role of Crossover on Optimization of a Function Problem Using Genetic Algorithms. *International Journal of Computer Science and Mobile Computing, 5*(7), 425–429.

Weisman, O., & Pollack, Z. (2002). *Neural Networks Using Genetic Algorithm*. Retrieved from http://www.cs.bgu.ac.il/NNUGA.

Whitley, D., Starkweather, T., & Fuquay, D. A. (1989). Scheduling Problems and Traveling Salesman: The Genetic Edge Recombination Operator. *ICGA*.

Whitley, D. (1995). Genetic Algorithms and Neural Networks. In J. Periaux & G. Winter (Eds.), *Genetic Algorithms in Engineering and Computer Science* (pp. 191-201). John Wiley & Son Corp.

Wright, A. H. (1991). Genetic Algorithms for Real Parameters Optimization. *Foundation of Genetic Algorithms*, *1*, 205-218. doi:10.1016/B978-0-08-050684-5.50016-1

Applied Computer Science, vol. 15, no. 3, pp. 34–44
doi:10.23743/acs-2019-19

Submitted: 2019-08-04
Revised: 2019-08-27
Accepted: 2019-09-02

EMD, EEMD, knee joint, vibration, kinetic chain

Anna MACHROWSKA [0000-0003-3289-2421]*,
Robert KARPIŃSKI [0000-0003-4063-8503]*,
Przemysław KRAKOWSKI [0000-0001-7137-7145]** ,
Józef JONAK[0000-0003-4658-4569]*

DIAGNOSTIC FACTORS FOR OPENED AND CLOSED KINEMATIC CHAIN OF VIBROARTHROGRAPHY SIGNALS

Abstract

The paper presents results of preliminary research of vibroarthrography signals recorded from one healthy volunteer. The tests were carried out for the open and closed kinematic chain in the range of motion 90° – 0° – 90°. Analysis included initial signal filtration using the EMD algorithm. The aim was to investigate the occurrence of differences in the values of selected energy and statistical parameters for the cases studied.

1. INTRODUCTION

Anterior knee pain can be caused by multiple factors and is one of the most common complaints of the patients (Powers, Bolgla, Callaghan, Collins & Sheehan, 2012). However, etiology of the condition is still controversial (Sanchis-Alfonso, 2014). Chondromacia of articular cartilage in patellofemoral joint as well as increased forces in the joint are the most common causes of the pain (Sanchis-Alfonso & Dye, 2017). Up to this date there is no simple, fast, accessible and reproducible diagnostic modality to detect chondral lesions in patellofemoral joint. Vibroarthrography in future might bring a solution to this problem, however up to this date there is no standardized protocol of examination especially regarding patellofemoral joint.

* Lublin University of Technology, Faculty of Mechanical Engineering, Department of Machine Design and Mechatronics, , Nadbystrzycka 36, 20-618 Lublin, Poland, a.machrowska@pollub.pl, r.karpinski@pollub.pl, j.jonak@pollub.pl
** Orthopedic Department, Łęczna Hospital, Krasnystawska 52, 21-010 Łęczna, Poland

Open and closed kinetic chain in exercises is the terms introduced by Steindler in 1955 (Charnley, 1955). From that time, attention was brought to the stress distribution in knee joint during certain exercises. In closed kinetic chain distal segment of the limb is opposed by “considerable resistance” whereas in open kinetic chain the distal part of the limb is free to move without additional resistance. Closed kinetic chain exercises such as squats or leg presses imitate physiological movement patterns and involve cooperation between various muscle groups. In open kinetic chain it is possible to isolate one muscle group which needs strengthening. Therefore open and closed kinetic chain generates different loading patterns on patella-femoral and tibio-femoral joints (Adouni & Shirazi-Adl, 2009; Barcellona & Morrissey, 2016). Great attention was put into this phenomenon in relation to rehabilitation after ligamentous reconstructions, or anterior knee pain due to its stress distributions (Cohen et al., 2001; Luque-Seron & Medina-Porqueres, 2016; Witvrouw, Danneels, van Tiggelen, Willems, & Cambier, 2004). Stress distribution differs in patellofemoral joint during open and closed kinetic chain exercises depending on flexion angle of the joint (Cohen et al., 2001). In clinical setting open kinetic chain is easier to perform on standard examination, however up to this date, there is insufficient information about the differences in vibroacoustic signals emitted by patellofemoral joint in open and closed kinetic chain. Moreover, it is not known whether open or closed kinetic chain provides more accurate evaluation of anterior compartment of the knee joint (Karpiński, Machrowska, & Maciejewski, 2019).

The aim of the work was to determine statistical and energy indicators characterizing vibroartrographic signals for an open and closed kinematic chain.

2. EMPIRICAL MODE DECOMPOSITION

Vibroarthrography (VAG) signals are inherently nonlinear and non-stationary. Failure in proper method and approach selection will invariably result in improper results and conclusion, which is further amplified due to complex and sensitive character of medical data as a whole (Maciejewski, 2015; Maciejewski, Surtel, & Dzida, 2015). Therefore, modern methods should be used for the analysis, allowing for proper interpretation of the results. A characteristic feature of the recorded VAG signals is the clear presence of low- frequency artifacts, which are the source of muscle tension, obtained during the tests (Luque-Seron & Medina-Porqueres, 2016). The methodology of knee joint state tests forces the limbs to flex and straighten, so it is not possible to exclude co-occurrence of muscle origin signals. For more accurate analysis of nonlinear and non- stationary VAG signals, the Empirical Mode Decomposition (EMD) algorithm was used. It allows the analysis of individual filtered signal components.

EMD is a popular signal processing method for the extraction of oscillation modes (Machrowska & Jonak, 2018). An unquestionable advantage of the algorithm is the possibility of using nonlinear and non- stationary input signals. The discussed tool has found a number of applications (Alickovic, Kevric & Subasi, 2018; Jonak, Machrowska, Podgórski & Bęc, 2016; Kolotkov, Anfinogentov & Nakariakov, 2016; Yaslan & Bican, 2017). As a part of the EMD procedure, the input signal is decomposed to a finite number of internal IMF (Intrinsick Mode Functions) components and a residual signal. The algorithm obtaining algorithm is based on the filtration process (sifting). In the input signal $x_1(t)$ local extremes are identified, then the signal envelope is constructed using interpolation with third order split functions (cubic spline). At each signal point, the average $m_1(t)$ and the difference between the input data $x(t)$ are determined (Huang et al., 1998):

$$h_1(t) = x(t) - m_1(t). \tag{1}$$

The $h_1(t)$ function is called intrinsic function (IMF) when it meets two conditions:

(1) In the selected set of data, the number of extremes and the number of zero crossings of the function are equal to or differ at most by one,
(2) At each point, the envelope's mean value defined by local maxima and minima is zero.

Sifting procedure is repeated k times, where $h_k(t)$ is given as an updated input signal:

$$h_k(t) = h_{k-1}(t) - m_k(t). \tag{2}$$

The filtration process is stopped when the condition of equality of zero crossings and local extremes is met. A residual signal $r_n(t)$ is then determined:

$$r_n(t) = x(t) - \sum_{i=1}^{n} c_i\,(t), \tag{3}$$

where $c_i(t)$ is the i^{th} internal function of IMF, while n is the highest possible number of modal oscillations. The residual signal $r_n(t)$ is then treated as an input signal for subsequent iterations. The sifting process is continued until the stoppage criterion is met. The basic condition for stopping is limitation of the standard deviation, determined for two successive results of the screening process. It is obtained on the basis of the equation (Huang et al., 1998):

$$SD = \frac{\sum_t |h_{i,k-1}(t) - h_{i,k}(t)|^2}{\sum_t h_{i,k-1}^2(t)}. \tag{4}$$

The sifting process ends when the SD value is less the pre-established initial one.

3. MATHERIALS AND METHODS

The test were performed on a 23 years old white Caucasian male without knee joint disorders. The vibroartrographic signal was recorded using a three-axis, miniature accelerometer sensor with Analog Devices ADXL325 analog output from the measuring range ± 5g per axis. The signal was sampled at 1000 Hz using an Texas Instruments analog measuring card connected to a PC. The sensor was attached to the skin using a double-sided adhesive tape about 1 cm above the top of the patella. The examination was carried out in a sitting position. The examined person had the task of extending and bending the raised limb in the range of 90° – 0° – 90° (OKC). The study of motion in a closed kinetic chain (CKC) included alternating standing up and sitting on a chair (movement in the range of 90° – 0° – 90°). The diagram showing the directions of distribution of individual axes is shown in Figure 1.

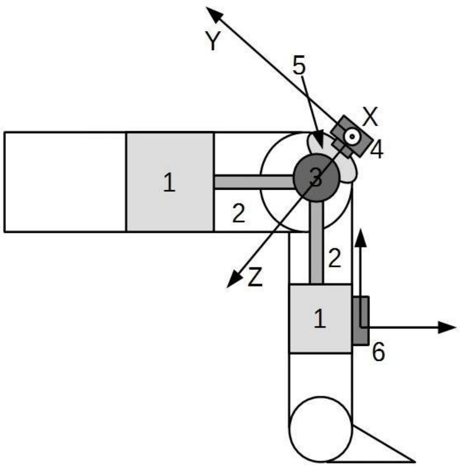

Fig. 1. Distribution of individual axes accelerometer sensor

4. RESULTS

Signal from the X axis resembles a sinusoidal waveform, for closed kinematic chain (CKC), the rise and fall times of the pulse slopes (movement in the concentric phase- muscle shortening and eccentric- muscle straightening) are definitely longer than for open kinematic chain (OKC). Above relationship is related to the longer motion range of the squatting with the CKC. The motion phases are also visible for the signal recorded in the Z axis. In the case of CKC, there are noticeable oscillations on the pulse crest, characteristic for knee locking after the concentric squat phase (Fig. 2 and Fig. 3). On the issue of OKC oscillations on the pulse top are not so regular due to the fact of a short- term isometric contraction in the in the final movement phase (full extension of the limb). Mentioned vibrations are reflected in 3rd and 4th IMFs. High frequency IMFs 1st and the 2nd, on the other hand, shows filtered vibrations of the knee joints, crossed by unconsolidated peaks associated with the friction phenomenon, analogous to the slide bearings surfaces. The lower frequency IMFs do not have such a significant physical meaning.

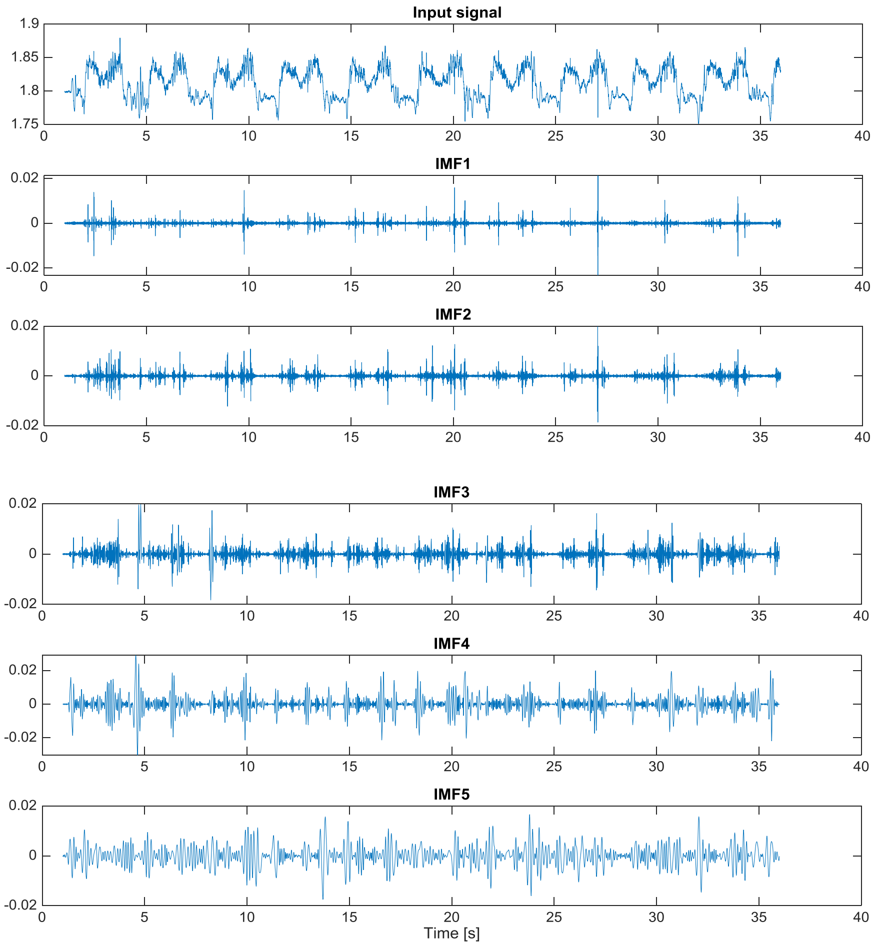

Fig. 2. Z axis – CKC

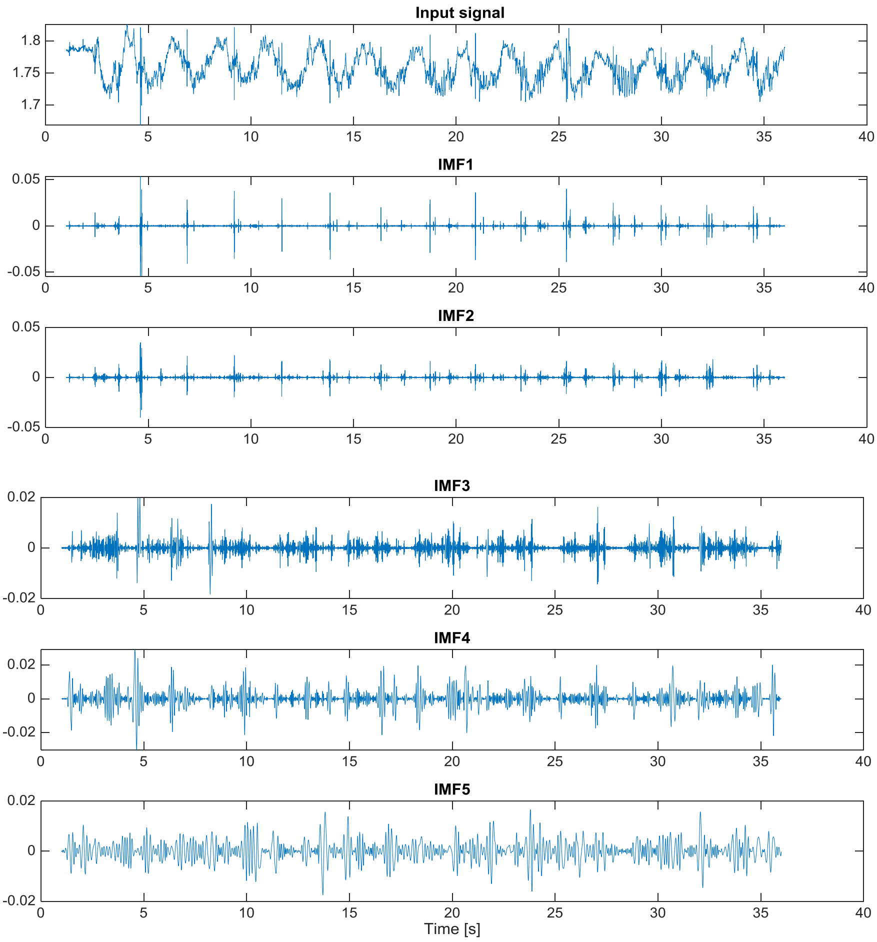

Fig. 3. Z axis – OKC

Signal energy is one of the most import ant factors to describe the signal. Values of signals energy for X axis is shown on figure 4. At higher frequencies, the energy values differ only slightly between OKC and CKC. In the lower frequency ranges (from IMF 6 up to 25 Hz) a closer differentiation of the signal energy value is visible. For the OKC energy values in the range of 10–25 Hz (IMF 6 and 7) are higher than for the CKC. The inverse relationship occurs at very low frequencies (from IMF 8).

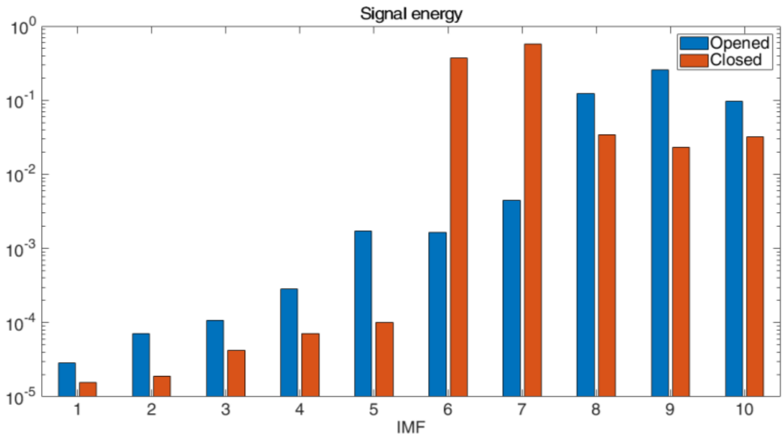

Fig. 4. X axis – signal energy for OKC and CKC

In the case of Y axis (Fig. 5), the highest signal energy values are observed in IMFs 5, 6 and 7 (15–30 Hz). In case of CKC, visible is tendency to taking higher values for higher frequency ranges in comparison to OKC. Thus the relationship between the transmission of joint structures vibration and type of kinematic chain is visible.

For Z axis (Fig. 6) higher values of the selected indicator are observed at low frequencies (IMF 7, 8 and 9), while the dependence of the occurrence of higher values for OKC is no longer as pronounced as for axes X and Y. There are no clear dominance of energy values for CKC in higher frequencies due to the sensor location.

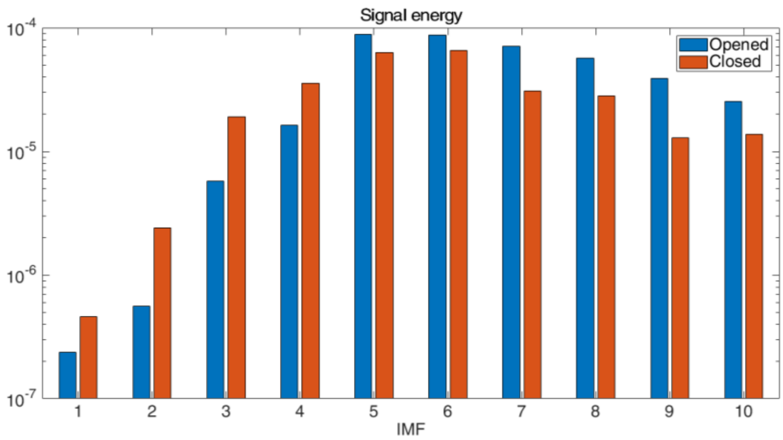

Fig. 5. Y axis – signal energy for OKC and CKC

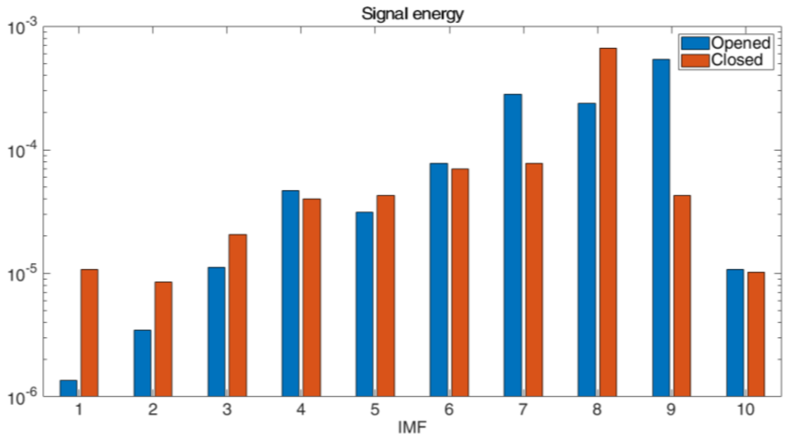

Fig. 6. Z axis – signal energy for OKC and CKC

Standard deviation parameter shows the scale of results scattering around the mean. Data from X axis (Fig. 7) are clearly more diverse for lower frequencies (IMF 6–10). For Y axis (Fig. 8) at higher frequencies (IMF 1–4), higher standard deviation values occur for CKC. The inverse relationship (higher standard deviation values for CKC) is visible in the lower frequency ranges (IMF 5–10). Above dependencies are not so clear the Z axis (Fig. 9) – higher indicator values can be only seen for higher frequencies (IMF 1–3), while for low frequencies the inverse relationship cannot be confirmed.

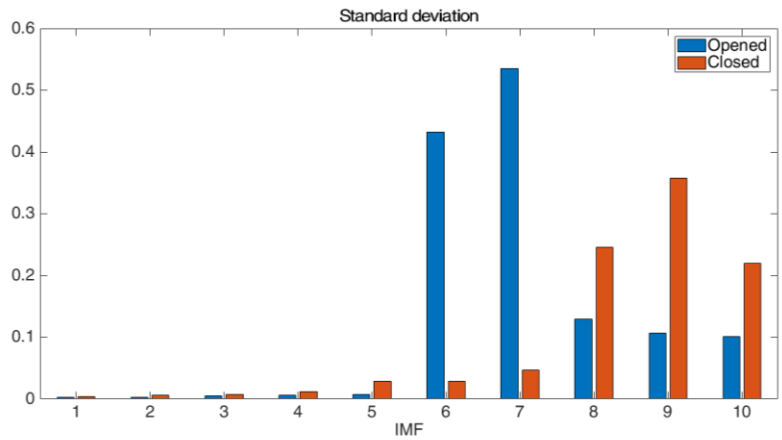

Fig. 7. X axis – standard deviation parameter for OKC and CKC

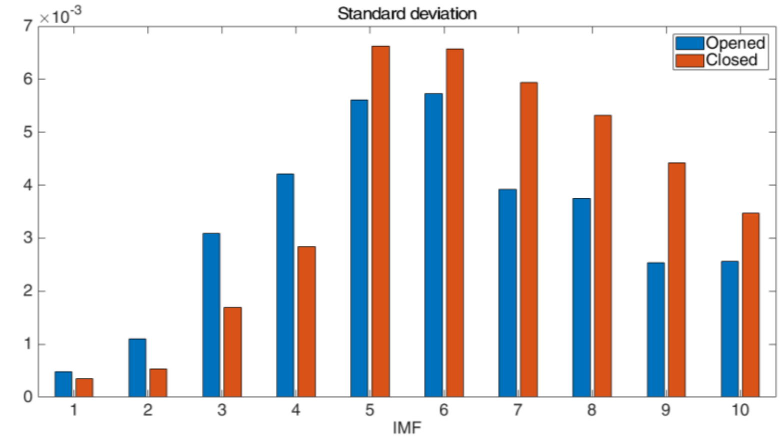

Fig. 8. Y axis – standard deviation parameter for OKC and CKC

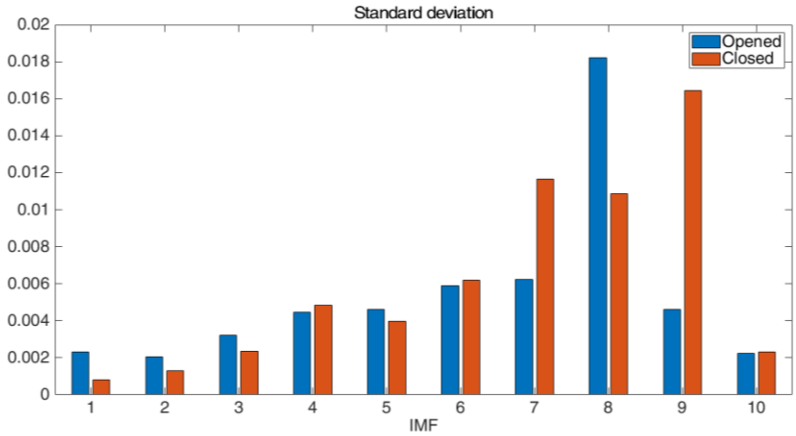

Fig. 9. Z axis – standard deviation parameter for OKC and CKC

5. CONCLUSIONS

The analysis of selected indicators of energy and statistical parameters allows to show the differences between the open and closed kinematic chain. An important factor is the correct positioning of the vibration sensor with the selection of the proper orientation of the sensor axis relative to the anatomical location (minimizing the attenuation of soft tissue and maximum use of bone conduction.)

The higher the signal energy at low frequencies in the Z axis for waveforms recorded in a closed kinematic chain due to the greater impact of vibration standard deviation takes higher values for signals recorded in the open kinetic chain.

The results obtained show that analysis in both the open and closed kinetic chains is important. Signal analysis for the open chain provides information related to the work of the unloaded limb, which allows a more accurate analysis of the functioning of cartilage structures due to the lower effect of muscle tension at high frequencies. In contrast, signal analysis for a closed kinetic chain provides us with information about the work of an anatomically loaded limb in real operating conditions.

Demonstrating the differences between the closed and open kinematic chains allows in the future a more accurate analysis and distinction of structures generating a vibroacoustic signal, which will allow analysis targeted at specific joint structures. Thanks to this analysis, it will be possible to assess the knee joint movement during walking, where signals generated by the open and closed kinematic chains overlap during walking.

REFERENCES

Adouni, M., & Shirazi-Adl, A. (2009). Knee joint biomechanics in closed-kinetic-chain exercises. *Computer Methods in Biomechanics and Biomedical Engineering*, *12*(6), 661–670. doi:10.1080/10255840902828375

Alickovic, E., Kevric, J., & Subasi, A. (2018). Performance evaluation of empirical mode decomposition, discrete wavelet transform, and wavelet packed decomposition for automated epileptic seizure detection and prediction. *Biomedical Signal Processing and Control*, *39*, 94–102. doi:10.1016/j.bspc.2017.07.022

Barcellona, M. G., & Morrissey, M. C. (2016). The effect of open kinetic chain knee extensor resistance training at different training loads on anterior knee laxity in the uninjured. *Manual Therapy*, *22*, 1–8. doi:10.1016/j.math.2015.12.011

Charnley, J. (1955). Kinesiology of the human body under normal and pathological conditions. *The Journal of Bone and Joint Surgery. British Volume*, *37–B*(4), 736–737. doi:10.1302/0301-620X.37B4.736

Cohen, Z. A., Roglic, H., Grelsamer, R. P., Henry, J. H., Levine, W. N., Van Mow, C., & Ateshian, G. A. (2001). Patellofemoral Stresses during Open and Closed Kinetic Chain Exercises: An Analysis Using Computer Simulation. *The American Journal of Sports Medicine*, *29*(4), 480–487. doi:10.1177/03635465010290041701

Huang, N. E., Shen, Z., Long, S. R., Wu, M. C., Shih, H. H., Zheng, Q., Yen, N.-Ch., Tung, Ch. Ch., & Liu, H. H. (1998). The empirical mode decomposition and the Hilbert spectrum for nonlinear and non-stationary time series analysis. *Proceedings of the Royal Society of London. Series A: Mathematical, Physical and Engineering Sciences*, *454*(1971), 903–995. doi:10.1098/rspa.1998.0193

Jonak, J., Machrowska, A., Podgórski, J., & Bęc, J. (2016). Identification of the operating parameters for the mechanical systeIdentification system using EMD algorithm. *MATEC Web of Conferences*, *83*, 05001. doi:10.1051/matecconf/20168305001

Karpiński, R., Machrowska, A., & Maciejewski, M. (2019). Application of acoustic signal processing methods in detecting differences between open and closed kinematic chain movement for the knee joint. *Applied Computer Science*, *15*(1), 36–48. doi:10.23743/acs-2019-03

Kolotkov, D. Y., Anfinogentov, S. A., & Nakariakov, V. M. (2016). Empirical mode decomposition analysis of random processes in the solar atmosphere. *Astronomy & Astrophysics*, *592*, A153. doi:10.1051/0004-6361/201628306

Luque-Seron, J. A., & Medina-Porqueres, I. (2016). Anterior Cruciate Ligament Strain In Vivo: A Systematic Review. *Sports Health: A Multidisciplinary Approach*, *8*(5), 451–455. doi:10.1177/1941738116658006

Machrowska, A., & Jonak, J. (2018). xEMD procedures as a data – Assisted filtering method. *AIP Conference Proceedings*, *1922*, 120007. doi:10.1063/1.5019122

Maciejewski, M. (2015). Zastosowanie i ograniczenia technologii informacyjnych w diagnostyce medycznej. *Informatyka, Automatyka, Pomiary w Gospodarce i Ochronie Środowiska*, *1*, 66–72.

Maciejewski, M., Surtel, W., & Dzida, G. (2015). Human ECG signal parameters estimation during controlled physical activity. In R. S. Romaniuk (Ed.), *Proc. SPIE 9662, Photonics Applications in Astronomy, Communications, Industry, and High-Energy Physics Experiments* (96621P). doi:10.1117/12.2205811

Powers, C. M., Bolgla, L. A., Callaghan, M. J., Collins, N., & Sheehan, F. T. (2012). Patellofemoral Pain: Proximal, Distal, and Local Factors—2nd International Research Retreat, August 31–September 2, 2011, Ghent, Belgium. *Journal of Orthopaedic & Sports Physical Therapy*, *42*(6), A1–A54. doi:10.2519/jospt.2012.0301

Sanchis-Alfonso, V. (2014). Holistic approach to understanding anterior knee pain. Clinical implications. *Knee Surgery, Sports Traumatology, Arthroscopy*, *22*(10), 2275–2285. doi:10.1007/s00167-014-3011-8

Sanchis-Alfonso, V., & Dye, S. F. (2017). How to Deal With Anterior Knee Pain in the Active Young Patient. *Sports Health: A Multidisciplinary Approach*, *9*(4), 346–351. doi:10.1177/1941738116681269

Witvrouw, E., Danneels, L., van Tiggelen, D., Willems, T. M., & Cambier, D. (2004). Open versus Closed Kinetic Chain Exercises in Patellofemoral Pain: A 5-Year Prospective Randomized Study. *The American Journal of Sports Medicine*, *32*(5), 1122–1130. doi:10.1177/0363546503262187

Yaslan, Y., & Bican, B. (2017). Empirical mode decomposition based denoising method with support vector regression for time series prediction: A case study for electricity load forecasting. *Measurement*, *103*, 52–61. doi:10.1016/j.measurement.2017.02.007

Applied Computer Science, vol. 15, no. 3, pp. 45–55
doi:10.23743/acs-2019-20

Submitted: 2019-09-10
Revised: 2019-09-19
Accepted: 2019-09-23

manufacturability, fuzzy logic

Józef MATUSZEK [0000-0003-1668-6329]*, *Tomasz SENETA**,
Aleksander MOCZAŁA [0000-0001-8001-7109]*

FUZZY ASSESSMENT OF MANUFACTURABILITY DESIGN FOR MACHINING

Abstract

The article attempts to assess the manufacturability design taking into account the assessment due to the processing, assembly process and organization of production. The evaluation was conducted by the fuzzy inference methods. An assessment was presented for machining based on the proposed fuzzy inference database.

1. INTRODUCTION TO APPLICATION METHODS FOR FUZZY SETS

Knowledge representation in the fuzzy rule-based system is enhanced by the use of linguistic variables and the language of their values, which are defined by context-dependent fuzzy sets, which determine the importance of a gradual membership function (Zadeh, 1965). On the other hand, fuzzy set inference methods, such as generalized Modus Ponens, generalized Modus Tollens, etc., form the basis for approximate inference (Zadeh, 1975). Therefore, fuzzy logic provides a unique framework for inference computational systems based on rules. This idea suggests the presence of two clearly different concepts in the inference methods of fuzzy sets: knowledge and reasoning. This clear separation of knowledge and reasoning (knowledge base) and processing structure is a key aspect of knowledge-based systems, so from this point of view fuzzy set inference methods can be considered a kind of knowledge-based system. The methods of inference of fuzzy sets in which two input variables (x1 and x2) and a single output variable (s) are involved, for example, sets of terms are related as follows: {small, medium, large}, {short, medium, long} and {bad, medium, good}.

* University of Bielsko-Biala, Faculty of Mechanical Engineering and Computer Science, Willowa 2, 43-309 Bielsko-Biała, Poland, jmatuszek@ath.bielsko.pl, tomasz.seneta@zf.com, amoczala@ath.bielsko.pl

The following base rule consists of five linguistic rules:

- R1W IF X1 is small and X2 is short, THEN Y is bad,
- R2W IF X1 is small and X2 is medium, then Y is bad,
- R3W IF X1 is medium and X2 is short, THEN Y is medium,
- R4W IF X1 is large and X2 is medium, THEN Y is medium,
- R5W IF X1 is large and X2 is long and Y is good.

The above method of inference can be represented by the decision table shown in Table 1.

Tab.1. Example table decision

	x1		
x2	small	medium	large
short	bad	medium	
medium	bad		medium
long			good

The Mamdani method (Fernández & Herrera, 2012) processing structure of fuzzy set inference consists of the following five elements – Fig. 1:

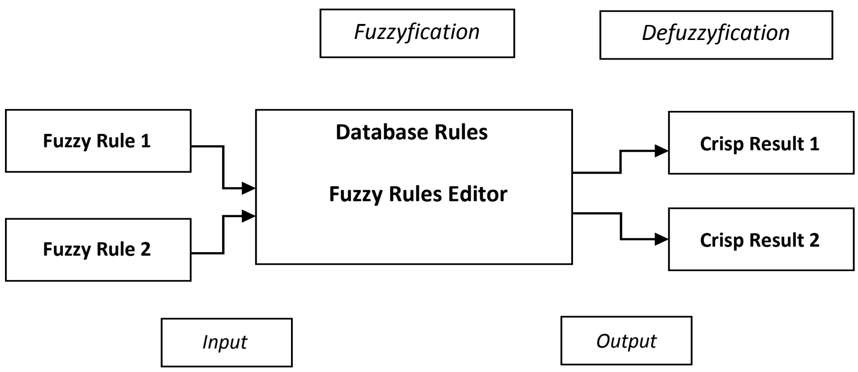

Fig. 1. Structure of the basic fuzzy model

- Input scaling that transforms parameter values – enter variables from its domain to the one in which the input fuzzy partitions are defined,
- A fuzzy interface that transforms explicit input into fuzzy values that serve as input to the fuzzy inference process,
- An inference engine that extracts data from blurry input data into several resulting fuzzy sets according to the information stored in the knowledge base,

– Defuzzification interface that converts fuzzy sets received from the inference process into a clear value,
– Output scaling that converts defragmented value from the output domain of fuzzy areas to output variables, creating a global result of the fuzzy set inference method.

Defuzzification (sharpening) is an action to provide the predicted value of a parameter. ***The center of gravity method*** consists in determining the value of y^*, which is the center of gravity of the area under the curve $\mu_{wyn}(y)$.

$$y^* = \frac{\int y \cdot \mu_{wyn}(y)dy}{\int \mu_{wyn}(y)dy} \tag{1}$$

The project reference model is of the type: multiple entries – multiple outputs (multiple input-multiple output MIMO).

2. FUZZY ASSESSMENT OF MANUFACTURABILITY

2.1. General description of the variables

A set of linguistic variables $V_i = \{V_1, ..., V_n\}$, and $\in N - \{0\}$ is given, defining input and output criteria of technology.The linguistic variable V_i is described by the quadrangle $[L_i, T_i(L), \Omega_i, M_i]$ where:

– $L_i = \{L_1, ..., L_n\}$, and $\in N - \{0\}$ is a set of linguistic variable names,
– $T_i(L_i) = \{T_1(L_1), ..., T_n(L_n)\}$, and $\in N - \{0\}$ is a set of countable determinations of linguistic variables,
– $t_{ij} = \{t_{11}, t_{12}, ..., t_{nm}\}$, $i, j \in N - \{0\}$, $t_{ij} \in T_i(L_i)$ is set of linguistic values of linguistic variables,
– $\Omega_i = \{\Omega_1, ..., \Omega_n\}$, $i \in N - \{0\}$ is a set of linguistic ranges of V_i variables,
– $M_i = \{M_i, ..., M_n\}$, $i \in N - \{0\}$ is a set of semantic rules,
– $m_{ij} = \{m_{11}, m_{12}, ..., m_{mn}\}$, $i, j \in N - \{0\}$, $m_{ij} \in M_i$ is a range of variation of the linguistic value t_{ij} with an assessment of belonging from 0 to 1.

2.2. Procedure – list of variables

The fuzzy method course of action results from project management schemes adopted according to PMI – according to AIAG (Kuo, Huang & Zhang, 2001). Assessment of machining processability and subsequent assembly process assessment, correspond to the prototyping phase during product design and development (Lalaoui & El Afia, 2018), and the assessment of the production organization technology corresponds to the pilot series and preserver phase during validation and then serial production (Favi, Germani & Mandolini, 2016).

In terms of manufacturability processing variables being indicators evaluating product design for the future feasibility of the machining technology (Deka & Behdad, 2019) and compliance with selected requirements – Fig. 2:

- V_1 – Technological Capabilities of the Machine Park/Accuracy,
- V_2 – CAD/CAM Software Capability,
- V_3 – Machining Capabilities of Available Tools,
- V_4 – Material meeting the project requirements,
- V_5 – Energy Consumption,
- V_6 – Waste Environmental Aspects.

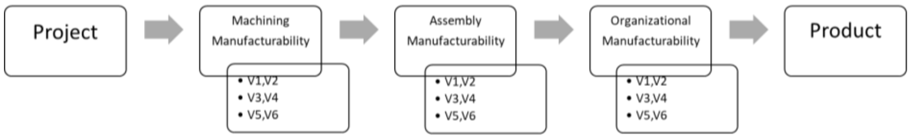

Fig. 2. Procedure – list of variables

In terms of manufacturability assembly (Matuszek & Seneta, 2017) variables being indicators evaluating product design for the feasibility of installation in accordance with the principles assemblability and shortest installation time :

- V_1 – Access,
- V_2 – Maneuverability,
- V_3 – Orientation,
- V_4 – Maneuverability,
- V_5 – Assemblability,
- V_6 – Processes.

In terms of manufacturability organization of production variables being indicators evaluating product design in terms of organizational and technical capabilities, quality and maintenance (Matuszek, Seneta & Moczała, 2018):

- V_1 – Disassembly,
- V_2 – Reuse,
- V_3 – Standardization of components,
- V_4 – Target cost,
- V_5 – Mounting quality,
- V_6 – Number of special elements in maintenance.

Sets of V_i variables can be modified and changed depending on the nature of the target process for which we design the product. This gives the fuzzy method a significant advantage in terms of flexibility. In the example presented, the set of variables V_i was prepared for medium-sized plant and small-lot production.

3. EVALUATION OF MACHINING MANUFACTURABILITY

3.1. The manufacturability evaluation processing procedure

An example of the assessment of machinability of processing consists of three sub-stages of analysis for which linguistic variables are described in Table 2:

Tab. 2. Sub-stages of machining efficiency evaluation - linguistic variables Sub-step 1

V_i	L_i	$T_i(L_i)$	t_{ij}	Ω_i	M_i
V_1	Technological Capabilities of the Machine Park/Accuracy	$T_1(L_1)$	t_{11} – unfulfilled t_{12} – deviates significantly t_{13} – deviates slightly t_{14} – fully meets	[0–4]	M_1
V_2	CAD/CAM Software Capability	$T_2(L_2)$	t_{21} – unfulfilled t_{22} – deviates significantly t_{23} – deviates slightly t_{24} – fully meets	[0–4]	M_2

Substage 2

V_i	L_i	$T_i(L_i)$	t_{ij}	Ω_i	M_i
V_3	Machining Capabilities of Available Tools	$T_3(L_3)$	t_{31} – unfulfilled t_{32} – deviates significantly t_{33} – deviates slightly t_{34} – fully meets	[0–4]	M_3
V_4	Material meeting the project requirements	$T_4(L_4)$	t_{41} – unfulfilled t_{42} – deviates significantly t_{43} – deviates slightly t_{44} – fully meets	[0–4]	M_4

Substage 3

V_i	L_i	$T_i(L_i)$	t_{ij}	Ω_i	M_i
V_5	Energy consumption	$T_5(L_5)$	t_{51} – unfulfilled t_{52} – deviates significantly t_{53} – deviates slightly t_{54} – fully meets	[0–10]	M_5
V_6	Waste Environmental Aspects	$T_6(L_6)$	t_{61}– unfulfilled t_{62} – deviates significantly t_{63} – deviates slightly t_{64} – fully meets	[0–10]	M_6

3.2. Machining Manyfacturability Assessment – sub-step 1

The processability of the workpiece (sample housing) is determined, assuming that it depends on two factors, which are:

- Technological Capabilities of the Machine Park/Accuracy,
- CAD/CAM Software Capability.

Tab. 3. Fuzzification of input variables

Technological Possibilities Of The Machine Park/Accuracy	**Rating**
Fully fall within the capabilities of machines/accuracy	100
It deviates slightly from the machine's capabilities/accuracy	60
It deviates from the machine capabilities/accuracy significantly	30
Machine capabilities/accuracy not met completely	0
CAD/CAM SOFTWARE CAPABILITY	**Rating**
CAD/CAM capabilities not met	0
It deviates significantly from the CAD/CAM	30
It deviates slightly from the CAD/CAM	60
Fully fits CAD/CAM capabilities	100

Tab. 4. Fuzzy relations for the variable TECHNOLOGICAL POSSIBILITIES

TECHNOLOGICAL POSSIBILITIES				
	Unfulfilled	**It deviates significantly**	**It deviates slightly**	**Fully meets**
0	1	0	0	0
30	0	1	0	0
60	0	0	1	0
100	0	0	0	1

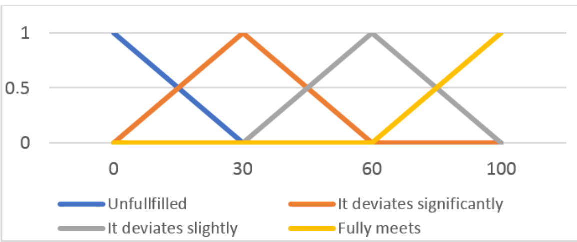

Fig. 3. Membership function graph for TECHNOLOGICAL POSSIBILITIES

The membership function for Technological Capabilities is described by the formulas:

$$\mu_{\text{UNFULFILLED}}(x) = \begin{cases} \dfrac{30 - x}{30 - 0} \; for \; 0 < x < 30 \\ 0 \; for \; 30 \; \leq x \; \leq 100 \end{cases}$$

$$\mu_{\text{DEVTES SIGNIFICANTLY}}(x) = \begin{cases} \dfrac{x}{30 - 0} \; for \; 0 < x < 30 \\ \dfrac{60 - x}{60 - 30} \; for \; 30 < x < 60 \\ 0 \; for \; 60 \; \leq x \; \leq 100 \end{cases}$$

$$\mu_{\text{ DEVIATES SLIGHTLY}}(x) = \begin{cases} 0 \; dla \; x \; \leq 30 \\ \dfrac{x - 30}{60 - 30} \; dla \; 30 < x < 60 \\ \dfrac{100 - x}{100 - 60} \; dla \; 60 < x < 100 \end{cases}$$

$$\mu_{\text{FULLY MEETS}}(x) = \begin{cases} 0 \; dla \; x \; \leq 60 \\ \dfrac{x - 60}{100 - 60} \; dla \; 60 < x < 100 \end{cases}$$

Tab. 5. Fuzzy relations for the variable SOFTWARE CAPABILITY

SOFTWARE CAPABILITY				
	Unfulfilled	**It deviates significantly**	**It deviates slightly**	**Fully meets**
0	1	0	0	0
30	0	1	0	0
60	0	0	1	0
100	0	0	0	1

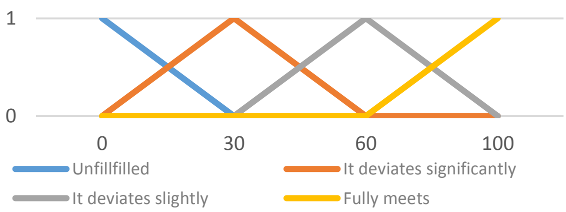

Fig. 4. Membership function graph for SOFTWARE CAPABILITY

The membership function for Software Capability is described by the formulas:

$$\mu_{\text{UNFULFILLED}}(x) = \begin{cases} \dfrac{30-x}{30-0}\ for\ 0 < x < 30 \\ 0\ for\ 30\ \leq x\ \leq 100 \end{cases}$$

$$\mu_{\text{DEVIATES SIGNIFICANTLY}}(x) = \begin{cases} \dfrac{x}{30-0}\ for\ 0 < x < 30 \\ \dfrac{60-x}{60-30}\ for\ 30 < x < 60 \\ 0\ for\ 60\ \leq x\ \leq 100 \end{cases}$$

$$\mu_{\text{ DEVIATES SLIGHTLY}}(x) = \begin{cases} 0\ for\ x\ \leq 30 \\ \dfrac{x-30}{60-30}\ for\ 30 < x < 60 \\ \dfrac{100-x}{100-60}\ for\ 60 < x < 100 \end{cases}$$

$$\mu_{\text{FULLY MEETS}}(x) = \begin{cases} 0\ for\ x\ \leq 60 \\ \dfrac{x-60}{100-60}\ for\ 60 < x < 100 \end{cases}$$

The course of fuzzification with the Mamdani rule, the basis of inference rules (tab. 6) was carried out for the selected workpiece according to expert assessments:

- Technological capabilities = 20,
- Software capability = 55,
- Rule 10 Technological capabilities – Deviates significantly and Software capability – Deviates significantly in min (0.67, 0.17) = 0.17,
- Rule 11 Technological possibilities – Deviates significantly and Software capability – Deviates slightly to a degree of min (0.67, 0.83) = 0.67,
- Rule 14 Technological possibilities Unfulfilled and also Software capability – Deviates significantly to a degree of min (0.33, 0.17) = 0.17,
- Rule 15 Technological possibilities Unfulfilled and Software capability – Deviates slightly to a degree of min (0.33, 0.83) = 0.33,
- **Inference processing for manufacturability – substep 1.**

From rules 10, 11, 14 and 15 – MAX, so we activate the rules: 11. Technology 1 takes the value for Technology Capabilities 20 and Software Capability 55:

Tab. 6. Base rules of inference manufacturability evaluation processing – Substage 1

1	IF	TECHNOLOGICAL POSSIBILITIES FULLY MEETS	AND	SOFTWARE CAPABILITY UNFULFILLED	THAN	MANFACTURABILITY 1 MEDIUM
2	IF	TECHNOLOGICAL POSSIBILITIES FULLY MEETS	AND	SOFTWARE CAPABILITY DEVIATES SIGNIFICANTLY	THAN	MANFACTURABILITY 1 MEDIUM HIGH
3	IF	TECHNOLOGICAL POSSIBILITIES FULLY MEETS	AND	SOFTWARE CAPABILITY DEVIATES SLIGHTLY	THAN	MANFACTURABILITY 1 MEDIUM HIGH
4	IF	TECHNOLOGICAL POSSIBILITIES FULLY MEETS	AND	SOFTWARE CAPABILITY FULLY MEETS	THAN	MANFACTURABILITY 1 HIGH
5	IF	TECHNOLOGICAL POSSIBILITIES DEVIATES SLIGHTLY	AND	SOFTWARE CAPABILITY UNFULFILLED	THAN	MANFACTURABILITY 1 MEDIUM LOW
6	IF	TECHNOLOGICAL POSSIBILITIES DEVIATES SLIGHTLY	AND	SOFTWARE CAPABILITY DEVIATES SIGNIFICANTLY	THAN	MANFACTURABILITY 1 MEDIUM
7	IF	TECHNOLOGICAL POSSIBILITIES DEVIATES SLIGHTLY	AND	SOFTWARE CAPABILITY DEVIATES SLIGHTLY	THAN	MANFACTURABILITY 1 MEDIUM HIGH
8	IF	TECHNOLOGICAL POSSIBILITIES DEVIATES SLIGHTLY	AND	SOFTWARE CAPABILITY FULLY MEETS	THAN	MANFACTURABILITY 1 MEDIUM HIGH
9	IF	TECHNOLOGICAL POSSIBILITIES DEVIATES SIGNIFICANTLY	AND	SOFTWARE CAPABILITY UNFULFILLED	THAN	MANFACTURABILITY 1 MEDIUM LOW
10	IF	TECHNOLOGICAL POSSIBILITIES DEVIATES SIGNIFICANTLY	AND	SOFTWARE CAPABILITY DEVIATES SIGNIFICANTLY	THAN	MANFACTURABILITY 1 MEDIUM LOW
11	IF	TECHNOLOGICAL POSSIBILITIES DEVIATES SIGNIFICANTLY	AND	SOFTWARE CAPABILITY DEVIATES SLIGHTLY	THAN	MANFACTURABILITY 1 MEDIUM LOW
12	IF	TECHNOLOGICAL POSSIBILITIES DEVIATES SIGNIFICANTLY	AND	SOFTWARE CAPABILITY FULLY MEETS	THAN	MANFACTURABILITY 1 MEDIUM
13	IF	TECHNOLOGICAL POSSIBILITIES UNFULFILLED	AND	SOFTWARE CAPABILITY UNFULFILLED	THAN	MANFACTURABILITY 1 LOW
14	IF	TECHNOLOGICAL POSSIBILITIES UNFULFILLED	AND	SOFTWARE CAPABILITY DEVIATES SIGNIFICANTLY	THAN	MANFACTURABILITY 1 MEDIUM LOW
15	IF	TECHNOLOGICAL POSSIBILITIES UNFULFILLED	AND	SOFTWARE CAPABILITY DEVIATES SLIGHTLY	THAN	MANFACTURABILITY 1 MEDIUM LOW
16	IF	TECHNOLOGICAL POSSIBILITIES UNFULFILLED	AND	SOFTWARE CAPABILITY FULLY MEETS	THAN	MANFACTURABILITY 1 MEDIUM

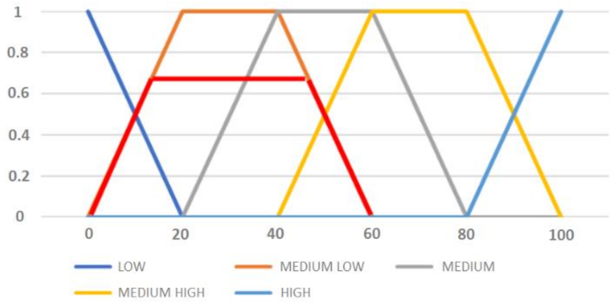

Fig. 5. Membership function graph Machining efficiency – sub-step 1

For technology – the low average (range <0; 60>) takes the value of min (0.67; technology – medium) – the value lower 0.67 or the value of the function technology – medium – low (Fig. 5).

Therefore, after the defuzzification process, the assessment is:

$$\begin{cases} y = \frac{x}{20} \\ y = 0.67 \end{cases} \qquad 0.67 = \frac{x}{20} \qquad x = 20 * 0.67 = 13.4$$

$$\begin{cases} y = \frac{60-x}{60-40} \\ y = 0.67 \end{cases} \quad 0.67 = \frac{60-x}{20} \quad 60 - x = 20 * 0.67 \quad 60 - x = 13.4 \quad x = 46.6$$

$$r = \frac{\int_0^{80} y \cdot \mu_{B'}(y)dy}{\int_0^{80} \mu_{B'}(y)dy}$$

$$r = \frac{\int_0^{13,4} y \cdot \frac{y^2}{20}\, dy + \int_{13,4}^{46,6} y \cdot 0.67\, dy + \int_{46,6}^{60} y \cdot \frac{60-y}{20}\, dy}{\int_0^{60} \mu_{B'}(y)dy}$$

$$\int_0^{60} \mu_{B'}(y)dy = P_1 \qquad P_1 = \frac{(60+33.2)\cdot 0.67}{2} = 31.2$$

$$r = \frac{y^3}{60} + \frac{y^2}{3} + \frac{1}{20} \cdot \left(30y^2 - \frac{y^2}{3}\right) = 40.1 + 664 + 229.24 = 933.34$$

$$r = \frac{933.34}{31.2} = 29.91$$

The value of the sample assessment of Machining Manufacturability Sub-step 1 is 29.9.

3. CONCLUSIONS

Attempt to assess manufacturability assessment takes into account the structure due to the machining, assembly process and organization of production. The assessment was carried out according to the fuzzy set inference methods. The manufacturability evaluation procedure is proposed in the steps, which start their ratings linguistic variables divided into sub-steps. An example of the evaluation due to machining on the basis of the proposed base of fuzzy inference can be extended for the assembly process steps and organization of production.

REFERENCES

Deka, A., & Behdad, S. (2019). Part separation technique for assembly-based design in additive manufacturing using genetic algorithm. *Procedia Manufacturing*, *34*, 764–771. doi:10.1016/j.promfg.2019.06.208

Favi, C., Germani, M., & Mandolini, M. (2016). Design for manufacturing and assembly vs. design to cost: toward a multi-objective approach for decision-making strategies during conceptual design of complex products. *Procedia CIRP*, *50*, 275–280. doi:10.1016/j.procir.2016.04.190

Fernández, A., & Herrera, F. (2012). Linguistic fuzzy rules in data mining: follow-up mamdani fuzzy modeling principle. In: E. Trillas, P. Bonissone, L. Magdalena, J. Kacprzyk (Eds.), *Combining Experimentation and Theory. Studies in Fuzziness and Soft Computing* (vol. 271, pp. 103–122). Berlin, Heidelberg: Springer. doi:10.1007/978-3-642-24666-1_8

Kuo, B. T. C., Huang, S. H., & Zhang, H. C. (2001). Design for manufacture and design for 'X': concepts, applications, and perspectives. *Computers & Industrial Engineering*, *41*(3), 241–260.

Lalaoui, M., & El Afia, A. (2018). A Fuzzy generalized simulated annealing for a simple assembly line balancing problem. *IFAC-PapersOnLine*, *51*(32), 600–605. doi:10.1016/j.ifacol.2018.11.489

Matuszek, J., & Seneta, T. (2017). Evaluation of design manufacturability in new product production launches by Lucas DFA method. *Mechanik*, *7*, 523–525.

Matuszek, J., Seneta, T., & Moczała, A. (2018). Evaluation of design manufacturability in assembly processes by modified Lucas Design for Assembly method. *Mechanik*, *7*, 532–534. doi:10.17814/mechanik.2018.7.75

Zadeh, L. A. (1965). Fuzzy sets. *Information and Control*, *8*(3), 338–353. doi:10.1016/S0019-9958(65)90241-X

Zadeh, L. A. (1975). The concept of a linguistic variable and its application to approximate reasoning – I. *Information Sciences*, *8*(3), 199–249. doi:10.1016/0020-0255(75)90036-5

Applied Computer Science, vol. 15, no.3, pp. 56–64
doi:10.23743/acs-2019-21

Submitted: 2019-07-12
Revised: 2019-08-03
Accepted: 2019-09-12

distance education, online examination,
authentication, assessment, Biometric system

Hamid JAN[0000-0003-2065-8515]*, *Beena HAMID***

THE APPLICATION OF FINGERPRINTS AUTHENTICATION IN DISTANCE EDUCATION

Abstract

Currently the distance education has obtained a wider ever acceptance. One of the main tasks of distance education is the process of checking student's knowledge by online examination. To conduct a fair examination and prevent unauthorized users to appear in the examination, different biometric technologies are used; we in this paper implement a fingerprint biometric system for distance education students and found by survey that the students are comfortable with fingerprint biometric system.

1. INTRODUCTION

The invention of computer technology has changed our lives and found new directions. The ways of communication and getting information through Web is another change for people. Distance education through web technology or online education is the new way of getting education emerged from World Wide Web (Alavi & Leidner, 2016; Takahashi, Abiko & Negishi, 2006). These technologies are very attracting and interesting but also face various threats, especially when tests are conducted online. (King, Guyette & Piotrowski, 2009) studied and come to the conclusion that 73.6% of the students think that cheating is easy in the online exam as compared to conventional exam. These were the students selected for the sample.

* Sarhad university of Science & Information Technology, Landi Akhund Ahmad, Ring Road, Peshawar 25000,Pakistan, hod.csit@suit.edu.pk
** Jalya Khan Institute of Modern Sciences, Ghani Khan Road, Shaheedan Salarabad, Charsadda 25000, Pakistan, beenhamidjan@gmail.com

Distance learning is a modern form of education and is the interaction of the teacher and students with each other at a distance or on internet (King, Guyette & Piotrowski, 2009). It provides the learning process different from the conventional form of education. The problems of distance learning can be divided into two groups: pedagogical problems and technical problems. In this paper, we considered only technical problems, in particular, the problem of identifying the true user during Examination.

The place of the student and the teacher is different in online examination, because communication is done through the Internet. As the distances increases between teacher and student, the chances of committing negligence increases, and revealing the wrong actions of the students is quite difficult. To avoid such unfair means, the actions of the students must be continuously supervised during the examination. In supervising the first move may be the use of an authentication method, that is, the identification of the student, which is the right person who is eligible for the exam occasionally a student who has been registered in the exam is different from the student who wrote the exam. Therefore, authentication plays a role in determining the correct user.

A new method to authenticate people based on their biometrics has become known for many years (Green & Romney, 2005; Frischholz & Dieckmann, 2005). William (2002), for example, explains that biometric data are unique physical characteristics of a person, such as fingerprints, iris, face, fingerprints, etc. Biometric fingerprint systems are very common and are known for their accuracy, ease and proven record (Aggarwaltt, Rathat, Jeat & Bollet, 2008; Ali, Ali, Shahzad & Malik, 2006; Ratha, Connell & Bolle, 2001).

However, like any other biometric system, fingerprints also represent several threats and risks to the authentication process (Maltoni, Maio, Jain & Prabhakar, 2003). Education should not be thought as distance or conventional, unless it is associated with assessments and exams. Student assessment is an important part of the education and training system. First, it is important to know that how much knowledge is required for a student and secondly the students themselves need to know about their knowledge. The most tried assessment procedure due to its clarity is the use of MCQs type exam.

The interactions of students with online materials and the collection of all information for examination from such material are very helpful. It is also handy to support the examiner in his work.

2. RELATED WORK

Althaff et al. (2009) offers a unimodal approach that ensures the security of online exams by using facial recognition techniques. They use the methods of discrete casino transformation (DCT) and Karhunen-Loeve transformation (KLT) to capture the facial image functions, and then compare these results with facial recognition. This method can be further extended by comparing faces with a protected image.

Agulla et al. (2008) provides uniform protection technologies using biometric authenticity of the Internet. This method uses biochecker software, which is handy for verification of images on user side. Visualize user images and handy for user behavior monitoring. The drawback of this method is that you need powerful servers to run this software.

Hsieh & Leu (2011) provides unimodal technique for implementing a unique authentication method based on passwords. This method supply independent passwords based on location and time of a mobile user. By using this password only, the application on mobile device can be accessed, such as Internet banking. This helps in reduction the risk of intrusion. This method can be used during the student authentication process.

Taiwo Ayodele et al. (2011) offered an automatic learning method that prevents theft, impersonation of exams online. This method shows the student's behavior during the exam, thus avoiding negligence.

Apampa et al. (2010) Proposes a multiple-step approach to the model, presenting authentication methods to initiate a student session and follow-up student monitoring while the examination is in progress. To authenticate, the student has three options, i.e by face recognition, by passwords or by tokens. After authentication the student is continuously check through the webcam. If some unfair means or risks are identified, the student will be asked to authenticate again.

Nasser Modiri et al. (2011) offered a multimode technique, in which the system is designed to conduct distance examinations in secure domain. To do this, the student provides user-id and passwords at the time of registration and then the student supervision is done through the webcam. It assists to monitor students' behavior during the examination.

3. METHODOLOGY OF FINGERPRINT AUTHENTICATION

The working diagram of scanner that was used in fingerprint Authentication (Maltoni, Maio, Jain & Prabhakar, 2003) is shown in figure 1.

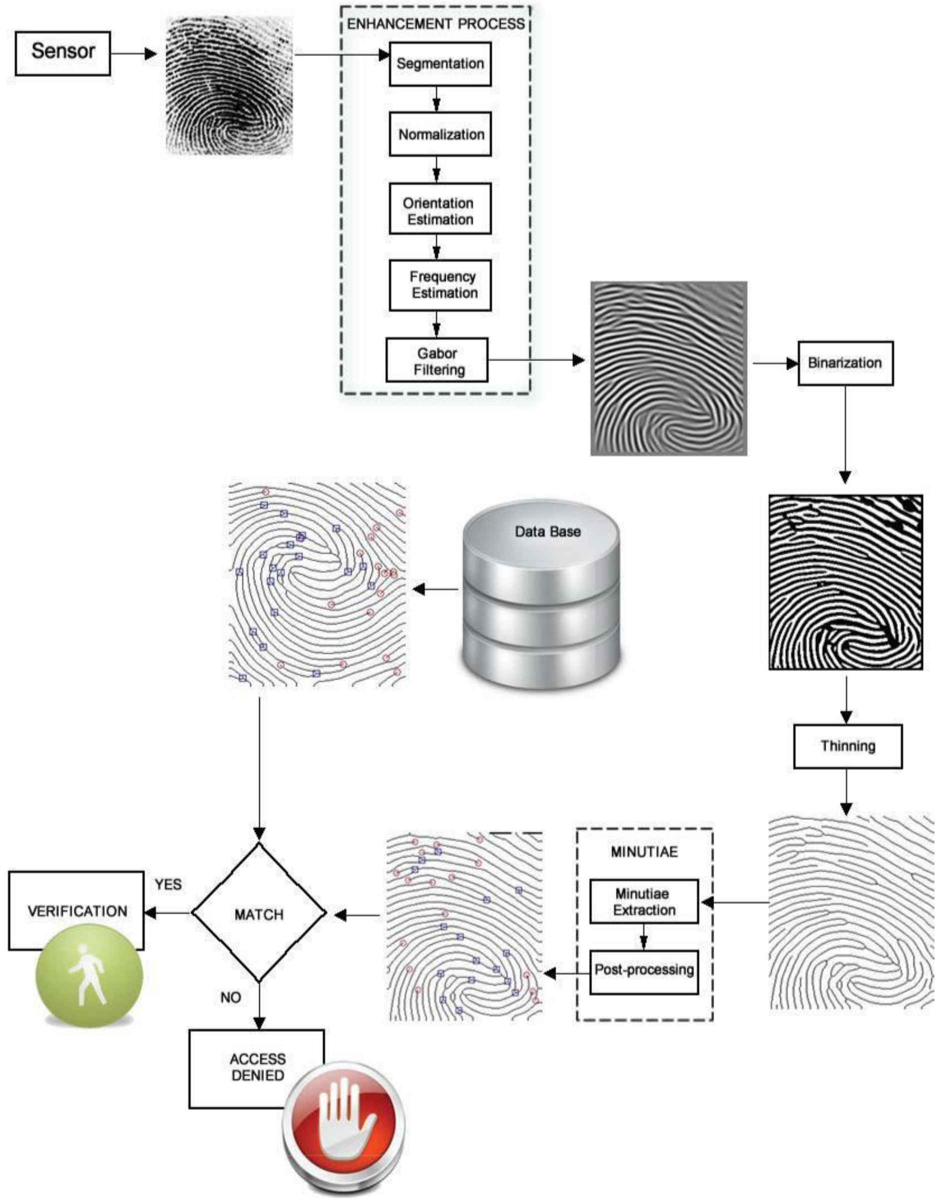

Fig. 1. Fingerprint authentication system

The fingerprint consists of the following two types of features:

1. The Global Features: They are core and delta. The core is the inner most point and delta is the location where three ridges meet.
2. The Local Features: The lines on fingerprint are called Ridges and the spaces between them are called valleys. These ridges form different patterns and are called minutiae points. The most common minutiae points are ridge bifurcation and ridge ending**.**

With the help of local and global features of fingerprint, we can differentiate users. The global and local features of finger prints are shown in figure 2.

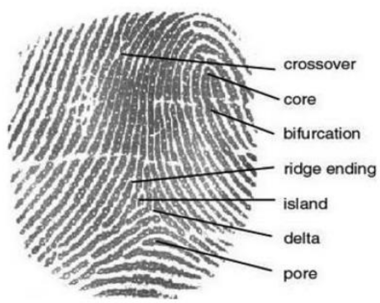

Fig. 2. Local and Global features of fingerprints

Students will be able to appear in exam online. Each student will be given access to a computer in the classroom, connected to the server. The internet connection will not be available during exam. The student will authenticated first through biometric system by matching his fingerprints. Once the student is recognized by the system, the system allows him to complete the exam. The test of the student is send for checking to the teacher electronically and the system also send the copy of test to the printer for student.

Once the student is recognized by the system, his identity will be known and now the student can be punished, if found using unfair means in the examination. There are many advantages and disadvantages of conducting exam online. The ability to track the actions of a student identified by system, allows us to constantly evaluate him and giving student the best experience. Any online activity can be vulnerable, so a reliable security policy will be required. Fingerprint Biometrics appears again as a way of reducing the likelihood of threats.

4. RESULT AND DISCUSSION

During the examination, 100 students were verified on fingerprint biometric system. The detail of these student were presented in figures 3,4 and 5. Most of them are in the range from 17 to 30 years old, Students of Computer Science at Comwave College Islamabad, a Distance Learning Centre of SUIT. Students in Computer science Department mostly come after completing twelve years of schooling. Almost all (91.3%) are men. All of them were enrolled in the different subjects.

The purpose of the experiment was to analyze the attitude of students towards a new tool for controlling access to e-learning. 80% of students think that fingerprint registration is a very easy or easy way to use online courses. Those who welcome the use of fingerprint biometric system said they look more secure, it’s simple and faster than other access tools. Those who oppose fingerprint biometric system consider that the password is sufficient. The data in Table 1 clearly supports the choice of a fingerprint biometric technology.

Tab. 1. The choice of best Biometric System

Biometric Choice	Frequency	%age	Cum.%
Fingerprint	80	80.0	80.0
Face	5	5.0	85.0
Iris	13	13.0	97.0
Voice	2	2.0	100.0
Total	100	100.0	

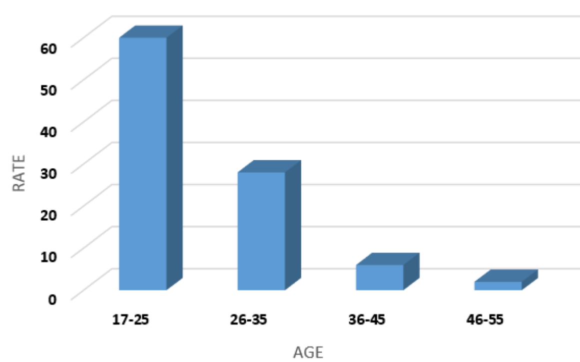

Fig. 3. The Age of Students

To find about the ease of use of a new fingerprint interface, students find it very easy or easy to use (80.0%) (see Table 2).

Tab. 2. The opinion poll of students

Opinion	Frequency	%age	Cum.%
Very Easy	45	45.0	45.0
Easy	35	35.0	80.0
Difficult	17	17.0	97.0
Useless	3	3.0	100.0
Total	100	100	

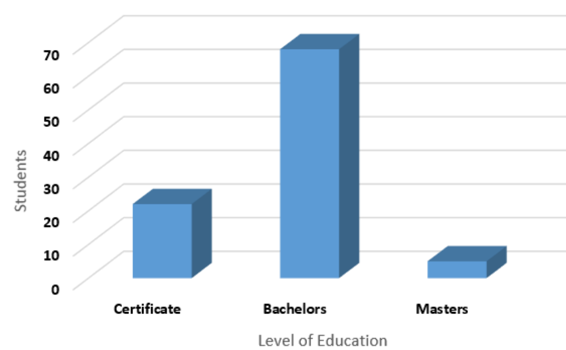

Fig. 4. The Level of Education

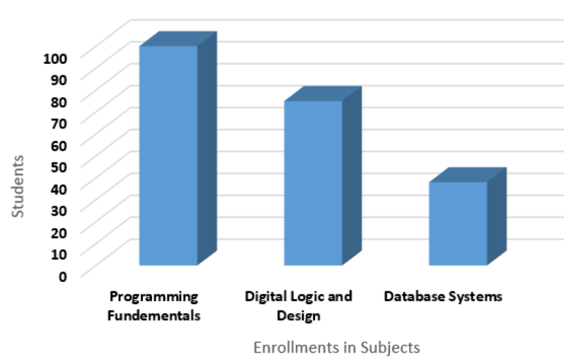

Fig. 5. Total enrollment of Students in Each Subject

Students were analyzed for their level of knowledge about biometric system and to what extent they have used it. Many students were new to these methods and hardly have used biometric systems (see Table 3).

The main challenge of survey was whether the students think the fingerprint biometric system verification appropriate for accessing online courses. The students were divided into two groups. The group one contains those who accept the fingerprint verification and the group two includes those who did not accept it. Two-dimensional analysis of tree segmentation to assess which category is supported by many students is applied.

Tab. 3. Knowledge of Students about Biometric System

Knowledge	Frequency	%age	Cum.%
Expert Level	1	1.0	1.0
Intermediate Level	11	11.0	11.0
Elementary Level	15	15.0	26.0
no Knowledge	74	74.00	100.00
(Total)	100	100.00	

Two questions were asked from the students. Question no. 1 was: "What do you think about the verification via fingerprint to access online courses?". 77% students think that verification via fingerprint is very easy while 23% students think that verification by such method is very difficult. Question no. 2 was: "Which one of the biometric technologies would you select?". The total students in favor of biometric technology were seventy seven (77). Seventy (70) students selected Fingerprint Biometric technology while the other seven (7) students selected the other technology.

5. CONCLUSION

A fingerprint matching technique based on local features of fingerprints was used for verification and registration. The technique performed well when tested for online examination. The students were keen to use the biometric system for online learning. The students think that it is a faster and easy way to verify and register for online courses. Most of the students have never used the biometric system and have very little knowledge about biometric systems. Eventually the fingerprint biometric system was implemented in the distance education online examination and introduce a new way of conducting examination in distance.

REFERENCES

Aggarwaltt, G., Rathat, N. K., Jeat, T. Y., & Bollet, R. M. (2008). Gradient based Textural Characterization of Fingerprints. In *2008 IEEE Second International Conference on Biometrics: Theory, Applications and Systems* (pp. 1–5). Arlington, VA. doi:10.1109/BTAS.2008.4699383

Agulla, E. G., Rifón, L. A., Castro, J. L. A., & Mateo, C. G. (2008). Is my student at the other side? Applying Biome tric Web Authentication to E-Learning Environments. In *2008 Eighth IEEE International Conference on Advanced Learning Technologies* (pp. 551–553). Santander, Cantabria. doi:10.1109/ICALT.2008.184

Alavi, M., & Leidner, D. (2016). Research commentary: Technology mediated learning-a call for greater depth and breadth of research. *Information Systems Research*, *12*(1), 1–10. doi:10.1287/isre.12.1.1.9720

Ali, I., Ali, U., Shahzad, M. I., & Malik, A. W. (2006). Face and fingerprint biometrics integration model for person identification using gabor filter. In *IEEE International Conference on Computer Systems and Applications* (pp. 140–143). Dubai, UAE. doi:10.1109/AICCSA.2006.205081

Althaff, I., Syusaku, N., Karim, O., &Yoshimi, F. (2009). Face-based Access Control and Invigilation Tool for e-Learning Systems. In *2009 International Conference on Biometrics and Kansei Engineering* (pp. 40–44). Cieszyn. doi:10.1109/ICBAKE.2009.43

Apampa, K. M., Wills, G., & Argles, D. (2010). An approach to presence verification in summative e-assessment security. In *2010 International Conference on Information Society* (pp. 647–651). London.

Ayodele, T., Shoniregun, C. A., & Akmayeva, G. (2011). Toward e-learning security: A machine learning approach. In *International Conference on Information Society (i-Society 2011)* (pp. 490–492). London.

Frischholz, R. W., & Dieckmann, U. (2000). Bioid: A Multimodal Biometric Identification System. *Computer*, *33*(2), 64–68.

Green, N., & Romney, G. W. (2005). Establishing Public Confidence in the Security of Fingerprint Biometrics. In *005 6th International Conference on Information Technology Based Higher Education and Training* (pp. S3C/15-S3C/18). Santo Domingo. doi:10.1109/ITHET.2005.1560332

Hsieh, W., & Leu, J. (2011). Design of a time and location based One-Time Password authentication scheme. In *2011 7th International Wireless Communications and Mobile Computing Conference* (pp. 201–206). Istanbul. doi:10.1109/IWCMC.2011.5982418

King, C. G., Guyette, R. W., & Piotrowski, C. (2009). Online exams and cheating: An empirical analysis of business students 'views'. *The Journal of Educators Online*, *6*(1), 1–11.

Maltoni, D., Maio, D., Jain, A. K., & Prabhakar, S. (2003). *Handbook of Fingerprint Recognition*. London: Springer.

Modiri, N., Farahi, A., & Ketabi, S. (2011). Providing security framework for holding electronic examination in virtual universities. In *The 7th International Conference on Networked Computing and Advanced Information Management* (pp. 73–79). Gyeongju.

Ratha, N. K., Connell, J. H., & Bolle, R. (2001). An analysis of minutiae matching strength. In: J.Bigun & F. Smeraldi (Eds.), *Audio- and Video-Based Biometric Person Authentication. AVBPA 2001. Lecture Notes in Computer Science* (vol. 2091). Berlin, Heidelberg: Springer. doi:10.1007/3-540-45344-X_32

Takahashi, Y., Abiko, T., & Negishi, E. (2006). An Ontology-based System for Network Security. In *19th International Conference on Advanced Information Networking and Applications (AINA'05) Volume 1 (AINA papers)* (pp. 197–202 vol.1). Taipei, Taiwan. doi:10.1109/AINA.2005.116

Williams, J. W. (2002). Biometrics or ... biohazards? In *Proceedings of the 2002 Workshop on New Security Paradigms NSPW '02* (pp. 97–107). doi:10.1145/844118.844120

Applied Computer Science, vol. 15, no.3, pp. 65–72
doi:10.23743/acs-2019-22

Submitted: 2019-08-30
Revised: 2019-09-01
Accepted: 2019-09-22

Rapid Prototyping, surgery planning, fractures

Przemysław KRAKOWSKI [0000-0001-7137-7145]*
Józef JONAK [0000-0003-4658-4569]**
Robert KARPIŃSKI [0000-0003-4063-8503]**
Łukasz JAWORSKI [0000-0002-4384-5754]***

USEFULNESS OF RAPID PROTOTYPING IN PLANNING COMPLEX TRAUMA SURGERIES

Abstract

Orthopaedic trauma surgery is a complex surgical speciality in which anatomy, physiology and physics are mixed. Proper diagnosing and based on that planning and performing surgery is of crucial matter. This article presents usefulness of 3D reconstruction in diagnostics and surgical planning. It focuses on utility of computed tomography reconstruction in trauma surgery. Moreover, two cases in which this technique was used is described. Complex 3D reconstruction proved its usefulness and in future it may become a modality of choice for planning complex trauma procedures in which standard implants and approaches are insufficient.

1. INTRODUCTION

Trauma to the lower extremity can be a devastating incident for every individual. Among various injuries affecting lower extremity, tibial fractures are one of the most common. The incidence of all tibia fractures is estimated 13 in 100000 persons per year (Decruz, Antony Rex & Khan, 2019). These fractures can be divided into

* Orthopaedic Department, Łęczna Hospital, Krasnystawska 52, 21-010 Łęczna, Poland
** Lublin University of Technology, Faculty of Mechanical Engineering, Department of Machine Design and Mechatronics, Nadbystrzycka 36, 20-618, Lublin, Poland, j.jonak@pollub.pl, r.karpinski@pollub.pl
*** Independent researcher, Lublin, Poland

proximal, shaft and distal tibia fractures differing in optimal treatment method, surgical approach and anticipated treatment result. Every fracture treatment can be perceived as a mix of anatomy, physiology and physics. Fractures affecting joints such as knee or ankle if treated improperly lead to malunion, joint range of motion loss and persistent pain. Even though fractures affecting proximal and distal end of tibia are less common than affecting diaphyseal region(Court-Brown & Caesar, 2006), the impact of these fractures on daily living is much greater if treated incorrectly. Therefore, planning of surgical treatment is of vital importance in order to create best possible outcome for the patient. Complex joint fractures require meticulous planning. Up to this date the gold standard in fracture diagnosis is conventional X ray Introduced in 1895 by Wilhelm Conrad Röntgen (On a New Kind of Rays, 1896). Before that, orthopaedic diagnostic was limited to simple observation of limb alignment or pathological movement on fracture site. The invention was introduced to everyday practice. Up to this day, plain X-rays are the work horse for trauma surgeons (American College of Surgeons, 2012; Bégué, 2014). It is cheap, widely used and available in almost any trauma setting. The sensitivity of radiography In orthopaedic diagnostics usually 2 views are required in 90 degree rotation of the films. However, in some cases such as scaphoid fractures, around 25% of fractures can be overlooked on initial X-rays (Jenkins, Slade, Huntley & Robinson, 2008). Similarly in paediatric orthopaedics, fractures often are occult and not visible on first presentation on plain X-rays due to unique characteristics of the paediatric skeleton which can cause troubles with diagnosing the fracture (Segal & Shrader, 2013). In 1961 Oldendorf (1961) published his work which was a mile stone for creating commercially available computed tomography (CT) scanners which was introduced in 1972 (Richmond, 2004). Computed tomography can bring a great insight into the fracture lines, however plain CT in transversal cuts can be misleading in clinical setting. Therefore, complex 3D reconstruction of the fractures is necessary for proper planning. CT is routinely used in articular fractures, where up to 31% of articular surface depression cannot be visible on plain radiograph (Dale, Ha & Chew, 2013). Apart from obvious misdiagnosed fractures In this article we are presenting a case studies of two patients treated in Orhtopaedic Department of Leczna Hospital with complex articular fractures, where surgical planning was performed on high resolution 3D reconstructions in order to facilitate the surgery.

2. CASE PRESENTATIONS

A 50 year old female suffered a complex fracture of distal tibia and fibula after being hit by a car. At the time of admission through physical examination was performed. The physical evaluation revealed distal tibia deformation, tenderness and swelling. The initial X-rays showed complex, articular distal tibia fracture. Until planned surgery the patient was immobilised in a cast. The CT scans were obtained and 3D reconstructions were rendered. The planning of surgery was performed on 3D reconstructions of the fracture sites. The 3D reconstructions enabled detailed surgical planning. And significantly aided during procedure, while all necessary implants were prepared in advance with the knowledge of exact screw length which were to be used. During the surgery itself, knowledge of implants length was a great help during the procedure while it was a simple and fast method of confirmation of implant placement. And if there was a mismatch between planned and measured implant the surgeon had a feedback that probably the placement or angle of the implant is false. This enabled the operating surgeon for anatomical reduction of the fracture and adequate placement of implants. Postsurgery X-rays show excellent reduction and fixation on Figures 1–2.

Fig. 1. AP postoperative X-ray

Fig. 2. Lateral postoperative X-ray

A 30 year old female was admitted to the hospital due to lateral tibial condyle fracture sustained during a standing height fall. The patient had a prior history of juvenile osteoporosis and multiple bone deformations were encountered including proximal tibia deformation. Moreover the length of the bones was shortened which is typical for metabolic bone diseases (Skowrońska-Jóźwiak & Lorenc, 2006). The fracture was diagnosed as Schatzker type I fracture. In normal setting this type of fracture is rather straightforward in treatment, however in this case due to bony ends deformations and abnormal limb length 3D reconstruction was a great assistance in surgical planning. It was seen that typical proximal tibial implants would not fit to the deformed bone, therefore on basis of 3D reconstruction a trial implants were introduced in order to select the best fitting implants. Based on 3D reconstructions a straight plate, which was bended to fit the bone was introduced. Additional fixation was achieved by inserting additional screws apart from plate. Proper implant placement regardless of congenital deformity of proximal tibia is shown on Figures 3–4.

Fig. 3. AP postoperative X-ray

Fig. 4. Lateral postoperative X-ray

3. DEVELOPING OF THE VIRTUAL MODELS

3D models of the analyzed cases were based on a series of 2D images perpendicular to the axis of long bones obtained by computed tomography. The images were exported to a file in the DICOM (Digital Imaging and Communications in Medicine) format. This format allows the exchange and interpretation of medical data related to diagnostic images in medicine. It is mainly used in the processing of computed tomography (CT) images, magnetic resonance imaging (RM). Data in the DICOM format usually has a large volume, but it allows you to maintain high image quality. In the next step, the image series were implemented in Materialise Mimics 17.0, where, based on the source files, the program calculates cross-sections in two parallel planes arranged perpendicular to the long axis of the bone. Then, using the conversion function from two-dimensional data in the form of pixels to three-dimensional pixels called voxels. Creating a virtual model using the tresholding function is based on thresholding radiological density values expressed in the Hounsfield Scale.

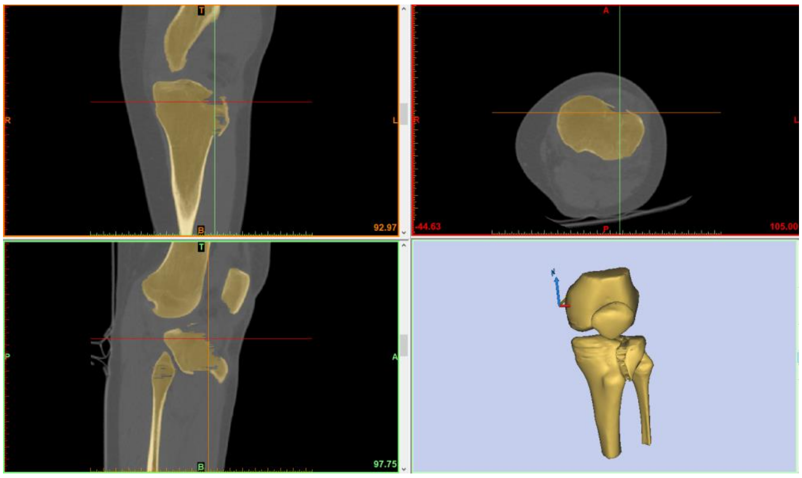

Fig. 5. Calculation of 3D model for proximal tibia fracture

The range of this scale is from –1000 HU for air, to about 3100 HU for bone tissue. It is represented by 12-bit images, where the areas closer to white correspond to structures that absorb more radiation, while the areas closer to black correspond to structures that absorb less radiation. Specific ranges of variation HU units correspond to the anatomical structures. The radiological density range for bone tissue is from +300 to +400 HU for spongy bone and from +1800 to +1900 HU for cortical bone. In the case of the analyzed set of images, structures with radiological density from 226 to 1852 HU were isolated. When the tissue mask with the desired radiological density is ready, it begins to calculate the 3D model based on highlighted tissues on layers in three perpendicular planes of the 3D coordinate system. This process for both analyzed cases is presented in Fig. 5 and Fig. 6.

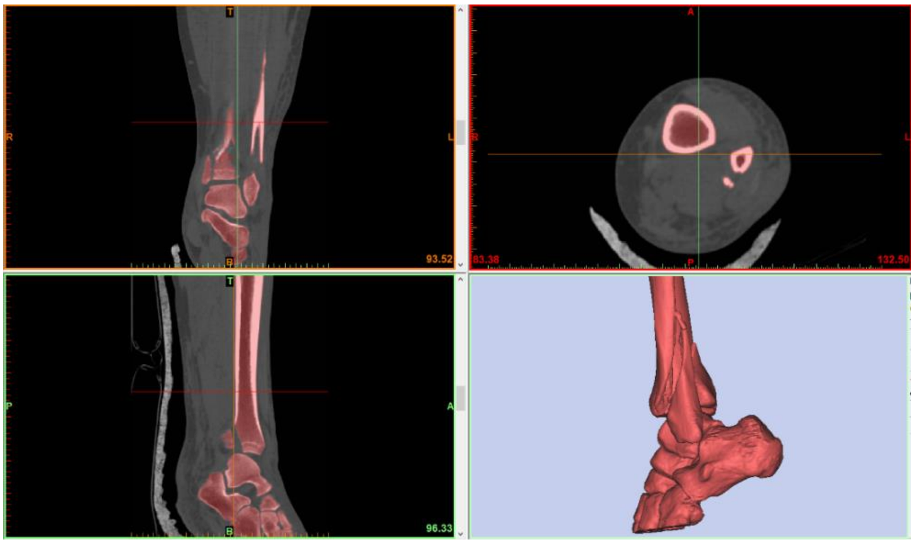

Fig. 6. Calculation of 3D model for distal tibia fracture

For better model quality, voids inside the bone were filled using the "Fill cavities from polylines" tool, which fills the empty strokes (polylines) created on the basis of cross-section sketches of the initial 3D model on each layer of the image. The results are shown in Figures 7 and 8.

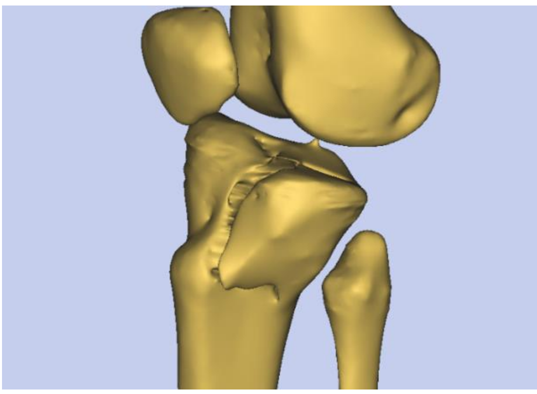

Fig. 7. Final 3D model of proximal tibia fracture

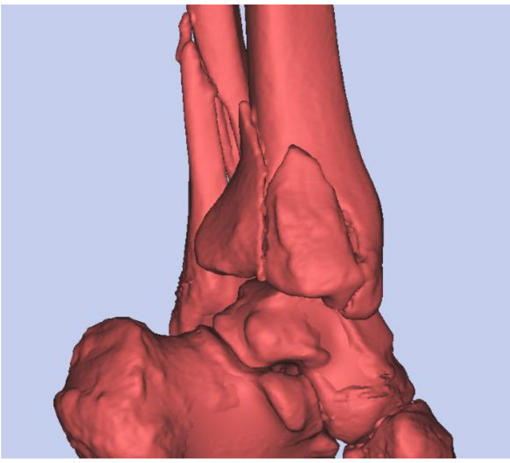

Fig. 8. Final 3D model of distal tibia fracture

The models obtained in this way provide the operator with much more information about fracture, especially in terms of the size and distribution of bone fragments. It is also possible to estimate the volume of cavities, which allows you to prepare the right amount of material to fill them. The use of Rapid Prototyping technology in the broadly understood planning of orthopedic procedures allows for the appropriate selection of surgical instruments, which can reduce the time of the procedure and reduce its costs in comparison with procedures performed without using this technology. Moreover, thanks to additive manufacturing processes in form of 3D printing, physicians are able to practise each procedure on life-size models, derived from digital models (e.g. in STL file format) and 3D printed using affordable plastic materials.

4. CONCLUSIONS

Trauma surgery requires complex and often multidisciplinary approach. Radiological assessment of the fracture sites and adjacent soft tissues is crucial for proper surgery planning. Several imaging modalities may be incorporated in diagnostic and planning protocol including conventional radiography, CT or MRI. Nevertheless, each trauma case can differ significantly from previous cases and may require individual approach. In simple fractures, the surgery is rather straightforward. However, intraarticular fractures, especially in deformed limbs can be a challenging and restoring individual anatomy may not be possible without high resolution 3D reconstructions with trial implant templates placement can be a great help in surgical planning. It gives insight into the fracture which cannot be obtained otherwise.

REFERENCES

American College of Surgeons. (2012). *Advanced trauma life support: ATLS ; student course manual* (9. ed). Chicago, Ill: American College of Surgeons.

Bégué, T. (2014). Articular fractures of the distal humerus. *Orthopaedics & Traumatology: Surgery & Research*, *100*(1), S55–S63. doi:10.1016/j.otsr.2013.11.002

Court-Brown, C. M., & Caesar, B. (2006). Epidemiology of adult fractures: A review. *Injury*, *37*(8), 691–697. doi:10.1016/j.injury.2006.04.130

Dale, J. D., Ha, A. S., & Chew, F. S. (2013). Update on Talar Fracture Patterns: A Large Level I Trauma Center Study. *American Journal of Roentgenology*, *201*(5), 1087–1092. doi:10.2214/AJR.12.9918

Decruz, J., Antony Rex, R. P., & Khan, S. A. (2019). Epidemiology of inpatient tibia fractures in Singapore – A single centre experience. *Chinese Journal of Traumatology*, *22*(2), 99–102. doi:10.1016/j.cjtee.2019.01.004

Jenkins, P. J., Slade, K., Huntley, J. S., & Robinson, C. M. (2008). A comparative analysis of the accuracy, diagnostic uncertainty and cost of imaging modalities in suspected scaphoid fractures. *Injury*, *39*(7), 768–774. doi:10.1016/j.injury.2008.01.003

Oldendorf, W. H. (1961). Isolated flying spot detection of radiodensity discontinuities – Displaying the internal structural pattern of a complex object. *IRE Transactions on Bio-Medical Electronics*, *BME-8*, 68–72.

On a New Kind of Rays. (1896). *Nature*, *53*(1369), 274–276. doi:10.1038/053274b0

Richmond, C. (2004). Sir Godfrey Hounsfield. *BMJ*, *329*(7467), 687.1. doi:10.1136/bmj.329.7467.687

Segal, L. S., & Shrader, M. W. (2013). Missed fractures in paediatric trauma patients. *Acta Orthopaedica Belgica*, *79*(6), 608–615.

Skowrońska-Jóźwiak, E., & Lorenc, R. S. (2006). Metabolic bone disease in children: Etiology and treatment options. *Treatments in Endocrinology*, *5*(5), 297–318.

Applied Computer Science, vol. 15, no. 3, pp. 73–86
doi:10.23743/acs-2019-23

Submitted: 2019-07-16
Revised: 2019-08-08
Accepted: 2019-09-03

Data Mining, classification, clustering, association, regression, algorithms bottleneck

Workineh TESEMA[*]

INEFFICIENCY OF DATA MINING ALGORITHMS AND ITS ARCHITECTURE: WITH EMPHASIS TO THE SHORTCOMING OF DATA MINING ALGORITHMS ON THE OUTPUT OF THE RESEARCHES

Abstract

This review paper presents a shortcoming associated to data mining algorithm(s) classification, clustering, association and regression which are highly used as a tool in different research communities. Data mining researches has successfully handling large amounts of dataset to solve the problems. An increase in data sizes was brought a bottleneck on algorithms to retrieve hidden knowledge from a large volume of datasets. On the other hand, data mining algorithm(s) has been unable to analysis the same rate of growth. Data mining algorithm(s) must be efficient and visual architecture in order to effectively extract information from huge amounts of data in many data repositories or in dynamic data streams. Data visualization researchers believe in the importance of giving users an overview and insight into the data distributions. The combination of the graphical interface is permit to navigate through the complexity of statistical and data mining techniques to create powerful models. Therefore, there is an increasing need to understand the bottlenecks associated with the data mining algorithms in modern architectures and research community. This review paper basically to guide and help the researchers specifically to identify the shortcoming of data mining techniques with domain area in solving a certain problems they will explore. It also shows the research areas particularly a multimedia (where data can be sequential, audio signal, video signal, spatio-temporal, temporal, time series etc) in which data mining algorithms not yet used.

[*] Jimma University, Faculty of Computing, Department of Information Technology, Jimma, Ethiopia, workineh.tesema@ju.edu.et

1. INTRODUCTION

Data mining is a process of exploring huge data, typically business related data which is called big data (Rehman, 2017). This process is performed to find hidden patterns and relationship present in the data. The overall objective of the data mining process is to extract knowledge from a large dataset and transform it into a comprehensible structure for further use (Bavisi, Mehta & Lopes, 2014). Data mining is the process of automatically finding implicit, previously unknown, and potentially useful information from large volumes of data (Yadav, Wang & Kumar, 2013). Therefore, the role of data mining algorithms has become vital to researchers in science, medicine, business, and security domains. Recent advances in data extraction techniques have resulted in tremendous increase in the input data size of data mining applications (Kalyani, Bharathi & Rao, 2016). Data mining algorithm is the tool that involves retrospective analysis to extract diamonds of knowledge from historical data and predict outcome of the future (Talia, Trunfio & Marozzo, 2016). Data mining can automate the process of finding patterns and relationships in raw data and the results can be utilized for decision support. That is why data mining is used, especially in science, business, health, security, and informatics areas (Massaro et al., 2017). Data mining is a technology that uses various techniques to discover hidden knowledge from heterogeneous and distributed historical data stored in large databases, warehouses and other massive information repositories (Kotu & Deshpande, 2015).

In researches, data mining algorithm is the tool used for retrieving hidden knowledge from noisy data. Hence, the volume of data enhanced from time-to-time it is difficult to retrieve knowledge. So, the role of data mining was help to retrieving using different algorithms. There are a lot of data mining algorithms that were used to conduct researches. Many researchers and students were used the existing algorithms. Some algorithms need data to be feed into it to get certain knowledge (Kotu & Deshpande, 2015). Sometimes the quality of data has impact on the performance of the algorithms; hence the algorithms were measured by its performance and evaluations metrics on imported dataset (Massaro, Maritati & Galiano, 2018).

Therefore, data mining algorithm is the heart of the data-mining process. These algorithms determine how cases are processed and hence provide the decision-making capabilities needed to classify, segment, associate, and analyze data for processing.

1.1. Shortcoming of Data Mining Algorithms

On the other hand, data mining algorithms have been unable to maintain the same rate of growth. Consequently, there is an increasing need to understand the bottlenecks associated with the execution of these algorithms in modern architectures. According to Ozisikyilmaz B. (2009) to analysis of the data mining applications, there is an architecture problem. The architecture variation in user expectations and satisfaction relative to the actual hardware performance to develop more efficient architectures that are customized to end-users.

Additionally, data mining algorithms were need preprocessing stages to retrieve hidden knowledge (Massaro, Barbuzzi, Vitti, Galiano, Aruci & Pirlo, 2016). This pre-processing stage is time and budget consuming, because commonly the input dataset owns features (noisy, null values, missed values, duplicate values, incomplete values), which require a transformation and cleaning step, in order to match the input format and assumptions of the data mining algorithms being considered (Wimmer & Powell, 2015). On the other hand, the data mining stage involves typically the use of one or more inductive learning algorithms, requiring that the user iterates over several steps, especially when the results are not good enough, either in terms of performance (accuracy) or understanding of the rules generated for the model (Al-Khoder & Harmouch, 2015). The other bottleneck of data mining algorithms is dynamic nature of data which refers to high voluminous and continuously changing information which is not stored earlier for analyzing and processing like static data. It is difficult to maintain dynamic data as it changes with time (Gulli & Pal, 2017). Many algorithms are used to analyze the data of interest. These data can be sequential, audio signal, video signal, spatio-temporal, temporal, time series etc (Nguyen, Woon, & Ng, 2015).

1.2. Recent Researches Towards Data Mining Algorithms

The finding of the research paper by Massaro et al. (2018) to improve the best performing predictive model k-Nearest Neighbor (k-NN) exhibited the best performance. The performance comparison has been performed between Support Vector Machine (SVM), k-Nearest Neighbor (k-NN), gradient boosted trees, decision trees, and deep learning algorithms. The gradient boosted trees approach represents an alternative approach having the second best performance.

The other finding of the study conducted by S.R. Joseph et al. (2016) on data mining algorithms presents overview of various algorithms necessary for handling large datasets and the strengths and limitations of data mining algorithms. This work argued that data mining algorithms classification, regression, and clustering have limitations as a large of volume of dataset. These algorithms have a bottleneck to handle a large volume data, to identify associations, to identify patterns and to analyze a large size of datasets. The study clearly showed that choosing the appropriate algorithm for specific purpose is a big challenge. While different algorithms used to perform the same business task, each algorithm come up with a different result, and some algorithms yield more than one type of results. Therefore, data mining algorithms has a jam to identify pattern from a huge dataset and they produce different results.

Clustering is one of a data mining algorithm which is used to partition meaningful data into useful clusters which can be understandable and has analytical value. In the paper after giving a brief viewpoint of data mining and clustering techniques, a comparative study of various partitioning algorithms was done. The paper analyses four important partitioning algorithms known as K-means, K-Medoids, CLARA and CLARANS. The study presents a comparative table to understand merits and demerits of each of the algorithms. The analysis shows that CLARA and CLARANS are comparatively more efficient and scalable than other algorithms. However algorithms such as K-Means and K-Medoid can be further modified to make them equally efficient and scalable. The paper shows that not all partitions algorithms are efficient to handle large datasets. The exploration of partitioning algorithms opens new vistas for further development and research (Swarndeep Saket & Pandya, 2016). However, further research is required to study efficiency parameters of each of the partitioning algorithms.

Clustering is the basic composition of data mining analysis, plays a significant role in different modern science research. On one hand, many tools for cluster analysis have been created, along with the information increase and subject intersection. On the other hand, each clustering data mining algorithm has its own strengths and weaknesses, due to the complexity of information (Xu & Tian, 2015). The main purpose of the paper is to introduce the basic and core idea of each commonly used clustering algorithm, specify the source of each one, and analyze the advantages and disadvantages of each one. It is hard to present a complete list of all the clustering algorithms due to the diversity of information, the intersection of research fields and the development of modern computer technology. So 19 categories of the commonly used clustering algorithms, with high practical value and well-studied, are selected and one or several typical algorithm(s) of each category is(are) discussed in detail so as to give readers a systematical and clear view of the important data analysis method, clustering (Xu & Tian, 2015).

1.3. Types of Data Mining Algorithms

Data mining involves primarily the following four classes of tasks presented below.

1.3.1. Classification

a. Decision Tree

Decision trees arrange information in a tree-like structure, classifying the information along various branches. Each branch represents an alternative route, a question. This structure can be used to help you predict likely values of data attributes.

b. CART

Another type of algorithm is CART which is educated from trained dataset. Decision tree has a leaf node where non-leaf node represents a feature and each leaf represent a value that can take the feature. Decision tree instances are classified by path starts from the root and ends at a leaf node branches based on instance feature values (Zafarani, Abbasi & Liu, 2014). Construction of decision trees is based on heuristics.

c. J48

J48 is a Java implementation of C4.5 in Weka package is referred to as J48. This algorithm is used to handle both nominal and numeric values as well as handle missing values.

d. C4.5

C4.5 is used to continue data and avoids over fitting of data. Over fitting is a big problem at the time of displaying result of decision tree. C4.5 improves computational efficiency and handles training data with missing and numeric value.

1.3.2. Clustering

Clustering algorithms are data mining algorithms that work related data grouped together. Therefore, it groups like data together in various groups. There is no prearranged arrangement for grouping these data; alike data are assimilated, and the analysis of the significance of such groupings is left to the user. Clustering is useful to see patterns in data, such as trying to identify geographic regions that are likely to respond well to a certain sales campaign.

a. K-means Algorithm

K-means algorithm is the most largely used algorithm in many researches. This algorithm is a commonly used for grouping technique. The nature of k-means is starts with a collection of data and attempts to group them into ‘k’ number of groups based on certain specific distance measurements. K-means clustering algorithm generates a specific number of disjoint, flat (non-hierarchical) clusters.

b. DBSCAN

DBSCAN is also another algorithm works based on the density. This clustering algorithm has played a great role in finding the density of the non-linear shapes of the structure. DBSCAN uses the concept of density reach ability and density connectivity.

c. K-Nearest Neighbor

K-nearest neighbor (KNN) is an algorithm works based on the similarity measure. It stores available cases and classifies new cases based on a similarity measure, for instance distance functions. A case is categorized by a majority vote of its neighbors, with the case being assigned to the most common amongst its k nearest neighbors measured by a distance function. If k = 1, then the case is assigned to the class of its nearest neighbor. This algorithm is used in statistical estimation and pattern recognition as a nonparametric technique.

d. Expectation-Maximization

Expectation-Maximization (EM): EM-based algorithm is a soft clustering technique; it is robust to noise and able to handle missing data. In the initial step, the EM-based algorithm guesses the parameters of the model, such as the maximum number of clusters and their centers. Then, it iteratively performs two alternating steps, the Expectation (E) and the Maximization (M). In the Expectation step, for each data object, current parameters of the model used to calculate its membership for each cluster. In the Maximization step, re-estimate the model parameters; for instance, re-calculate the new centers to maximize the likelihood between the model and the assumed model (Xu & Tian, 2015).

e. Support Vector Machine

One of the initial shortcomings of the SVMs is its costly computational complexity in the training phase, which leads to inapplicable algorithms in the large datasets. However, this problem is being solved with great success. One approach is to break a large optimization problem into a series of smaller problems, where each problem only involves a couple of carefully chosen variables so that the optimization can be done efficiently. The process iterates until all the decomposed optimization problems are solved successfully.

A more recent approach is to consider the problem of learning SVMs as that of finding an approximate minimum enclosing ball of a set of instances (Štulec, Petljak & Kukor, 2016). These instances, when mapped to an N-dimensional space, represent a core set that can be used to construct an approximation to the minimum enclosing ball. Solving the SVMs learning problems on these core sets can produce good approximation solutions in very fast speed. For example, the core vector machine and the further ball vector machine (Otha & Higuci, 2013) can learn SVMs for millions of data in seconds.

f. PageRank

PageRank produces a static ranking of Web pages in the sense that a PageRank value is computed for each page off-line and it does not depend on search queries. The algorithm relies on the democratic nature of the Web by using its vast link structure as an indicator of an individual page's quality. In essence, PageRank interprets a hyperlink from page x to page y as a vote, by page x, for page y. However, PageRank looks at more than just the sheer number of votes, or links that a page receives. It also analyzes the page that casts the vote. Votes casted by pages that are themselves "important" weigh more heavily and help to make other pages more "important". This is exactly the idea of rank prestige in social networks (Xu & Tian, 2015).

1.3.3. Regression

On the other hand, regression and association were algorithms largely used for a research purpose.

a. Linear Regression

This method is works based on statistics for predicting the value of a dependent and independent variables where the relationship between the variables can be described with a linear model.

b. Logistic Regression

This algorithm is based on the classification analog of regression. Logistic regression is preferable when trees in the same situations and effects are small and predictors contribute additively (when there are no interactions).

1.3.4. Association

a. Apriori approach

The bottlenecks of the apriori approach is reduces the size of candidate frequent itemsets by using apriori property. However, it still requires two nontrivial computationally expensive processes. It requires as many database scans as the size of the largest frequent itemsets. In order to find frequent k-itemsets, the apriori algorithm needs to scan database k times. Breadth-first (i.e., level-wise) search a candidate generation and test the frequency of true appearance of the itemsets. It may generate a huge number of candidate sets that will be discarded later in the test stage.

One of the most popular data mining approaches is to find frequent itemsets from a transaction dataset and derive association rules. Given a set of transactions, the problem of mining association rules is to generate all association rules that have support and confidence no less than the user-specified minimum support (called minsup) and minimum confidence (called minconf), respectively. Finding frequent itemsets (itemsets with support no less than minsup) is not trivial because of the computational complexity due to combinatorial explosion. Once frequent itemsets are obtained, it is straightforward to generate association rules with confidence no less than minconf. Apriori and AprioriTid, proposed by R. Agrawal & R. Srikant (2015), are seminal algorithms that are designed to work for a large transaction dataset.

b. FP-Growth Algorithm

To break the two drawbacks of Apriori algorithm, FP-growth algorithm is used. FP-growth requires constructing FP-tree. For that, it requires two passes. FPgrowth uses divide and conquer strategy. It requires two scans on the database. It first computes a list of frequent items sorted by frequency in descending order (F-List) and during its first database scan. In the second scan, the database is compressed into a FP-tree. This algorithm performs mining on FP-tree recursively. There is a problem of finding frequent itemsets which is converted to searching and constructing trees recursively. The frequent itemsets are generated with only two passes over the database and without any candidate generation process. There are two sub processes of frequent patterns generation process which includes: construction of the FP-tree, and generation of the frequent patterns from the FP-tree (Kumbhare & Chobe, 2014).

1.5. Data Mining Architecture

Data visualization techniques are becoming very useful methods to discover patterns in datasets, because they impact directly the human visual system, currently the most powerful pattern recognizer and discoverer (Shneiderman, 2003). There is a wide variety of techniques, which may be used in the several stages of the KDD process: in the pre-processing stage, to get a rough feeling of the features of the dataset; in the data mining stage, to discover patterns, such as clusters of items, correlations or dependencies among attributes, or to visualize the model produced by the data mining algorithm, in order to have a better understanding how the responses are generated by the model. Among the most common visualization techniques to mine knowledge from data are 2D, 3D scatter-plots, and scatter-plot matrix.

1.6. Limitations of Data Mining Algorithms

As this review paper shows that the bottleneck of data mining algorithms especially in researches are inefficiency of the algorithms on a large size of datasets and multimedia data. Data mining algorithms were not handling a large volume, heterogeneous data including multimedia data and spatial data (Wu et al., 2007). The performance of data mining algorithms are low on multimedia data (video signal, audio signal, sequential data, spatio-temporal, temporal, time series) and spatial data. Additionally, the presentation of data mining results to easily view and understand the output of the data mining algorithms there is a need to use knowledge representation (decision tree, rules, equations, semantic networks) and visualization techniques (such as graphs, bar charts, etc. (Huang & Hou, 2017).

However, many data mining algorithms work with static datasets. This requires that the algorithm be completely rerun any time the database changes. Since data mining problems are often not precisely stated, interfaces may be needed with both domain and technical experts. Although some techniques may work well, they may not be accepted by users if they are difficult to use or understand. Determining the intended use for the information obtained from the data mining tool is a challenge. Indeed, how business executives can effectively use the output is sometimes considered the most difficult part. Because the result are type that have not previously been known. Business practices may have to be modified to determine how to effectively use the information uncovered (Massaro, Maritati & Galiano 2018).

Some data mining algorithms, like k-NN, are easy to build but quite slow in predicting the target variables. Algorithms such as the decision tree take time to build but can be reduced to simple rules that can be coded into almost any application. The trade-offs between production responsiveness and build time need to be considered and if needed, the modeling phase needs to be revisited if the response time is not acceptable by business application. The quality of prediction, accessibility of input data and the response time of the prediction remain the most important quality factors in the business application. Therefore, this review work presents an inefficiency of data mining algorithms specifically in research work. The role of this review is also to give a clue idea for researchers and to what extent the efficiency of data mining algorithms helpful on the quality of retrieve hidden pattern from datasets. The summary of these algorithms has been shown as a table 1 below.

Tab. 1. Summary on Inefficiency of Data Mining Algorithms

No.	Algorithm	The study	Explored Bottleneck of the Algorithm
1.	Apriori	S. R. Joseph *et al.*, (2016) Data mining Algorithms: an overview, & G. Negandhi (2007) Apriori Algorithm Review for Finals	– It is reduces the size of candidate frequent itemsets by using Apriori property. – It requires many database scans as the size of the largest frequent itemsets. – It needs more search space and the input-output cost increases. – It increases the number of database scan hence it increases in computational cost. – It discovers a huge quantity of rules, when some being irrelevant.
2.	C4.5	N. Rehman (2017) Data Mining Techniques Methods Algorithms and Tools	– It requires target attribute that will have only discrete values. – Small change in data can cause different decision trees to be built. – In small training set, the C4.5 algorithm does not work very well (less accurate and/or efficient).
3.	CART	R. Zafarani, M. Abbasi and H. Liu (2014)	– It has unstable decision tree. – It splits variable only by one.
4.	Decision tree	R. Zafarani, M. Abbasi and H. Liu (2014), Social Media Mining, Cambridge University Press	– It cannot predict the value of a continuous attribute. – It provides error prone results on too many classes. – Irrelevant attribute affect construction of decision tree in a bad manner. – Small change in data can change the decision tree completely. – Performs poorly with many class and small data. – It does not function well with categorical variables having multiple levels. – It brought Over fitting problem.
5.	EM	N. Rehman (2017) Data Mining Techniques Methods Algorithms and Tools	– It is slow convergence. – Inability to provide estimation to the asymptotic variance-covariance matrix of the maximum likelihood estimator. – The EM algorithm does not require the gradient. – It can be used in cases where some data values are missing, although this is less relevant in the 1d case.

Tab. 1. Summary on Inefficiency… – cont.

6.	K-Means	J. Swarndeep Saket , & S. Pandya (2016) An Overview of Partitioning Algorithms in Clustering Techniques	– Every time starting with a random set of initial clusters and repeat a number of times to obtain an optimal. – It is difficult in comparing quality of the clusters produced. – It is difficult to predict what K should be when fixed number of clusters can make. – It doesn't work well with non-globular cluster.
7.	K-Mediod	"	– Due to its time complexity k-mediods is more costly than k-means algorithm. – It doesn't scale well for a large datasets. – The results produced and total run time depends upon initial partitions.
8.	KNN	S. Bavisi, *et al.*, (2014) A Comparative Study of Different Data Mining Algorithms	– It has poor run time performance. – It requires high calculation complexity – It considers no weight difference between samples. – It is sensitive to irrelevant and redundant feature. – Sensitiveness to noisy or irrelevant attributes. – It is a weak as a classifier for an IDS is its large storage requirements. – It is highly susceptible to the curse of dimensionality and slow in classifying test tuples.
9.	Naive Bayes	"	– It provides less accuracy. – The precision of algorithm decreases if the amount of data is less. – It will consider the probability of attribute to be zero (zero problem). – Independence assumption is often violated in the real world.
10.	Neural Networks	H.-C Huang, &, C.-I. Hou (2017)	– It has poor interpretability. – It takes time for long training. – Inability to interpret the learned model. – It has high complexity.
11.	PageRank	D. Xu & Y. Tian (2015) A Comprehensive Survey of Clustering Algorithms	– It is computed value for each page off-line and it does not depend on search queries. – Older pages may have higher rank – so even if a new page has some very good contents but it may not have many links in the early state. – PageRank can be easily increased.

Tab. 1. Summary on Inefficiency… – cont.

12.	SVM	S. R. Joseph *et al.*, (2016) Data Mining Algorithms: An Overview	– It is hard to interpret and memory intensive. – It is a classifier high algorithmic complexity and extensive memory requirements. – Depend on the choice of the kernel. – High complexity. – Difficult to design multi-class classifiers.
13.	DBSCAN	D. Xu, & Y. Tian (2015) A Comprehensive Survey of Clustering Algorithms	– It has trouble when the clusters have widely varying densities. – It also has trouble with high-dimensional data. – It is expensive when the computation of nearest neighbors requires computing all pairwise proximities. – To set an input parameters it is high sensitivity. – It is poor cluster descriptors.
14.	Linear regression	S. R. Joseph *et al.*, (2016) Data Mining Algorithms: An Overview	– It is limited to predicting numeric output. – It has a lack of explanation about what has been learned can be a problem. – It doesn't work well for data with continuous or binary outcomes.
15.	Logistic Regressio n	"	– It is a classic problem on text classification. – It is not stable when one predictor explain the response variable. – It requires more assumptions and sensitive to outliers.
16.	Density Based	"	– It fails in various density clusters. – It fails in neck type of dataset.

3. CONCLUSION

This review article attempts to answer which data mining algorithm(s) is efficient in the research work, the bottleneck associated with the algorithms and research area in data mining. Data mining algorithms are a tool used to retrieve hidden knowledge from datasets. It is a KDD process to identify the pattern and its relationship in huge dataset. Recent advances in data extraction techniques have resulted in tremendous increase in the input data size of data mining applications. Different algorithms provide different perspectives on the complete nature of the pattern. However, the size of dataset was increased from time-to-time in different fields for research purposes. This review paper basically to show a directions and used as a guide and help the researchers specifically to identify the shortcoming of data mining techniques with domain area in solving a certain problems they will explore. It also shows the research areas not yet started particularly in multimedia where data can be sequential, audio, video, spatio-temporal and time series. Therefore, the reviewed paper shows that it becomes difficult to handle a large datasets in order to identify associations and patterns. And it indicates an overview of architecture and algorithms used in large datasets.

REFERENCES

Agrawal, R., & Srikant, R. (2015). Fast algorithms for mining association rules. In *Proc. of the 20th International Conference on Very Large Data Bases (VLDB)* (pp. 487–499). Santiago, Chile.

Al-Khoder, A., & Harmouch, H. (2015). Evaluating Four Of The most Popular Open Source and Free Data Mining Tools. *International Journal of Academic Scientific Research*, *3*(10), 13–23.

Bavisi, S., Mehta, J., & Lopes, L. (2014). A Comparative Study of Different Data Mining Algorithms. *International Journal of Current Engineering and Technology*, *4*(5), 3248–3252.

Gulli, A., & Pal, S. (2017). *Deep Learning with Keras-Implement neural networks with Keras on Theano and Tensor Flow*. Birmingham, UK: Packt Publishing.

Huang, H. C., & Hou, C. I. (2017). Tourism Demand Forecasting Model Using Neural Network. *International Journal of Computer Science & Information Technology (IJCSIT)*, *9*(2), 19–29.

Joseph, S. R., Hlomani, H., & Letsholo, K. (2016). Data Mining Algorithms: An Overview. *International journal of Computers and Technology*, *15*(6), 6806–6813.

Kalyani, J., Bharathi, H. N., & Rao, J. (2016) Stock Trend Prediction Using News Sentiment Analysis, *International Journal of Computer Science & Information Technology (IJCSIT)*, *8*(3), 67–76.

Kotu, V., & Deshpande, B. (2015). *Predictive Analytics and Data Mining – Concepts and Practice with RapidMiner*. Elsevier.

Kumbhare, T. A., & Chobe, S. V. (2014) An Overview of Association Rule Mining Algorithms. *International Journal of Computer Science and Information Technologies*, *5*(1), 927–930.

Massaro, A., Barbuzzi, D., Vitti, V., Galiano, A., Aruci, M., & Pirlo, G. (2016), Predictive Sales Analysis According to the Effect of Weather. In *Proceeding of the 2nd International Conference on Recent Trends and Applications in Computer Science and Information Technology* (pp. 53–55). Tirana, Albania.

Massaro, A., Galiano, A., Barbuzzi, D., Pellicani, L., Birardi, G., Romagno, D. D., & Frulli, L., (2017). Joint Activities of Market Basket Analysis and Product Facing for Business Intelligence oriented on Global Distribution Market: examples of data mining applications. *International Journal of Computer Science and Information Technologies*, *8*(2), 178–183.

Massaro, A., Maritati, V., & Galiano, A. (2018). Data Mining Model Performance of Sales Predictive Algorithms Based On Rapidminer Workflows. *International Journal of Computer Science & Information Technology (IJCSIT)*, 10 (3) 39–56. doi:10.5121/ijcsit.2018.10303

Negandhi, G. (2007). *Apriori Algorithm Review for Finals* (SE 157B). Spring Semester.

Nguyen, H.-L., Woon, Y. K., & Ng, W. K. (2015). A Survey on Data Stream Clustering and Classification. *Knowledge and Information Systems*, *45*(3), 535–569. doi:10.1007/s10115-014-0808-1

Otha, M., & Higuci, Y. (2013). Study on Design of Supermarket Store Layouts: the Principle of Sales Magnet, World Academy of Science. *Engineering and Technology*, *7*(1), 209–212.

Ozisikyilmaz, B. (2009). *Analysis, Characterization and Design of Data Mining Applications and Applications to Computer Architecture* (Unpublished doctoral dissertation). Northwestern University, Evanston, Illinois.

Rehman, N. (2017). Data Mining Techniques Methods Algorithms and Tools. *International of Computer Science and Mobile Computing*, *6*(7), 227–231.

Shneiderman, B. (2003). Inventing discovery tools: Combining information visualization with data mining. In *The Craft of Information Visualization Readings and Reflections Interactive Technologies* (pp.378-385). Morgan Kaufmann. doi:10.1016/B978-155860915-0/50048-2

Štulec, I., Petljak, K., & Kukor, A. (2016). The Role of Store Layout and Visual Merchandising in Food Retailing. *European Journal of Economics and Business Studies*, *4*(1), 139–152.

Swarndeep Saket, J., & Pandya, S. (2016). An Overview of Partitioning Algorithms in Clustering Techniques. *International Journal of Advanced Research in Computer Engineering & Technology (IJARCET)*, *5*(6), 1943–1946.

Talia, D., Trunfio, P., & Marozzo, F. (2016). *Data Analysis in the Cloud: Models and Techniques for Cloud-Based Data Analysis.* Elsevier Science.

Wimmer, H., & Powell, L. M. (2015) A Comparison of Open Source Tools for Data Science, In *Proceedings of the Conference on Information Systems Applied Research* (v8 n3651). Wilmington, North Carolina USA.

Wu, X., Kumar, V., Ross Quinlan, J., Ghosh, J., Yang, Q., Motoda, H., McLachlan, G. J., Ng, A., Liu, B., Yu, P. S., Zhou, Z.-H., Steinbach, M., Hand, D. J., & Steinberg, D. (2007). *Top 10 algorithms in data mining*. London, UK: Springer-Verlag London Limited.

Xu, D., & Tian, Y. (2015). A Comprehensive Survey of Clustering Algorithms. *Annals of Data Science*, *2*(2), 165–193. doi:10.1007/s40745-015-0040-1

Yadav, Ch., Wang, S., & Kumar, M. (2013) Algorithm and approaches to handle large Data-A Survey, *International Journal of Computer Science and Network*, *2*(3), 1307.5437.

Zafarani, R., Abbasi, M., & Liu, H. (2014). Social Media Mining. Cambridge: Cambridge University Press. doi:10.1017/CBO9781139088510

Applied Computer Science, vol. 15, no. 3, pp. 87–102
doi:10.23743/acs-2019-24

Submitted: 2019-08-01
Revised: 2019-08-15
Accepted: 2019-09-03

inertia moment, induction motor, wavelet transformation, backlash zone, membership function

Marcin TOMCZYK[0000-0002-5383-7168]*,
Anna PLICHTA[0000-0001-6503-308X]**, *Mariusz MIKULSKI****

APPLICATION OF IMAGE ANALYSIS TO THE IDENTIFICATION OF MASS INERTIA MOMENTUM IN ELECTROMECHANICAL SYSTEM WITH CHANGEABLE BACKLASH ZONE

Abstract

This paper presents a new method of identification of inertia moment of reduced masses on a shaft of an induction motor drive being a part of an electromechanical system. The study shows the results of simulations performed on the tested model of a complex electromechanical system during some changes of a backlash zone width. An analysis of wavelet scalograms of the examined signals carried out using a clustering technique was applied in the diagnostic algorithm. The correctness of the earliest fault detection has been verified during monitoring and identification of mass inertia moment for state variables describing physical quantities of a tested complex of the electromechanical system.

1. INTRODUCTION

Detection of undesirable changes of states of electromechanical processes takes the form of a sequence of intentional operations executed in assumed time using a set of machines and devices at a determined number of available resources. Faults and other destructive events can be the reasons for these changes of states (Korbicz, Kościelny & Kowalczuk, 2002).

* Electrical School No. 1 in Krakow them. Silesian Insurgents, Kamieńskiego 49, 30-644 Kraków, Poland, tomczykmarcin@poczta.fm
** Cracow Univeristy of Technology, Faculty of Physics, Mathematics and Computer Science, Institute of Computer Science, Warszawska 24, 31-155 Kraków, Poland, aplichta@pk.edu.pl
*** State University of Applied Sciences in Nowy Sącz, Institute of Technology, Zamenhofa 1a, 33-300 Nowy Sącz, Poland, mmikulsk1@poczta.onet.pl

In electromechanical systems, such detection is easier due to the possibility of examining the signals simultaneously in the time and frequency, which facilitates the selection of information and, subsequently, correct interpretation of the features that assign the caught signals to different undesirable states of the system indicating the appearance of the fault (Duda, 2007; Zając, 2009).

Recognition of images consists in detection, interpretation, and identification of the correct features in a certain set of the examined object. The process of ascribing the object to a single class is named identification, whereas the ascribing of objects to the respective classes is named classification (Looney, 1997).

There are several scientific studies on the new techniques of detection of faults in dynamic systems using time-frequency methods as well as image analysis. Among these papers, some are very recent (they were published in the last three years) and some are older. The following ones are worth mentioning:

- using the theory of waves in the identification of dynamic systems (Hasiewicz & Śliwiński, 2005; Wysocki, 2006),
- a comparative analysis of time-frequency methods in diagnostics of electric drives (Sajjad, Zaidi, Zanardelli, Aviyente & Strangas, 2007),
- analysis of the possibility of application of discrete wavelet transformation to the envelope of stator's current to the early detection of coil short circuits in induction motor indicating a fault (Wolkiewicz & Kowalski, 2015),
- sing of discrete packet wavelet analysis of signal of stator's current in the detection of faults in windings of stator's induction motor (Mathew, 2017),
- detection of rotor's cracks in induction motor using the algorithm of recognition of binary image created as a result of the transformation of the tested vector of the stator's current (Divdel, Moghaddam & Alipour, 2016),
- presentation of diagnostics of faults in three-phase induction motor using the method of extraction of features from the thermograms registered for the assumed states of working (Głowacz & Głowacz, 2017).

2. PRESENTATION OF MODEL OF THE INDUCTION MOTOR DRIVE USED IN SIMULATION TESTS OF FAULT IDENTIFICATION

The diagnostic tests have been conducted by means of a working machine in the form of a dynamic mass-absorbing-elastic element being a load to the induction motor. The nominal operating conditions of the induction motor were set, and the model has been placed in a stationary coordinate system related to the stator (model α, β, 0). The gradually increasing backlash zone occurs on the rod as a result of the line's slip on the surface of the drive wheel of the working machine.

Fig.1 shows a simplified form of a diagram of the tested complex electromechanical system.

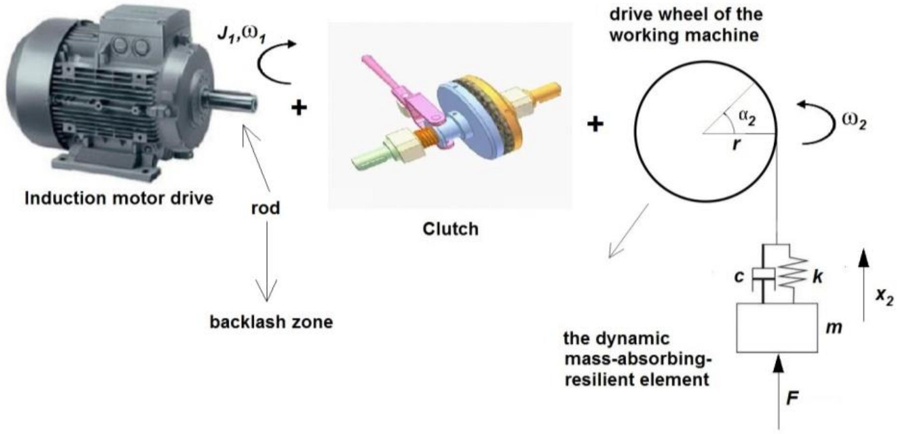

Fig. 1. Diagram of the tested complex electromechanical system – the induction motor drive is connected with the dynamic mass-absorbing-elastic element with the clutch

The following parameters of the induction motor were selected for the examination (parameters of its equivalent circuit are expressed in relative units): circuit stator relative resistance r_s = 0.059 [Ω], circuit rotor relative resistance r_w = 0.048 [Ω], relative reactance of the dispersion circuit stator x_s = 1.92 [Ω], relative reactance of the dispersion circuit rotor x_w= 1.92 [Ω], relative reactance of the dispersed circuit x_m= 1.82 [Ω], $w = x_s \cdot x_w - x_m \cdot x_m = 0.374$, mechanical time constant T_m = 0.86 [s]. All simulation tests have been conducted using MATLAB/Simulink environment.

3. DESCRIPTION OF EXECUTION OF IDENTIFICATION TESTS OF THE MASS INERTIA MOMENT IN THE ELECTROMECHANICAL SYSTEM CONTAINING FRICTION DESCRIBED BY MEANS POWER EQUATION OF OSTWALD AND DE WAELE

The tests have been carried out in four test groups, with the following four different values of apparent viscosity coefficient η_k: 0.0125 [$\mathrm{Pa \cdot s}^{n_1}$], 0.025 [$\mathrm{Pa \cdot s}^{n_1}$], 0.0375 [$\mathrm{Pa \cdot s}^{n_1}$], and 0.05 [$\mathrm{Pa \cdot s}^{n_1}$]. Each test group contained seven cases to study with different inertia moment values. The results of simulations for all the physical quantities and for every case of change of inertia moment of reduced masses and connected stiffly with the induction motor drive rotor J_1 have been written in the matrix $N_{1[7,2048]}$. The elements of the matrix N_1 have been written for each consistency index η_k. Value of an inertia moment J_1 have been determined as the percentage in relation to its nominal value J_1, down at value A% and up at value C%. Formal changes of inertia moment J_1 have been written in matrix K_1 in the following order: K_1 = [nominal value of the inertia moment (J_1 = 1.16 [$\mathrm{kg \cdot m^2}$]), A = 2.5% (J_1 = 1.131 [kg·m^2]), A = 5% (J_1 = 1.102 [kg·m^2]), A = 7.5% (J_1 = 1.073 [kg·m^2]), A = 17.5% (J_1 = 0.957 [kg·m^2]), C = 2.5 % (J_1 = 1.189 [kg·m^2]), C=5% (J_1 = 1.218 [kg·m^2])].

In each of the seven cases of changes of inertia moment J_1, simulation tests have been conducted for six backlash zone widths. The backlash zone width values have been taken in sequence from the matrix K_2, in the following order: [0.0025, 0.00375, 0.005, 0.0075, 0.009, 0.01]. All tests have been executed for the creep index n_1 value equal 0.93.

The wavelet type and its order have been selected in such a way that the shape of the basic wavelet approximately would be adequate to the character of the transient course of the tested physical quantity obtained as a result of a simulation for the case of the smallest backlash zone width. Based on the performed tests, the following selections of wavelets have been made for individual physical variables, with decomposition level 10:

a) linear acceleration of the induction motor drive a_1 – sym5,
b) electromagnetic moment of the induction motor drive m_{el} – db6,
c) angular speed of the induction motor drive rotor ω_1 – sym5,
d) linear acceleration of a mass a_2 – db6,
e) linear speed of a mass v_2 – sym5.

In all the conducted simulations it was assumed that the test of dynamics of the electromechanical system in backlash zone starts precisely when the expression specified in the left part of the following inequality (1) is smaller than its right part:

$$\left|\alpha_1 - \alpha_2\right| < \frac{K_{2(i)}}{r}; \quad i = 1,2..6 \tag{1}$$

where: r – radius of the drive wheel of a working machine [m],
$K_{2(i)}$ – value that has been taken sequentially from the K_2 matrix and corresponding to the given backlash value in mechanical connection,
i – an index number within the K_2 matrix.

The location change of the angle α_1 for rotating masses of the induction motor drive [rad] has been calculated using the formula: $\alpha_1 = \int \omega_1 \cdot dt$, and the location change of the angle α_2 of the drive wheel of the working machine [rad], has been calculated using the formula: $\alpha_2 = \int \omega_2 \cdot dt$, where ω_1 and ω_2 stand for angular speeds. The former refers to the angular speed of rotating masses of the induction motor drive [rad/s], and the latter to the speed of the drive wheel of the working machine [rad/s].

After satisfying the condition determined by inequality described by the formula (1) the load moment of the induction motor drive is set to zero in the tested electromechanical system.

In all the conducted simulation tests it was assumed that the tested matrix N_1 would contain 2000 samples of a signal, chosen in sequence from the moment of appearance of backlash zone in the tested model of the electromechanical system; additionally, 48 samples preceding this moment would be included. Therefore, the total number of samples will amount to the value of $2^{11} = 2048$, which enables effectively to carry out a multiresolution analysis.

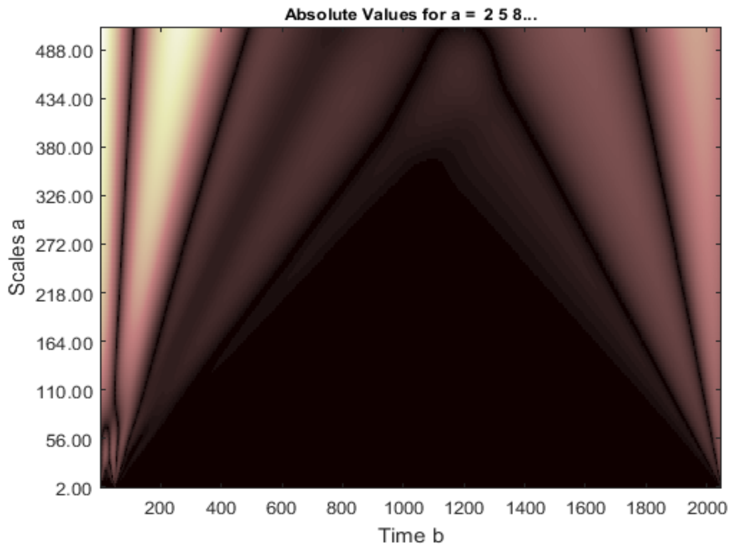

Fig. 2. Wavelet scalogram registered for test in which connection between the induction motor drive and the mechanical system loading him has been cut off until moment of backlash's taking.

Fig. 2 presents the wavelet scalogram depicting the linear acceleration of the induction motor drive a_1 with the inertia moment amounting to the value of true mass inertia moment J_1 decreased by about 7.5%. This simulation test has been conducted with backlash zone width = 0.005 at the consistency's coefficient $\eta_k = 0.025$ and the melt flow index $n_1 = 0.93$.

4. DESCRIPTION OF THE DIAGNOSTIC ALGORITHM USED IN PROCESSING OF THE WAVELET SCALOGRAMS BY MEANS OF IMAGE ANALYIS METHOD WITH USING OF A CLUSTERING TECHNIQUE

According to the presented diagnostic procedure, the values of inertia moment J_1 with the assumed backlash zone width values of matrix X_3 are determined using normalization of values of matrix's elements X_2.

For all the tested physical quantities, values of elements of matrix X_3 have been calculated as the transformation of the values X_2 to the range [k_3, $2\cdot k_3 – h_3$] according to the formula:

$$X_{3(e)(a,b)} = \left(\frac{\left(X_{2(e)(a,b)} - h_2\right)}{k_2 - h_2} \right) \cdot \left(k_3 - h_3\right) + k_3; \qquad (2)$$

$$a = 1,2...343;\; b = 1,2...436;\; e \in < 1,6 >$$

where: X_2 – values of matrix's elements calculated in the test,
h_2 – the minimal value of elements of matrix X_2 determined in the test,
k_2 – the maximal value of elements of matrix X_2 determined in the test,
h_3 – the initial value of the range containing normalized values X_2 in the test,
k_3 – the final value of the range containing normalised values X_2 in the test.

Therefore, the values of variables h_2 and k have been calculated according to the following formulas:

$$h_2 = \min(X_{2(e)(a,b)});\; a = 1,2...343;\; b = 1,2...436;\; e \in <1,6> \qquad (3)$$

$$k_2 = \max(X_{2(e)(a,b)});\; a = 1,2...343;\; b = 1,2...436;\; e \in <1,6> \qquad (4)$$

For all the tested physical quantities, values of elements of matrix X_2 have been calculated as the transformation of pixel colour intensities comprised in matrix X_1 to the range [k_3, $2\cdot k_3 – h_3$].

Normalization of values of the elements of the matrix X_1 used in simulation tests conducted at consistency coefficient η_k = 0.025 with the assumed backlash zone width can be described according to the formula:

$$X_{2(e)(a,b)} = \left(\frac{\left(X_{1(e)(a,b)} - h_1\right)}{k_1 - h_1} \right) \cdot \left(k_3 - h_3\right) + k_3; \quad a = 1,2...343;\; b = 1,2...436;\; e \in < 1,6 > \qquad (5)$$

where: X_1 – values of the elements of the matrix recorded in the test conducted with the nominal value of inertia moment J_1 (in the case of the undamaged drive with the induction motor),

h_1 – the minimal value of the elements of the matrix X_1 determined in the test,
k_1 – the maximal value of the elements of the matrix X_1 determined in the test,
h_3 – the initial value of the range containing normalized values X_1 determined in the test in which one assumed consistency coefficient $\eta_k = 0.025$ and nominal value of inertia moment J_1,
k_3 – the end value of the range containing normalised values X_1 determined in the test in which one assumed consistency coefficient $\eta_k = 0.025$ and nominal value of inertia moment J_1.

Calculations of values of variables h_1 and k_1 have been performed using the following formulas:

$$h_1 = \min(X_{1(e)(a,b)});\ a = 1,2...343;\ b = 1,2...436;\ e \in <1,6> \tag{6}$$

$$k_1 = \max(X_{1(e)(a,b)});\ a = 1,2...343;\ b = 1,2...436;\ e \in <1,6> \tag{7}$$

Values of variables h_3 and $k_{3,}$ which represent the beginning and end of the range to which the values of the elements of matrix X_2 have been transformed. For all the tested physical quantities, they have been determined using the minimal and maximal value, respectively, according to the formulas:

$$h_3 = \min(h_{4,}\ k_4) \tag{8}$$

$$k_3 = \max(h_{4,}\ k_4) \tag{9}$$

where: h_4, k_4 – values of variables obtained as a result of calculations conducted using variables calculated for parts of samples recorded in the test.

On the basis of results obtained in the series of tests, it was decided to divide of calculation of values of variables h_4 and k_4 into two cases for every simulation test conducted with the assumed backlash zone width:

- the first case concerns linear acceleration on the circuit of the drive wheel of the rotor a_1 and linear speed of the mass v_2,
- the second case concerns the electromagnetic moment of the induction motor m_{el}, angular speed of the rotor ω_1 and linear acceleration of the mass a_2.

In the first case, values of variables h_4 and k_4 have been calculated according to the following formulas:

$$h_4 = \min(X_{1(e)(j)}) - \max(X_{1(e)(j)});\ e \in <1,6>;\ j = 1,2...2048; \tag{10}$$

$$k_4 = \min(X_{1(e)(j)}) + \max(X_{1(e)(j)});\ e \in <1,6>;\ j = 1,2...2048; \tag{11}$$

In the second case, calculations of differences between the minimal and maximal values of arithmetic means of appropriate parts of the samples chosen from the matrix N_1 have been applied. However, values of variables h_4 and k_4 have been calculated, respectively, according to the formulas:

$$h_4 = (m_{e2} - m_{d2}) + (m_{e2} - m_{d2}) + (m_{e3} - m_{d3}) \tag{12}$$

$$k_{d4} = (m_{e1} - m_{d1}) - (m_{e2} - m_{d2}) - (m_{e3} - m_{d3}) - (m_{e4} - m_{d4}) \tag{13}$$

The minimal values m_{e1}, m_{e2}, m_{e3}, and m_{e4} used to determine the values of variables h_4 and k_4 have been calculated by means of the following formulas:

$$m_{e1} = \min(N_{1(e)(j)});\ e \in <1,6>;\ j = 1,2...768; \tag{14}$$

$$m_{e2} = \min(N_{1(e)(j)});\ e \in <1,6>;\ j = 1,2...1024; \tag{15}$$

$$m_{e3} = \min(N_{1(e)(j)});\ e \in <1,6>;\ j = 1,2...1280; \tag{16}$$

$$m_{e4} = \min(N_{1(e)(j)});\ e \in <1,6>;\ j = 1,2...1536; \tag{17}$$

The values of arithmetic means m_{d1}, m_{d2}, m_{d3} and m_{d4} have been calculated in the following way:

$$m_{d1} = \frac{\sum_{j=1}^{768} N_{1(e)(j)}}{768}; \quad e \in <1,6> \tag{18}$$

$$m_{d2} = \frac{\sum_{j=1}^{1024} N_{1(e)(j)}}{1024}; \quad e \in <1,6> \tag{19}$$

$$m_{d3} = \frac{\sum_{j=1}^{1280} N_{1(e)(j)}}{1280}; \quad e \in <1,6> \tag{20}$$

$$m_{d4} = \frac{\sum_{j=1}^{1536} N_{1(e)(j)}}{1536}; \quad e \in <1,6> \tag{21}$$

Values of elements of matrix N_1 have been determined according to the following order:

$$N_{1(e)(j)} = \left[M_{(e)(1)} >= M_{(e)(2)} >= .... >= M_{(e)(2048)} \right]; e \in <1,6>; \ j = 1,2...2048 \quad (22)$$

where: M – values of the elements of matrix M recorded in the test.

In the presented diagnostic method, determining of values of pattern matrices used in the identification of inertia moment J_1 was essential. Calculations in the algorithm were conducted according to the clustering method using *k-harmonic means* technique (Frąckiewicz, 2011).

An important element of the diagnostic method was conducting the most profitable initialisation of preliminary values of centres of clusters, membership function and weight function.

The initial values of centres of clusters used in simulations have been calculated by means of the value of variable k_3 obtained as a result of simulations conducted with consistency coefficient η_k = 0,025 [Pa·s^{n_1}] during which the inertia moment J_1 was changed at the assumed backlash zone width.

In simulations conducted by means of the described method, values of inertia moments J_1 have been used and chosen in sequence and according to the order assumed in matrix K_1.

Calculations of the initial values of centres of clusters S conducted according to the following formula:

$$S_{(e)(i)} = 1 - k_3; \quad e \in < 1,6 >; \ i = 1,2...7 \quad (23)$$

where: k_3 – the value of the variable determined according to the formula (8) by means of values of the matrix elements X_1 in simulations conducted for all the assumed changes of inertia moment J_1.

Values of membership function have been written in matrix M, whereas the values of weight function have been written in matrix W. The initial values in both matrices were set equal to 1 and determined in the following way:

$$M_{(i)(a,b)} = 1; \quad a = 1,2...343; \ b = 1,2...436; \ i = 1,2...7 \quad (24)$$

$$W_{(a,b)} = 1; \quad a = 1,2...343; \ b = 1,2...436 \quad (25)$$

In the next step of the algorithm, the above-described initial values of membership function M and weight function W have been changed using the following formulas (Frąckiewicz, 2011):

$$W_{(a,b)} = \frac{\sum_{i=1}^{7} \left\| X_{3(e)(a,b)} - S_{(e)(i)} \right\|^{-p-2}}{\left(\sum_{i=1}^{7} \left\| X_{3(e)(a,b)} - S_{(e)(i)} \right\|^{-p} \right)^2}; \tag{26}$$

a = 1,2...343; b = 1,2...436; $e \in$ <1,6>; p >= 2

$$M_{(i)(a,b)} = \frac{\left\| X_{3(e)(a,b)} - S_{(e)(i)} \right\|^{-p-2}}{\sum_{i=1}^{7} \left\| X_{3(e)(a,b)} - S_{(e)(i)} \right\|^{-p-2}}; \tag{27}$$

a = 1,2...343; b = 1,2...436; $e \in$ <1,6>; i = 1,2...7; p >= 2

where: p – additional optimisation parameter.

In the applied diagnostic method, the "soft" values of the membership function M have been calculated and met the following conditions (Frąckiewicz, 2011):

$$0 <= M_{(i)(a,b)} <= 1;\ a = 1,2...343;\ b = 1,2...436;\ e \in <1,6>;\ i = 1,2...7;\ p >= 2 \tag{28}$$

$$\sum_{i=1}^{7} M_{(i)(a,b)} = 1; \quad a = 1,2\ldots343;\ b = 1,2\ldots436;\ i = 1,2\ldots7 \tag{29}$$

Changes in the values of the membership function and the weight function have a significant impact on the values of the centres of clusters. It is then followed by determining a degree of membership of every value of the element of matrix X_3 to the particular clusters.

After updating of the values of the membership function M and weight function W, new values of centres of clusters S have been determined by means of the following formula (Frąckiewicz, 2011):

$$S_{(e)(i)} = \frac{\sum_{a=1}^{343} \sum_{b=1}^{436} \left(M_{(i)(a,b)} \cdot W_{(e)(a,b)} \cdot X_{3(e)(a,b)} \right)}{\sum_{a=1}^{343} \sum_{b=1}^{436} \left(M_{(i)(a,b)} \cdot W_{(e)(a,b)} \right)}; \quad e \in <1,6>;\ i = 1,2\ldots7 \tag{30}$$

In the conducted simulation tests, creation of pattern matrices as well as tested matrices have been conducted at the same assumed backlash zone width for all the tested physical quantities.

Values of all the elements of each pattern matrix have been calculated in the series of simulation tests in which the assumed consistency coefficient η_k = 0.025.

These values have been written to 7x7 matrix N_2. The tested values have been written into the 1x7 matrix N_3.

Values of the matrix's elements S have been written to the matrix containing pattern values N_2 and to the tested matrix N_3. Therefore, matrices N_2 and N_3 have been determined according to the following formulas:

$$N_{2(e)(f,i)} = S_{(e)(f,i)}); \; e \in <1,6>; \; f = 1,2...7; \; i = 1,2...7 \tag{31}$$

$$N_{3(e)(i)} = S_{(e)(i)}; \; e \in <1,6>; \; i = 1,2...7 \tag{32}$$

Determination of the values of the elements of matrix H enables one for correct identification of the value of inertia moment for the calculated wavelet scalogram of the physical quantity at the particular consistency coefficient η_k.

Values of matrix H can be expressed by means of the formula:

$$H_{(f)} = h_5 \cdot \sum_{i=1}^{7} \left| N_{2(f,i)} - N_{3(i)} \right|; \;\; f = 1,2...7; \;\; i = 1,2...7 \tag{33}$$

where: h_5 – the value of the variable used to improve the identification results.

Using of variable's value h_5 in calculations of matrix H clearly improves the results of the fault identification. The value of this variable causes the increase in the value obtained as a result of the summation of absolute values of differences between the values of the matrix containing pattern values N_2 and values of the tested matrix N_3.

The most profitable for identification simulations variable's value h_5 calculated for tests conducted with all set changes of value of inertia moment J_1 for assumed backlash zone width and in the group of analysis with the adopted consistency coefficient $\eta_k = 0.025$.

To calculate the variable's value h_5 the following formula is used:

$$h_5 = \frac{\max\left(S_{(e)(i)}, S_{1(e)(i)}\right)}{\min\left(\left|h_3\right|, k_3\right)}; \;\; e \in <1,6>; \; i \in <1,7> \tag{34}$$

Calculations of values of matrix's elements S_1 were conducted employing the same methodology as for calculations of values of matrix S. It can be described by the formula:

$$S_{1(e)(i)} = 1 - h_{d3}; \;\;\; e \in <1,6>; \; i = 1,2...7 \tag{35}$$

where: h_3 – the value of a variable determined according to the formula (8) by means of values of elements of matrix X_1 for simulation tests conducted for all the assumed changes of values of inertia moment J_1.

Index nr (for $nr \in <1, 7>$) in matrix H determines the column number in the matrix K_1, which contains the correct inertia moment of reduced masses on the shaft of induction motor drive. The value of index nr ($nr \in <1, 7>$) for $i = 1,2...7$ in matrix H has been determined using the following minimum function: $H_{(nr)} = \min(H_{(i)})$. Therefore, the number i of a column in the matrix K_1 refers to the corresponding to it index nr ($i = nr$).

5. RESULTS OF SIMULATIONS OF THE DIAGNOSTIC ALGORITHM APPLIED FOR IDENTIFICATION OF INERTIA MOMENT OF REDUCED MASSES ON SHAFT OF INDUCTION MOTOR DRIVE IN ELECTROMECHANICAL SYSTEM

In the tables presented below, in the column named *Test Parameters*, backlash zone widths have been placed assumed in the process of identification of the value of inertia moment of reduced masses connected stiffly with the motor's rotor J_1. Besides, in the following tables, one bolded the correct results that were obtained finally in the process of identification of fault and that are the final results of calculations of matrix H.

For all tested physical quantities, pattern matrices N_1 have been created in a series of tests in which the assumed value of consistency coefficient η_k was equal to 0.025 [$\mathrm{Pa} \cdot \mathrm{s}^{n_1}$]. Pattern matrices N_1 have been created for analyses in which an additional optimisation parameter p has been adopted corresponding to the assumed value of this variable. This value has been placed in the tables presented below.

Tab. 1. Exemplified results of tests in matrix *H* for linear acceleration of the induction motor drive a_1

Test parameters	Results	Test parameters	Results
inertia moment J_1 = 0.957, backlash zone = 0.00375, η_k = 0.0375, optimisation parameter p = 2	9.5409 8.4485 7.3105 6.0374 **0.0671** 10.5406 11.4658	inertia moment J_1 = 0.957, backlash zone = 0.00375, η_k = 0.0375, optimisation parameter p = 3	9.4615 8.3730 7.2421 5.9764 **0.0675** 10.4579 11.3810
inertia moment J_1 = 1.131, backlash zone = 0.01, η_k = 0.0375, optimisation parameter p = 3	0.0115 **0.0001** 0.0128 0.0276 0.1080 0.0212 0.0297	inertia moment J_1 = 1.131, backlash zone = 0.01, η_k = 0.0375, optimisation parameter p = 9	0.0150 **0.0002** 0.0166 0.0357 0.1333 0.0276 0.0380

Tab. 2. Exemplified results of tests in matrix *H* for electromagnetic moment of the induction motor drive m_{el}

Test parameters	Results	Test parameters	Results
inertia moment J_1 = 1.102, backlash zone = 0.0075, η_k = 0.0125, optimisation parameter p = 2	0.7347 0.3730 **0.0012** 0.4137 2.4923 1.0490 1.3497	inertia moment J_1 = 1.102, backlash zone = 0.0075, η_k = 0.0125, optimisation parameter p = 3	1.0650 0.5381 **0.0023** 0.5904 3.4786 1.5264 1.9718
inertia moment J_1 = 1.189, backlash zone = 0.01, η_k = 0.05, optimisation parameter p = 3	0.4008 0.8187 1.3102 1.7962 4.2535 **0.0050** 0.3993	inertia moment J_1 = 1.189, backlash zone = 0.01, η_k = 0.05, optimisation parameter p = 9	0.3424 0.7000 1.1203 1.5364 3.6411 **0.0046** 0.3415

Tab. 3. Exemplified results of tests in matrix *H* for angular speed of the rotor of the induction motor drive ω_1

Test parameters	Results	Test parameters	Results
inertia moment J_1 = 1.218, backlash zone = 0.005, η_k = 0.0125, optimisation parameter p = 2	0.8648 1.3365 1.8056 2.3249 4.8432 0.4357 **0.0604**	inertia moment J_1 = 1.218, backlash zone = 0.005, η_k = 0.0125, optimisation parameter p = 3	0.8659 1.3383 1.8080 2.3280 4.8496 0.4363 **0.0604**
inertia moment J_1 = 1.218, backlash zone = 0.0025, η_k = 0.05, optimisation parameter p = 3	0.9500 1.6000 2.2706 2.9889 6.4174 0.3959 **0.1762**	inertia moment J_1 = 1.218, backlash zone = 0.0025, η_k = 0.05, optimisation parameter p = 6	0.9391 1.5815 2.2445 2.9548 6.3460 0.3913 **0.1741**

According to the results of presented simulation tests, obtaining of correct results of identification of fault for all the tested physical quantities is possible if optimisation parameter p is equal or bigger than 2.

Tab. 4. Exemplified results of tests in matrix *H* for linear speed of the mass v_2

Test parameters	Results	Test parameters	Results
inertia moment J_1 = 1.218, backlash zone = 0.01, η_k = 0.0125, optimisation parameter p = 2	1.7737 2.7766 3.8581 5.0250 10.7233 0.8414 **0.0263**	inertia moment J_1 = 1.218, backlash zone = 0.01, η_k = 0.0125, optimisation parameter p = 3	1.8340 2.8699 3.9862 5.1898 11.0535 0.8704 **0.0272**
inertia moment J_1 = 1.073, backlash zone = 0.009, η_k = 0.0375, optimisation parameter p = 3	3.3018 2.2717 1.1624 **0.0330** 5.8461 4.2600 5.1521	inertia moment J_1 = 1.073, backlash zone = 0.009, η_k = 0.0375, optimisation parameter p = 6	1.8634 1.2977 0.6724 **0.0195** 3.6275 2.3761 2.8415

One should pay attention to the fact that if the value of additional optimisation parameter *p* exceeds 3, it triggers noticeable differences in results of fault's identification. Such conclusions can be drawn from the minimal values of matrix *H* obtained for the calculated wavelet scalograms. It can be noticed in all the presented tables.

6. CONCLUSIONS

The presented system of damage detection – based on image analysis enabling for the determination of centres of clusters by means of using the changes of value of membership function and weight function – found its application in the identification of the value of the inertia moment of rotating masses connected stiffly with the induction motor's rotor. The identification process has been conducted in the assumed time ranges.

The use of image analysis greatly increases the efficiency of analysis of non-stationary signals. This method, used in a diagnostic system, can effectively reduce the consequences of appearing of faults because it can be successfully applied already in the initial phase of the development of a fault. The conducted simulation confirmed the functioning of the proposed methodology of fault detection.

On the basis of the conducted research, it can be stated that the efficiency of detection process and fault identification can be greatly enhanced through ensuring appropriate ranges of changes of parameters and through the transformation the colour intensity of pixels recorded at wavelet scalogram in a system containing non-zero backlash zone to adequate ranges.

REFERENCES

Divdel, H., Moghaddam, M. H., & Alipour, G. (2016). A new diagnosis of severity broken rotor bar fault based modeling and image processing system. *Journal of Current Research in Science*, *S*(1), 771–780.

Duda, J. T. (2007). *Pozyskiwanie wzorców diagnostycznych w komputerowych analizach sprawności urządzeń. Diagnostyka procesów i systemów*. Warsaw, Poland: Akademicka Oficyna Wydawnicza EXIT.

Frąckiewicz, M. (2011). *Zastosowanie techniki KHM (k-średnich harmonicznych) w przetwarzaniu obrazów barwnych* (Unpublished doctoral dissertation). Silesian University of Technology, Gliwice.

Głowacz, A., & Głowacz, Z. (2017). Diagnosis of the three-phase induction motor using thermal imaging. *Infrared & Physics Technology*, *81*, 7–16.

Hasiewicz, Z., & Śliwiński, P. (2005). *Falki ortogonalne o zwartym nośniku*. Warsaw, Poland: Akademicka Oficyna Wydawnicza EXIT.

Korbicz, J., Kościelny, J. M., & Kowalczuk, Z. (2002). *Diagnostyka procesów. Modele. Metody sztucznej inteligencji. Zastosowania*. Warsaw, Poland: WNT.

Looney, C. G. (1997). *Pattern recognition using neural networks.* New York, USA: Oxford University Press.

Mathew, G. (2017). Fault detection in an induction motor drive using discrete wavelet packet transform. *IOSR Journal of Electrical and Eectronics Engineering (IOSR-JEEE)*, *12*(2), 01–06.

Wolkiewicz, M., & Kowalski, Cz. (2015). Diagnostyka uszkodzeń uzwojeń stojana silnika indukcyjnego z wykorzystaniem dyskretnej transformaty falkowej obwiedni prądu stojana. *Maszyny elektryczne: zeszyty problemowe*, *3*(107), 13–18.

Wysocki, H. (2006). *Zastosowanie nieklasycznego rachunku operatorów do identyfikacji liniowych układów dynamicznych*. Warsaw, Poland: Akademicka Oficyna Wydawnicza EXIT.

Zając, M. (2009). *Metody falkowe w monitoringu i diagnostyce układów elektromechanicznych (No. 371).* Cracow, Poland: Politechnika Krakowska.

Sajjad, S., Zaidi, H., Zanardelli, W. G., Aviyente, S., & Strangas, E. G. (2007). Comparative study of time-frequency methods for the detection and categorization of intermittent faults in electrical drives. In *Proc. IEEE Int. Symp. on Diagnostics for Electrical Machines, Power Electronics and Drives* (pp. 39–45). Cracow.